AMPLITUDE MODULATION OF ACOUSTIC SIGNALS BY OCEAN WAVES AND THE EFFECT ON SIGNAL DETECTION

James Blenn Perkins

NAVAL POSTGRADUATE SCHOOL
Monterey, California

THESIS

AMPLITUDE MODULATION
OF ACOUSTIC SIGNALS BY OCEAN WAVES
AND THE EFFECT ON SIGNAL DETECTION

by

James Blenn Perkins III

December 1974

Thesis Advisor: H. Medwin

Approved for public release; distribution unlimited.

UNCLASSIFIED

SECURITY CLASSIFICATION OF THIS PAGE (When Data Entered)

REPORT DOCUMENTATION PAGE

READ INSTRUCTIONS BEFORE COMPLETING FORM

1. REPORT NUMBER

2. GOVT ACCESSION NO.

3. RECIPIENT'S CATALOG NUMBER

4. TITLE (and Subtitle)
Amplitude Modulation of Acoustic Signals by Ocean Waves and the Effect on Signal Detection

5. TYPE OF REPORT & PERIOD COVERED
Master's Thesis; December 1974

6. PERFORMING ORG. REPORT NUMBER

7. AUTHOR(s)
James Blenn Perkins III

8. CONTRACT OR GRANT NUMBER(s)

9. PERFORMING ORGANIZATION NAME AND ADDRESS
Naval Postgraduate School
Monterey, California 93940

10. PROGRAM ELEMENT, PROJECT, TASK AREA & WORK UNIT NUMBERS

11. CONTROLLING OFFICE NAME AND ADDRESS
Naval Postgraduate School
Monterey, California 93940

12. REPORT DATE
December 1974

13. NUMBER OF PAGES
115

14. MONITORING AGENCY NAME & ADDRESS(if different from Controlling Office)
Naval Postgraduate School
Monterey, California 93940

15. SECURITY CLASS. (of this report)
Unclassified

15a. DECLASSIFICATION/DOWNGRADING SCHEDULE

16. DISTRIBUTION STATEMENT (of this Report)
Approved for public release; distribution unlimited.

17. DISTRIBUTION STATEMENT (of the abstract entered in Block 20, if different from Report)

18. SUPPLEMENTARY NOTES

19. KEY WORDS (Continue on reverse side if necessary and identify by block number)
Amplitude Modulation
Signal Processing
Signal Detection
Surface Scattered Sound
Ocean Wave Spectrum

20. ABSTRACT (Continue on reverse side if necessary and identify by block number)

A study was conducted of the amplitude modulation of an acoustic signal forward scattered from a wind-generated, model ocean surface. The demodulated spectrum of the surface scattered sound was compared with the model ocean spectrum while varying the acoustic frequency and angle of incidence. Several methods of enhancing signal detection through a knowledge of the ocean spectrum were studied. The most

DD FORM 1 JAN 73 1473 (Page 1)
EDITION OF 1 NOV 65 IS OBSOLETE
S/N 0102-014-6601

UNCLASSIFIED
SECURITY CLASSIFICATION OF THIS PAGE (When Data Entered)

(20. ABSTRACT Continued)

promising of these shows potential gains of the order of three decibels when the received signal is weak and fluctuating greatly, as at a Lloyd Mirror minimum.

Amplitude Modulation of Acoustic Signals by Ocean Waves and the Effect on Signal Detection

by

James Blenn Perkins III
Lieutenant Commander, United States Navy
B.S., United States Naval Academy, 1964

Submitted in partial fulfillment of the
requirements for the degree of

MASTER OF SCIENCE IN ENGINEERING ACOUSTICS

from the

NAVAL POSTGRADUATE SCHOOL
December 1974

ABSTRACT

A study was conducted of the amplitude modulation of an acoustic signal forward scattered from a wind-generated, model ocean surface. The demodulated spectrum of the surface scattered sound was compared with the model ocean spectrum while varying the acoustic frequency and angle of incidence. Several methods of enhancing signal detection through a knowledge of the ocean spectrum were studied. The most promising of these shows potential gains of the order of three decibels when the received signal is weak and fluctuating greatly, as at a Lloyd Mirror minimum.

TABLE OF CONTENTS

LIST OF FIGURES

ACKNOWLEDGEMENTS

The author wishes to extend his sincere appreciation to the following for their contributions to this work:

Dr. Herman Medwin provided invaluable guidance and advice in pursuing this research. Of particular note was his assistance in finding new approaches, or variations, when the effort was stalled or proceeding in an unprofitable direction;

Mrs. Carol Hickey was of great help in preparing computer programs and coping with the minicomputer system's limited storage capabilities;

Mr. William Smith assisted with excellent technical support and his experience from previous thesis projects saved significant wasted effort;

The support of the Naval Air Development Center in obtaining the required minicomputer is appreciated; through their auspices the maintenance support of Mr. Thomas Lee, Pinkerton Computer Consultants Inc., assured the continuity of this research;

The funding support of the Manager Anti-Submarine Warfare Systems Project Office (PM-4) made this work possible.

I. INTRODUCTION

It has long been known that received signals from distant underwater sound sources vary in time. The effect has been described as "builds and fades" of the signal. Though this effect is automatically interpreted by the human ear, which listens when the sound is present and tunes out when it disappears in the noise, little or no advantage of the phenomenon has been taken by the extensive signal processing equipment available today. Though nominally far superior to the ear in response-time and frequency resolution, this equipment often fails to achieve even parity with a human observer when processing a time varying, or modulated, signal. This is due primarily to the electronic equipment's narrow bandwidth and the fact that it integrates continuously rather than selectively.

It was the objective of this research to investigate some of the parameters affecting this phenomenon of a modulated acoustic signal with particular attention to determining, for surface affected signals:

1. The best laboratory modeling techniques.
2. The relation of the modulation frequency to the surface wave frequency.
3. The variation of the modulation amplitude and spectrum with frequency and source/receiver directivity.
4. The optimization of signal processing of an amplitude modulated signal by digital techniques.

In short an attempt was made to discover a "temporal filtering" scheme which could be used in concert with existing high speed frequency filtering techniques, such as the Fast Fourier transform, to enhance signal processing. The concept has been dubbed "EASE", Environmentally Adjusted Signal Enhancement.

II. THEORY

The subject of scattering of sound from the ocean surface has been treated by several authors utilizing nearly as many methods. The following is a summary of Refs.1 and 2 which point up those features of the scattered spectrum which are germane to understanding the relationships between sound fluctuations in the upper ocean and the ocean wave spectrum.

As Parkins summarizes the phenomenon: "When a monochromatic acoustic wave is incident on the surface of the ocean the envelope of reradiation varies in time or fades."

Assuming that the ocean is generated by a stationary homogeneous, Gaussian process, and that it is smooth enough so that multiple scattering can be neglected, the incident acoustic wave of harmonic time variation $e^{i\omega t}$ is given by:

$$\Phi_i = \Phi^+ e^{-\vec{k}_1 \cdot \vec{r}} e^{i\omega t}$$

with

$$k_1 = k_{1x}\hat{x} + k_{1y}\hat{y} + k_{1z}\hat{z}$$

$$= \frac{2\pi}{\lambda} [\ell\hat{x} + m\hat{y} + n\hat{z}]$$

Φ^+ is an amplitude term, ℓ, m, and n are the direction cosines and λ is the wave length of the incident acoustic wave. Other factors are defined in Figure 1.

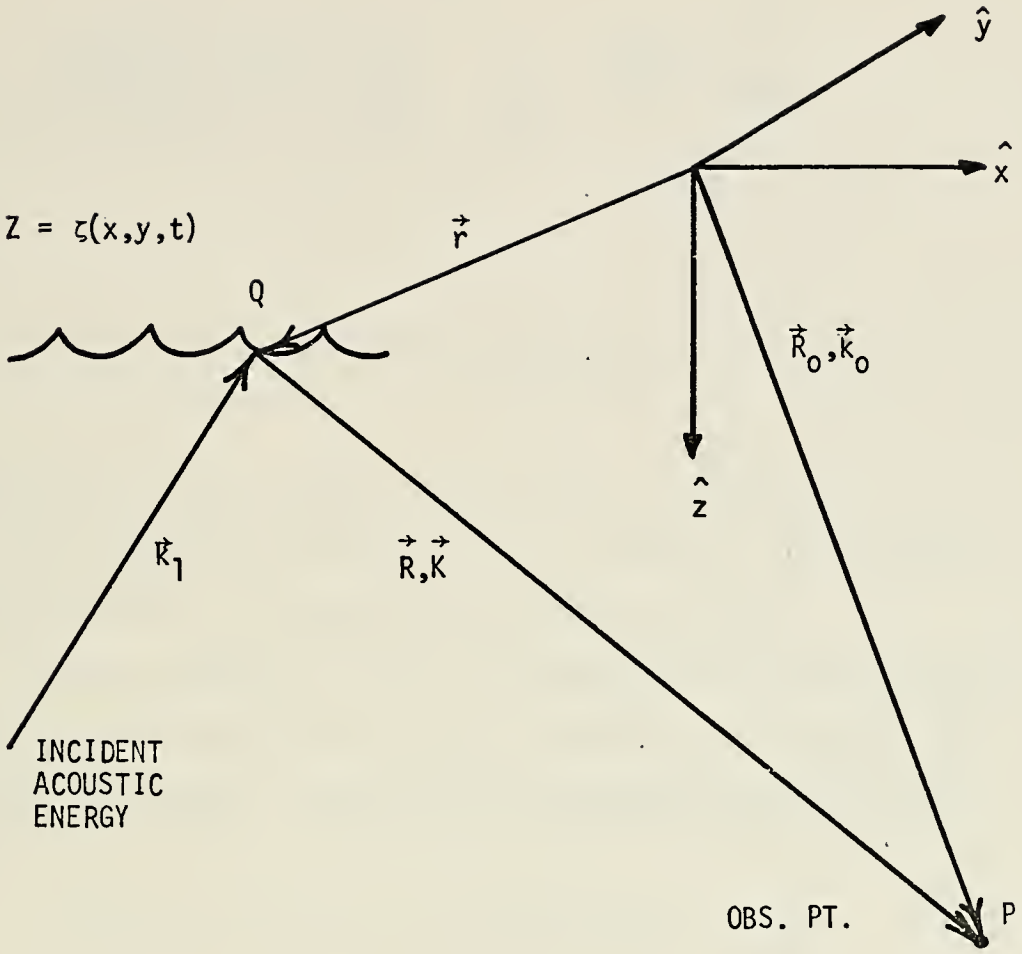

FIGURE 1. Coordinate System for Theoretical Development

Following the development of Beckmann and Spizzichino [Ref. 2] which stipulates a source free, isovelocity ocean, and using the Helmholtz Integral development of Stratton [Ref. 3], the farfield reradiated pressure may be expressed as:

$$\Phi_r = \frac{ie^{i(\omega t - kR_o)}}{2\pi R_o} \frac{\vec{K}\cdot\vec{k}_1}{K_z} \iint_L^L e^{i\vec{K}\cdot\vec{r}}\, dxdy$$

with:

$$\vec{K} = K_x\hat{x} + K_y\hat{y} + K_z\hat{z} = \vec{k}_o - \vec{k}_1$$

and other factors again as defined in Figure 1.

The irradiated area has been assumed to be an L x L aperture which is several wavelengths across.

In this research it was the spectral density of the reradiated pressure that was of interest. This may be obtained by first forming the autocovariance function,

$$R(\tau) = \langle \Phi_r(x,y,t)\ \Phi_r^*(x,y,t+\tau) \rangle$$

The autocovariance function having been found, the Wiener-Khinchin Theorem states:

$$S(\Omega) = \mathcal{F}\{R(\tau)\} = \int_{-\infty}^{\infty} R(\tau)\ e^{i\Omega\tau}\, d\tau$$

where Ω is the frequency of the reradiated (or scattered) sound.

Continuing with Parkins, and assuming that the surface irregularities are much smaller than the aperture, the expression for the spectral density of the scattered sound

is as given below. It should be noted at this point that the requirement for small surface irregularities corresponds to a roughness parameter,

$$\sqrt{g} = K_z\sigma = \frac{2\pi\sigma}{\lambda} [\cos \theta_1 + \cos \theta_2]$$

as defined by Beckmann and Spizzichino, much less than one. σ is the ocean RMS wave height, λ the acoustic wave length and θ_1 and θ_2 the angles of incidence and reflection, respectively (see Section IV.A.4 for a further discussion of $\sqrt{g}$).

The expression for the spectral density of the scattered sound is:

$$S(\Omega) = Be^{-K_z^2\sigma^2} [\delta(\Omega-\omega) \frac{16 \sin^2 K_x \ell \sin^2 K_y m}{K_x^2 K_y^2}$$

$$+ 2\ell^2 K_z^2 \sigma^2 \{[A'(K_x,K_y)]^2 \delta[\Omega-\omega-(K_x^2+K_y^2)^{\frac{1}{4}}(G)^{\frac{1}{2}}]$$

$$+ [A'(-K_x,-K_y)]^2 \delta[\Omega-\omega+(K_x^2+K_y^2)^{\frac{1}{4}}(G)^{\frac{1}{2}}]\}]$$

with: G the acceleration of gravity

A' the Neumann-Pierson directional wave spectrum

B the amplitude term

δ the Dirac delta

Parkins summarizes this equation: "....(this equation) shows the signal reradiated by a wind generated sea to have a specularly reflected component occurring at the incident frequency ω and two scattered components which are Doppler shifted by equal amounts from ω."

The spectrum of the reradiated sound is thus seen to be frequency modulated by the Doppler shift term and amplitude modulated by the wave spectrum. It is the amplitude modulation by the ocean waves that is considered in this research.

III. EXPERIMENTAL SETUP

This research was carried out using the Naval Postgraduate School OCEAN ACOUSTIC WAVE FACILITY (OAWF) with data collection and analysis accomplished with a hybrid computer setup designed by the Special Projects Group of NADC and affectionately referred to as OPHELEA (OCEAN PHYSICS ENVIRONMENT EFFECTS ANALYZER). All other equipment utilized was standard commercial electronic gear and the author feels that a detailed explanation of its functions and capabilities is unnecessary (see Equipment List - Section III.D).

A. OAWF

This facility consists of the unique combination of a wind-water tunnel and an anechoic tank (see Figures 2 and 3). Up to five 3/4 HP centrifugal fans (three in this case) comprise a Sea Exciter (Figure 4) which forces air down the wind-water tunnel, which is about 17 meters in length, generating waves which empty into an anechoic tank. The air space in the tunnel was standardized at 14.25 cm and the cross section of the entire tunnel measures about 1.2 meters square. Observation of the waves at various points along the tunnel is permitted by glass observation windows shown in Figure 5. Waves entering the 3x3x2.9 meter tank portion of the facility are constrained from diffracting by a plexiglass restraining barrier and are terminated by a

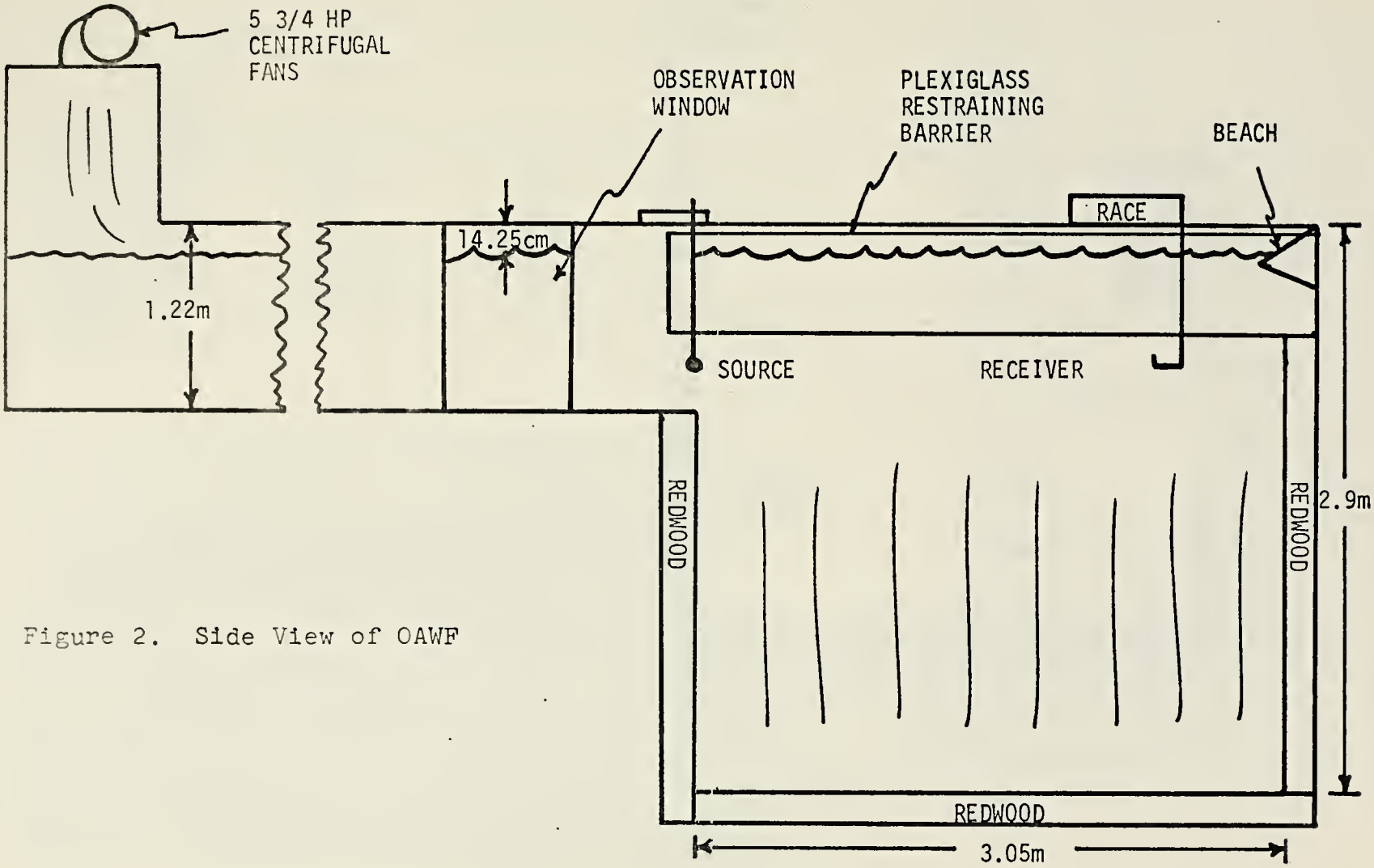

Figure 2. Side View of OAWF

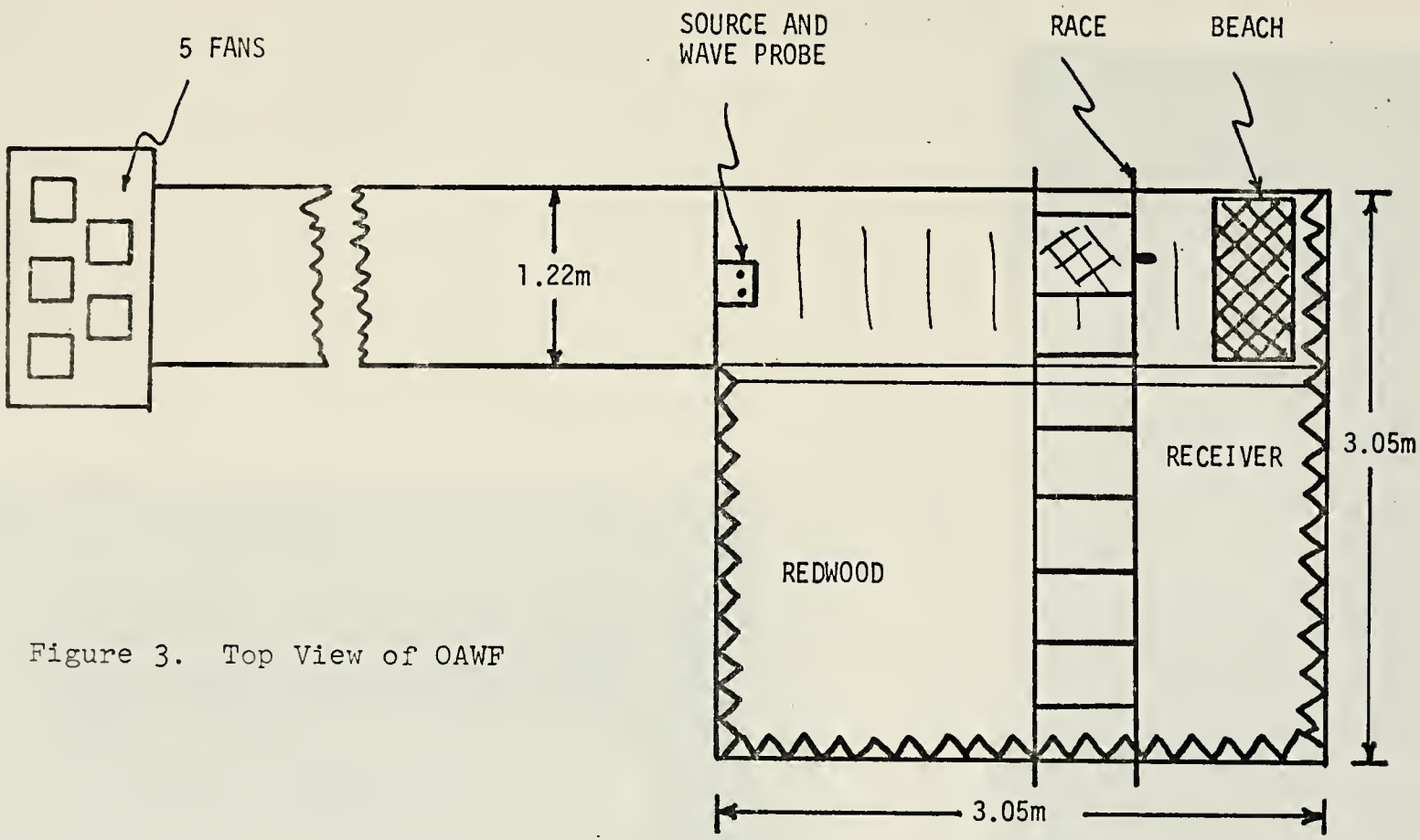

Figure 3. Top View of OAWF

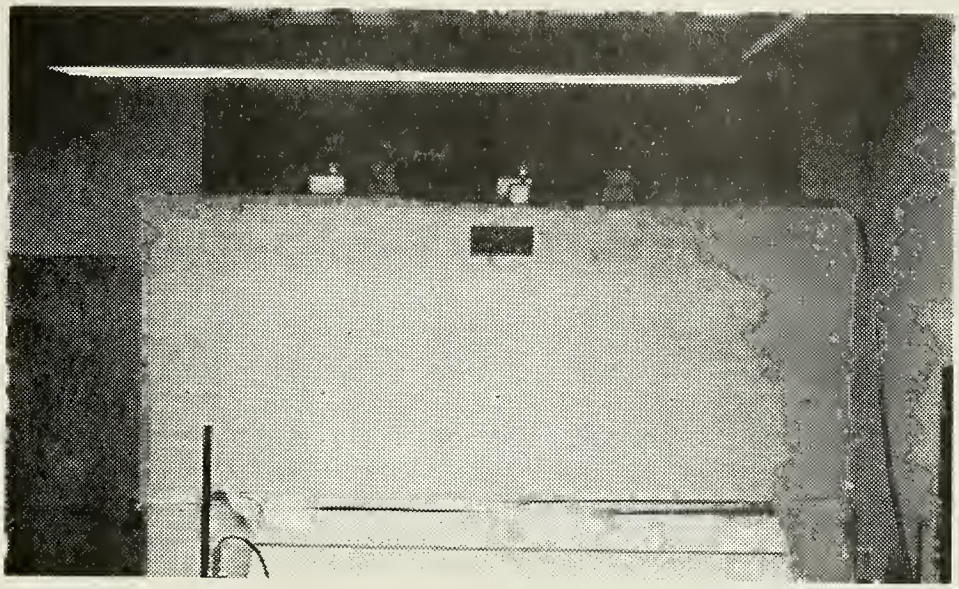

Figure 4. OAWF Sea Exciter

Figure 5.

OAWF Observation Window

"beach" to prevent reflections. The beach spans the width of the tank experimental area and consists of a screen covered wedge filled with stainless steel millings which cause incident waves to dissipate rather than reflect. The tank itself is lined with redwood 4x4's on all sides and the bottom which ensures excellent sound absorption at the boundaries as pointed out in Ref. 4. These redwood beams are oriented with a corner facing toward the tank interior, except on the wall bordering the waves which is flat, to further increase absorption. A movable race permits two-dimensional positioning of transducers to within one centimeter. This facility models the real ocean on a scale of about 50-1 and is shown in operation in Figures 6 through 8.

B. OPHELEA

The OPHELEA system consists of essentially three components which are interfaced to provide high speed analog to digital data collection and digital data processing with somewhat slower display. The design was developed by the Special Projects Section of the Naval Air Development Center in conjunction with Pinkerton Computer Consultants Inc., of Warminster, Pennsylvania. The three components are shown in Figure 9 and described below.

1. Interdata Model 70 Computer

This minicomputer is modularly constructed and features LSI and other state-of-the-art computer technology.

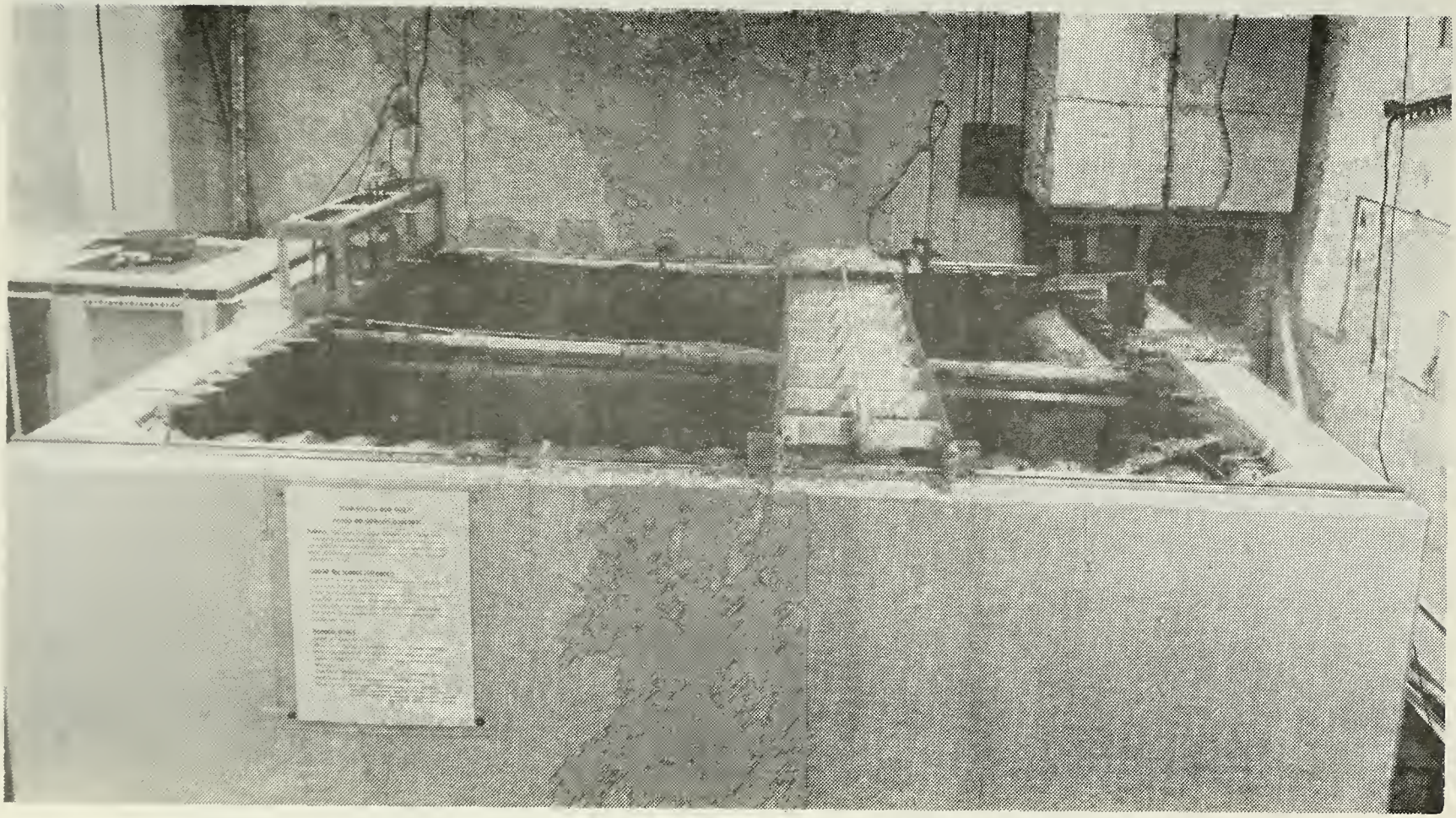

Figure 6. OAWF, Looking Down into Anechoic Tank

Figure 7. OAWF in Operation with Wave Peaks Shown Against the Plexiglass Restraining Barrier

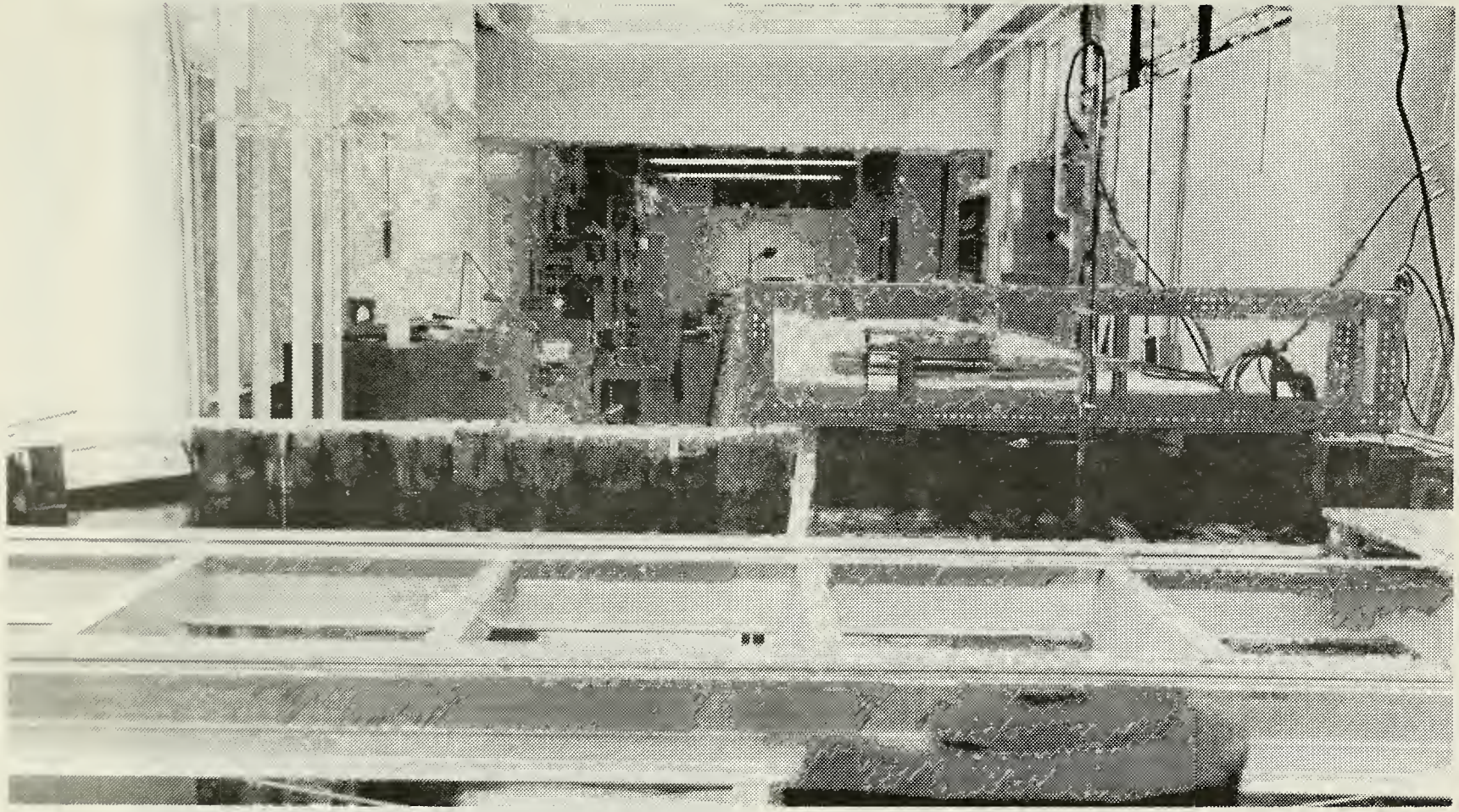

Figure 8. OAWF, Looking from the Tank Back up the Wind/Wave Tunnel Toward the Sea Exciter

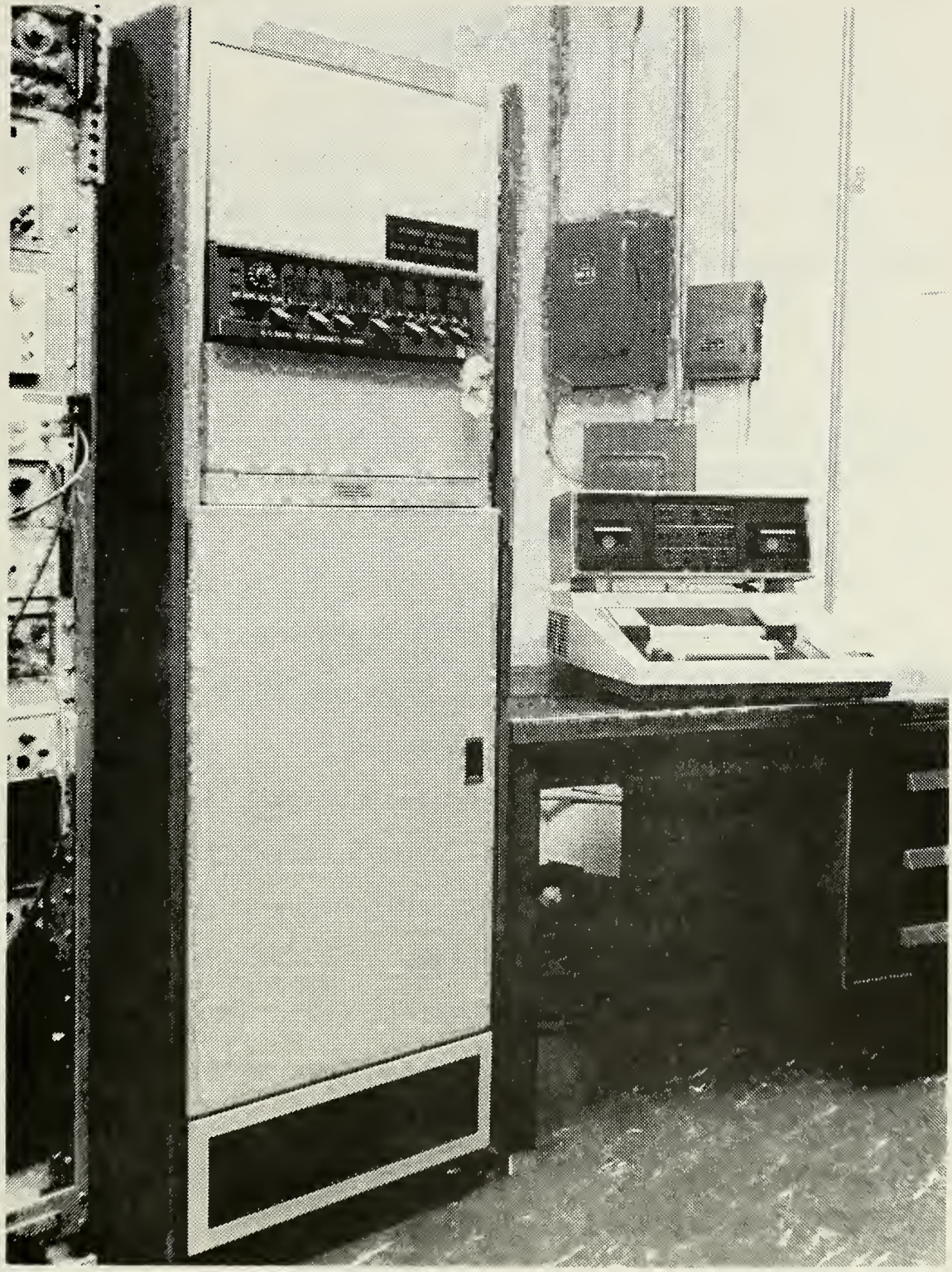

Figure 9. The OPHELEA System with Computer and A/D Converter in Large Cabinet to the Left

It is a 16 Bit half-word oriented digital computer that is FORTRAN programmable and has sufficient memory (32 thousand 8-bit bytes) capacity to process in excess of 8000 data points with an average size program. In this research it was programmed to perform a Fast Fourier Transform on input data and output spectral density vs. frequency. Some statistical analysis was also performed. This minicomputer occupies the upper half of the large cabinet shown in Figure 9.

2. Phoenix Analog to Digital Converters Model ADC 712

Two ADC 712 converters may be used separately or simultaneously. Each A/D converter is a high speed device capable of encoding up to ±10 volt input signals into 12 bits (11 bits + sign) of data, providing resolution to one part in 4095 (accuracy of 5mv in 20v). The maximum rate of conversion is 6.5 microseconds and it has performed reliably at a sampling rate of up to 300kHz. The A/D is driven by a "command to convert" signal consisting of a 5 volt positive pulse of at least 200 microseconds duration which is supplied by an external oscillator. Measurement is accomplished by successive comparisons against an internal reference voltage after which the value is converted to a digital number. The A/D converters are located in part of the lower half of the OPHELEA cabinet.

3. Texas Instruments Silent 700 Electronic Data Terminal Model 733

The TI 733 consists of a keyboard which is used as a programming and input/output control device, a printer which outputs data or answers queries of the computer on heat sensitive paper and a play back and record section which is used to read in computer programs and record/playback data. In this research, due to storage limitations, data were sometimes taken A/D, read out to tape cassettes, then reread in for processing after the appropriate program had been loaded. A capability of interfacing with the IBM-360/67 CP/CMS system, allowing direct access to the NPS computer facility, was also utilized in processing some statistical wave height information.

C. SEQUENCE OF OPERATION

The sequence of operation used most often in this research was as follows:

1. An analog signal (varying sound pressure, instantaneous wave height, etc.) was input to the A/D converter which, being triggered at twice the Nyquist rate (a value found to result in minimal aliasing effects), converted it to digital data.

2. Those data were then either:

   a. directly processed by the appropriate program which had been installed in the computer, or,

   b. read out to tape cassettes for later analysis as described above.

3. Reduced data and desired results were displayed on the paper readout of the terminal. Figure 10 is a pictorial description of this process.

D. EQUIPMENT LIST

In order to avoid needless repetition of the lengthy manufacturers' names for electronic equipment throughout this work, a number of abbreviations will be used instead. These short titles will be employed for the most part in block diagrams and schematics but may also appear in the text. The abbreviations, with the corresponding full equipment title/description are as listed below:

ABBREVIATION	MANUFACTURERS TITLE
CORRELATION COMPUTER	Princeton Applied Research Model 101 Correlation Function Computer
DC POWER SUPPLY	Hewlett-Packard Model 721A DC Power Supply
G.R. OSCILLATOR	General Radio Model 1312 Decade Oscillator
HP PRECISION AMP	Hewlett-Packard Model 463A Precision Amplifier
HP POWER AMP	Hewlett-Packard Model 467A Power Amplifier
KH FILTER-3342	Khron-Hite Model 3342 Filter
KH FILTER-3550	Khron-Hite Model 3350 Filter
O'SCOPE	Tektronix, Inc. Model 545B Oscilloscope

ABBREVIATION	MANUFACTURERS TITLE
PAR PREAMP	Princeton Applied Research Model 113 PreAmplifier (Note: HFRO and LFRO refer to the High/Low frequency roll off feature of the preamp – a filtering option)
WAVETEK 142	Wavetek Model 142 HF VCG Generator
WAVETEK 144	Wavetek Model 144 HF VCG Generator
X-Y RECORDER	Varian Aerograph Model F-100 Strip Chart Recorder

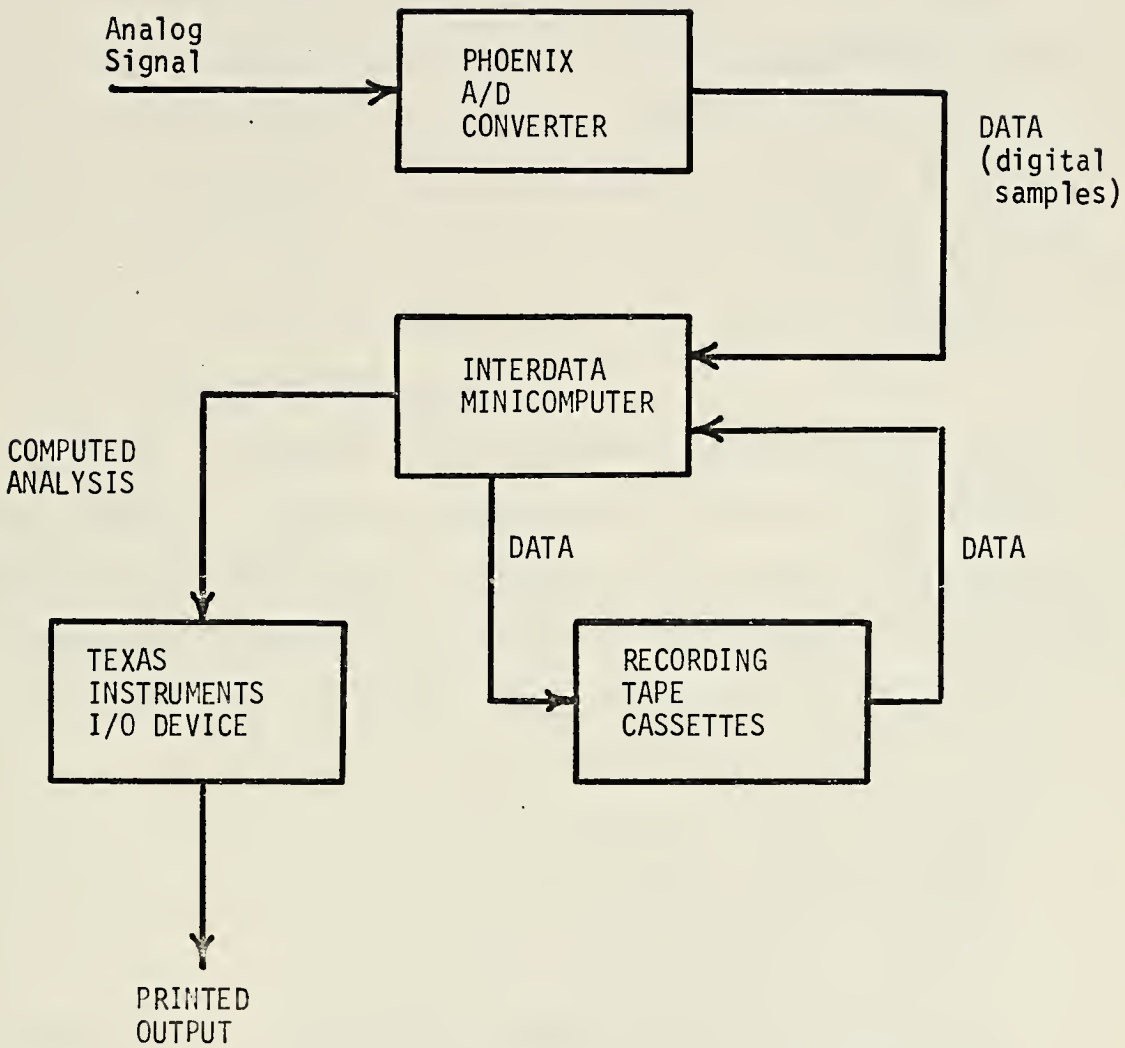

Figure 10. Data Processing Sequence

IV. EXPERIMENTAL PROCEDURES AND RESULTS

A. OAWF CHARACTERISTICS

In order both to ensure the validity of the research to follow and to gain an insight into the significant parameters affecting the scattering of sound from a real or model ocean, several preliminary experiments were conducted. In the sections that follow each will be fully discussed with setup diagrams, procedural explanations and results included.

1. Frequency Spectrum

In determining the frequency spectrum of the ocean wave heights, a highly linear probe designed at the Civil Engineering Department of Stanford University and pictured in Figures 11 and 12 was utilized. The probe is capacitive in nature, with a covered wire as the sensor. The wire serves as one electrode, the water as the other and the insulation is the dielectric of the capacitive element. The probe is excited by a 2.4 kHz sinusoidal carrier (amplitude 4.5 volts peak to peak). When the probe is immersed in the water wave system the output across a capacitive bridge (Figure 13) is amplitude modulated by the passing waves rising and falling around the wire and thereby changing the effective length of the capacitor. This AM signal is demodulated by the detector shown in Figure 14 and the resultant time varying DC signal, a replica of the instantaneous wave height at one point, is frequency analyzed by the OPHELEA system.

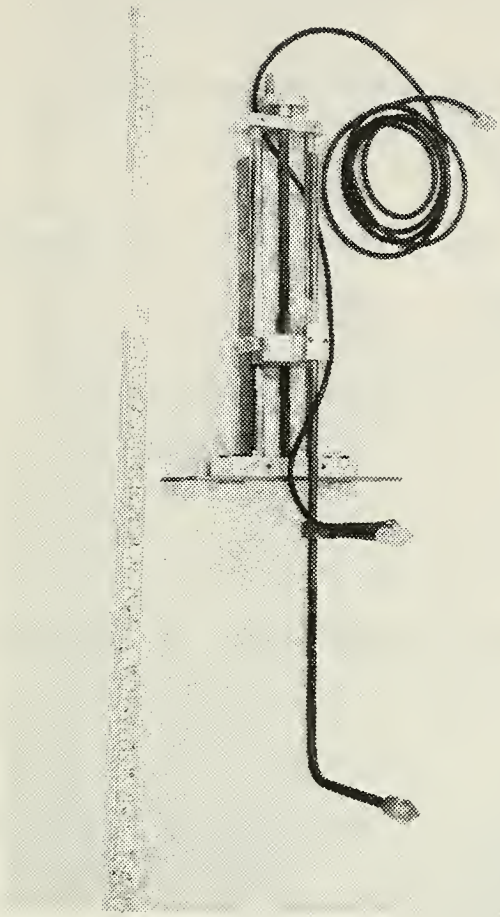

Figure 11. Stanford Wave Probe

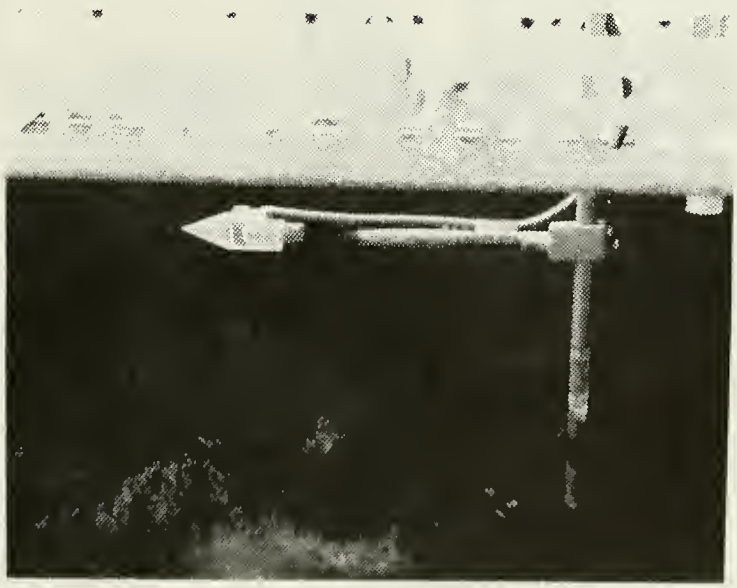

Figure 12.

Wave Probe in Operation

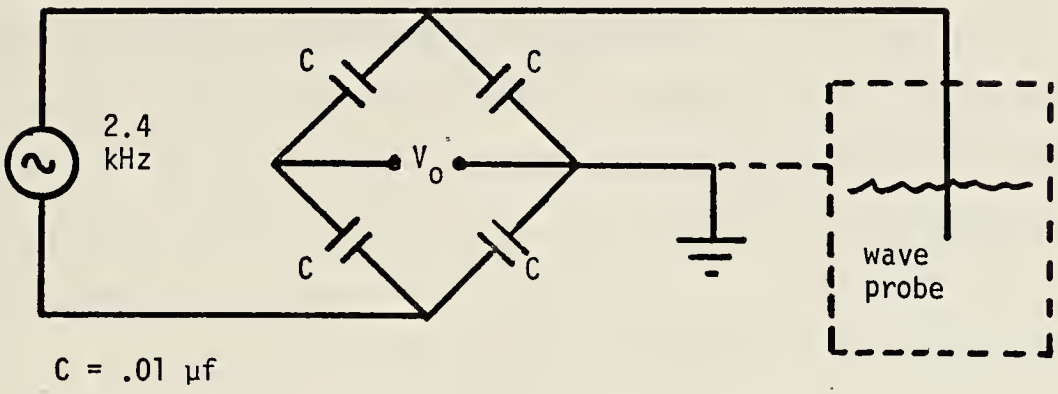

Figure 13. Wave Height Capacitive Bridge

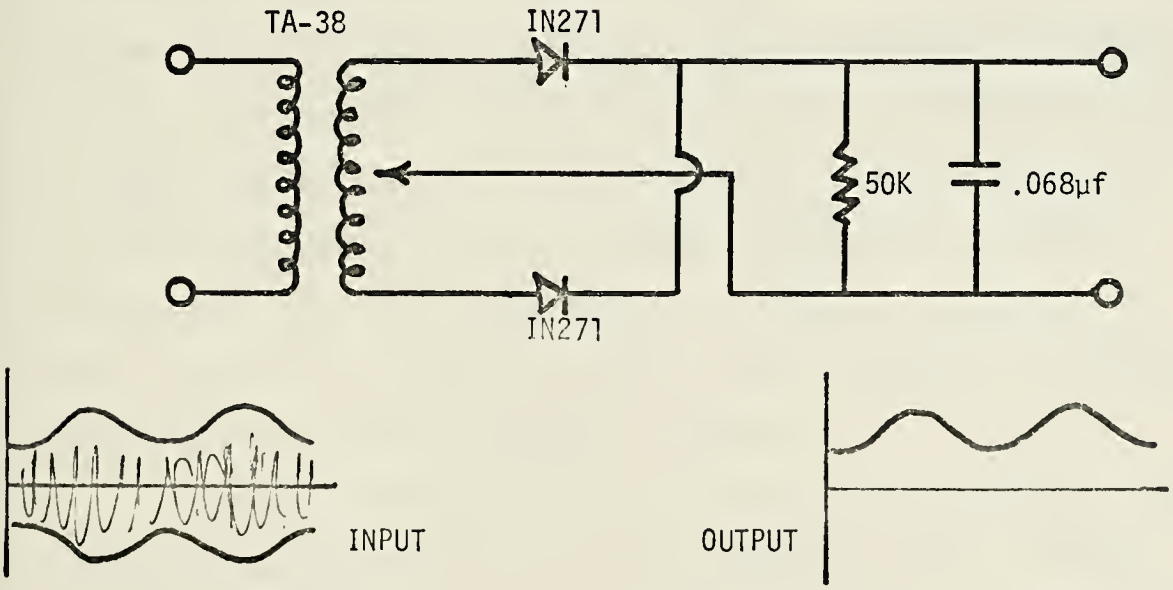

Figure 14. Wave Height Detector (Demodulator)

As noted above frequency analysis was accomplished by the OPHELEA system, using a program called PING 1C, a copy of which is included in Appendix A. In this case the program called for taking 256 A/D samples at a sampling rate of 20 Hz and computing a 128-point spectral density versus frequency output. These parameters provide a frequency resolution of greater than .08 Hz.

When taking A/D samples at sampling frequencies in excess of 20 kHz, a sinusoidal oscillator which is half-wave rectified by computer circuitry was used to provide the "command-to-convert" pulse train. At low frequencies however the sinusoidal pulse duration is too great and erroneous multiple triggering of the A/D converter results. Therefore the WAVETEK 144, with a positive pulse waveform and with its asymmetry control set for minimum pulse duration, was employed for the low sampling frequencies required for finding spectra of wave and demodulated scattered sound. A block diagram of the experimental setup is shown in Figure 15 and the normalized spectral density plot is shown in Figure 16. This plot is the average of forty runs conducted as outlined above (i.e., 40-128 point FFT analyses).

As can be seen from the figure, the predominant OAWF ocean frequency is about 2.5Hz as compared with a typical actual ocean frequency on the order of 0.1Hz. Though neither ocean is monochromatic, the OAWF spectrum is fairly narrow. Its bandwidth is about 0.6Hz at the half power points and

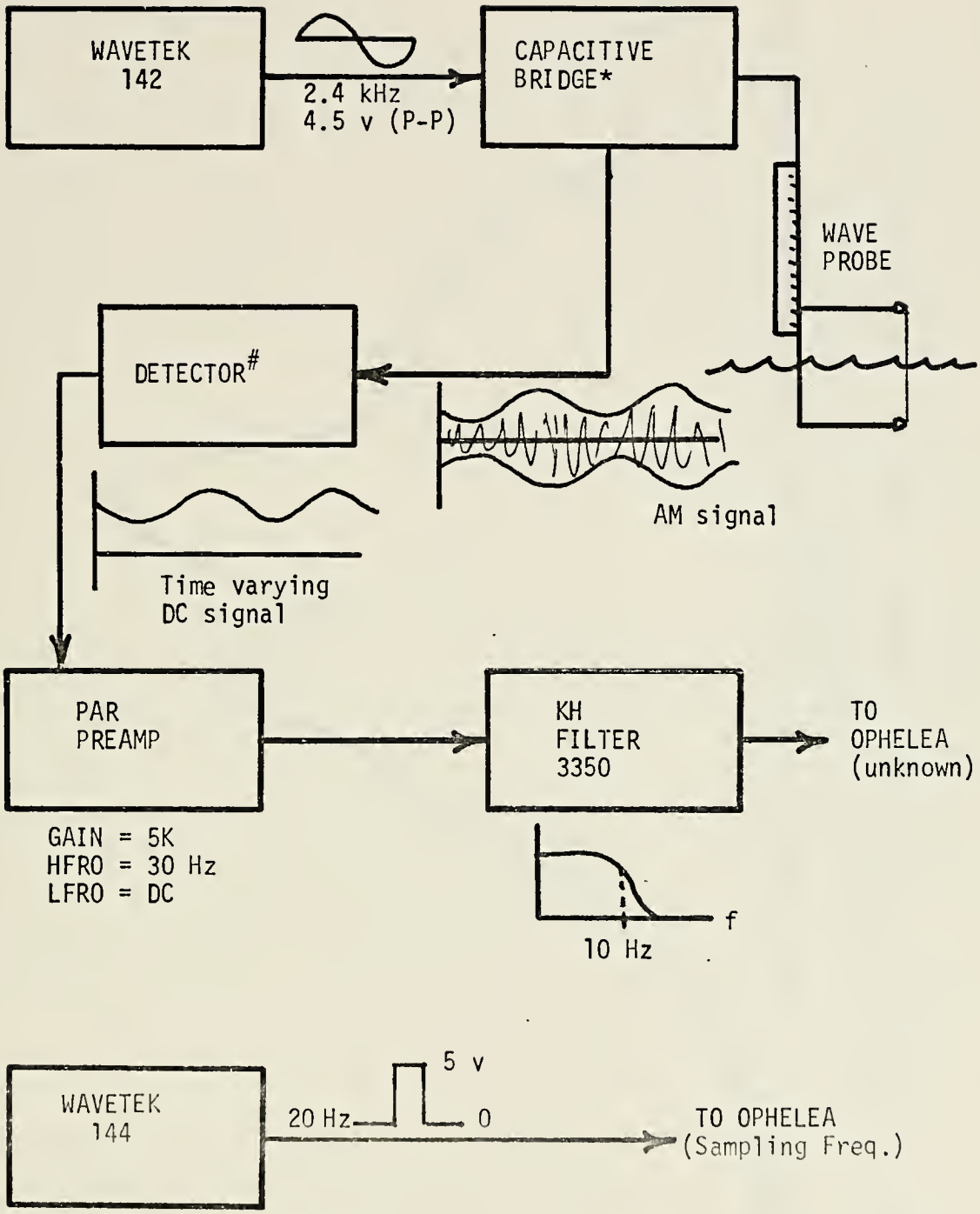

* See Figure 13
\# See Figure 14

Figure 15. Experimental Setup for Determining OAWF Surface Wave Spectrum

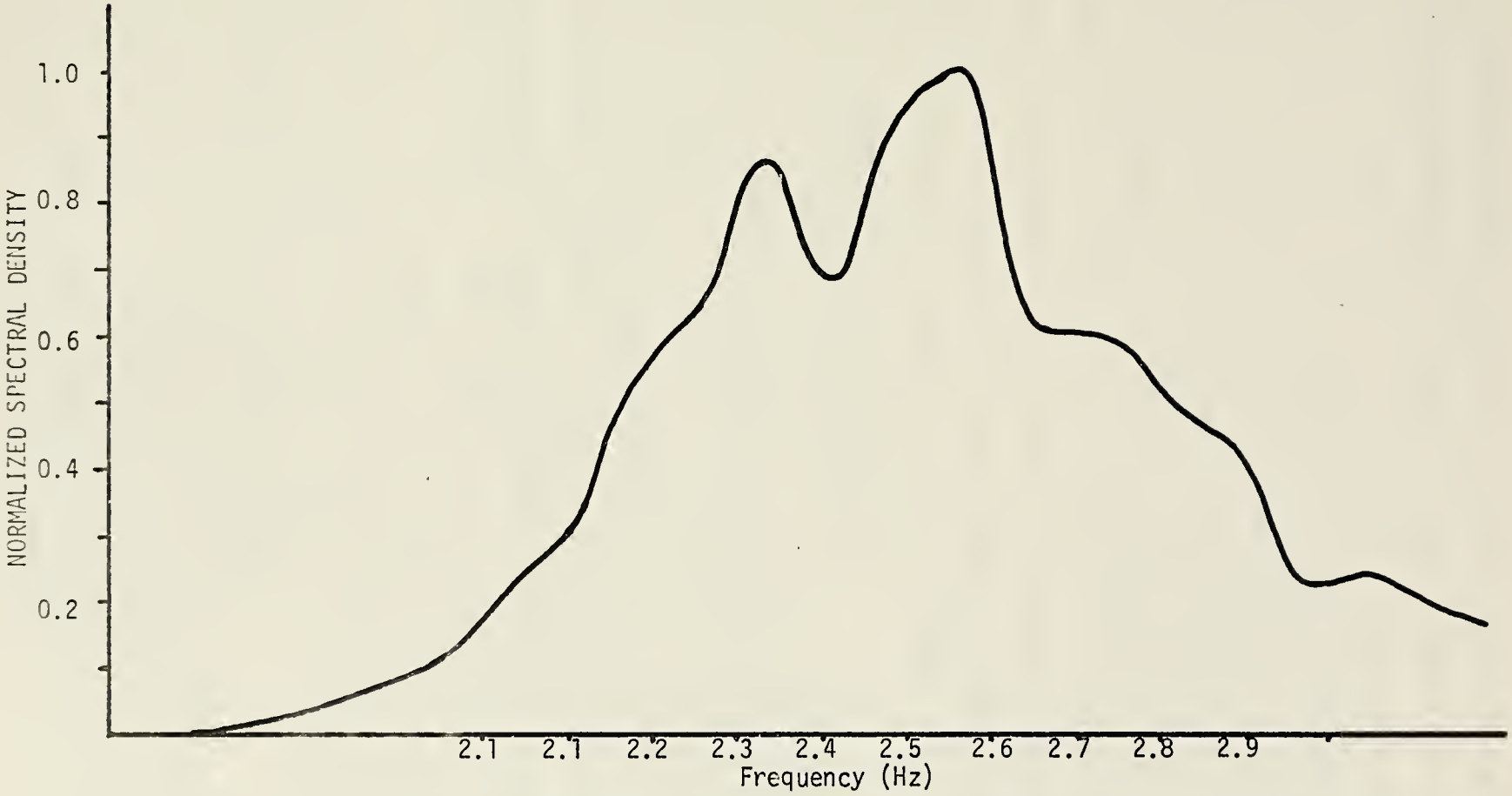

Figure 16. Normalized Wave Height Frequency Spectrum (Average of 40 Runs)

the spectral density tends to fall off less rapidly toward higher frequencies than does the actual ocean spectrum [Ref. 5]. This is due to the greater contribution of capillary waves in the OAWF waves. The irregularity at about 2.4Hz was felt at first to be merely a coincidental artifact which would disappear with additional averaging. However, though it smoothed some, it has persisted. The source of the irregularity may have been lack of adequate fetch for wave growth to an equilibrium spectrum. It is noted that a similar effect was observed in the work of Fowler and Scheibel [Ref. 6] at short fetch.

2. Probability Density Function

As Kinsman has noted [Ref. 7] the probability density function associated with wind driven ocean wave heights is nearly Gaussian. In order to verify that the OAWF sea met this criterion, wave height samples were collected using the setup shown in Figure 15 of the previous section and analysis was accomplished using the standard IBM-360/67 Library program "HISTF". This process was accomplished as follows:

a. Eight groups of 1024 wave height samples were taken from the previously described wave probe using the OPHELEA system and a program modestly entitled PERK 1A and were stored in the minicomputer memory.

b. The data were then read out to tape cassettes in a revised format compatible with the IBM-360 CP/CMS system.

c. Data were converted to punch cards using the CP/CMS system and analyzed using "HISTF".

The "HISTF" program outputs various statistical parameters and plots a histogram of the input data. Each of the eight data groups was analyzed and the results averaged. A graph of the resulting average histogram, as well as a comparable normalized Gaussian PDF, is shown in Figure 17. As can be seen, the histogram distribution is slightly skewed and displays negative kurtosis. Though not exactly agreeing with any one of Kinsman's seas, the variations are slight as is shown by the following comparison:

	Kinsman - record 072	OAWF - 3 Fans
Skewness	+.092	-.0245
Kurtosis	-.031	-.3549

The mean is also seen to be non-zero but is less than 0.1 centimeter.

3. Autocorrelation Function

The autocorrelation function of the ocean wave heights is characteristically that of band limited noise and takes the shape of an attenuated cosine [Ref. 8]. In finding the correlation function of the OAWF three fan ocean, essentially the same setup was used as in the previous two sections. However the output from the wave probe, characterizing the surface, was terminated, not in the OPHELEA system as before, but in a PAR CORRELATOR. This device is capable of computing either auto- or cross-correlation functions and displaying the result on an

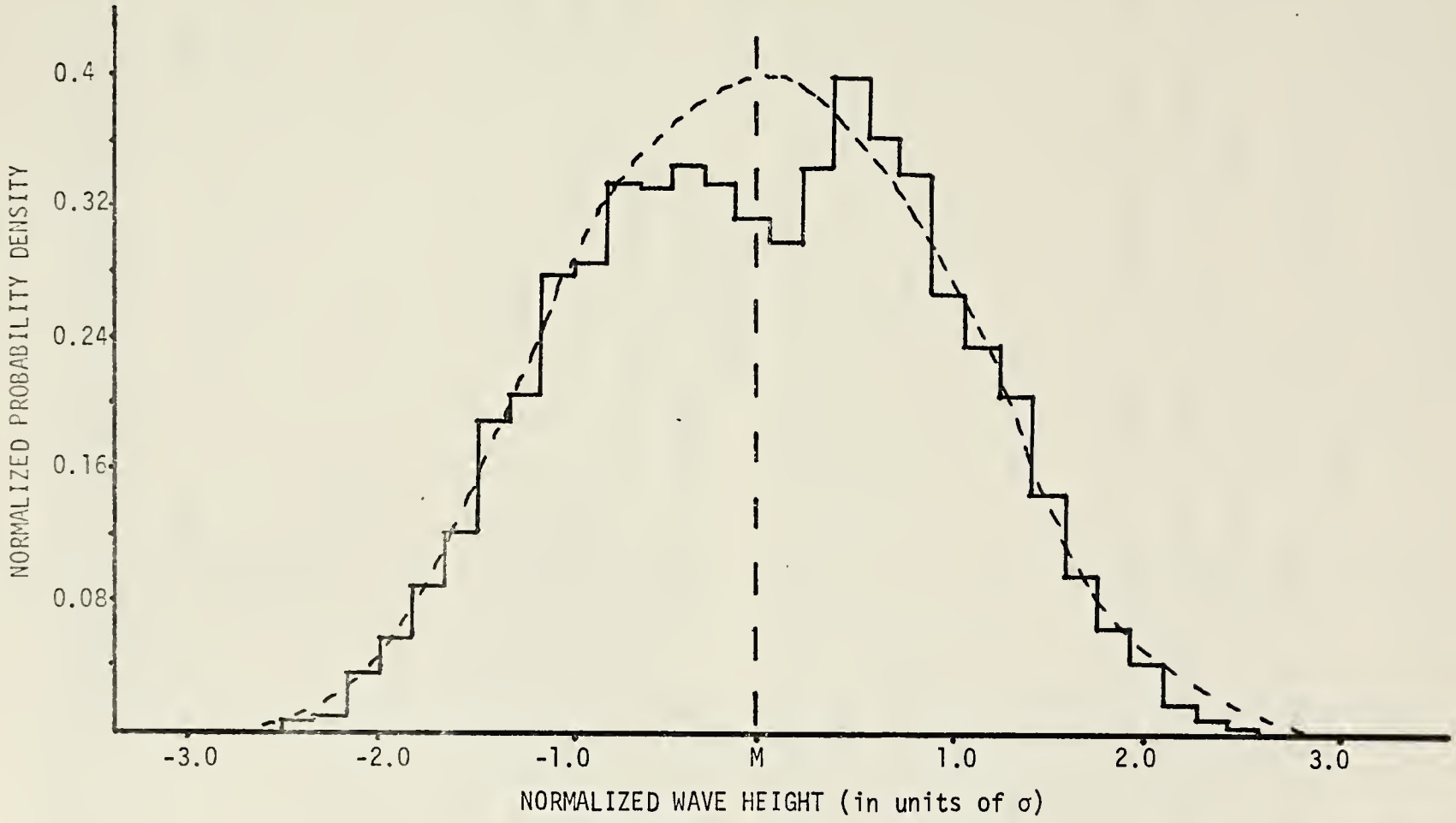

Figure 17. Wave Height Histogram and Corresponding Normalized Gaussian PDF

oscilloscope or a recorder. In this case an X-Y RECORDER was used. A diagram of the experimental setup is shown in Figure 18.

An average surface wave height correlation function for time lags, τ = 0.0 to 2.0 seconds, was arrived at by superimposing the eleven runs printed on the X-Y RECORDER and shown in Figure 19. The resultant average is shown in Figure 20 and can be seen to follow the expected form. The rate of "attenuation" is initially somewhat less than measured by Kinsman, with the OAWF correlation at the first peak down to 0.7 compared to 0.50 for Kinsman's ocean data. The second peak correlation conversely has dropped to about 0.3 while Kinsman's $C(\tau)$ remains at about 0.4 after time lags of two ocean periods.

The correlation function loses its consistency after two ocean periods as may be seen from Figures 19 and 21. Figure 21 shows the function computed with a precomputation period = T = 2.0 seconds set into the PAR CORRELATOR. With this setting the correlation function is computed for τ=2.0 to 4.0 seconds or in effect the function of Figure 19 is continued for another two seconds. For this longer time lag, it is difficult to see any repeatability in successive correlation functions.

While the OAWF values are somewhat different from those of the Kinsman ocean, the similarity in shape is obvious. This validation of the ocean model will be of importance

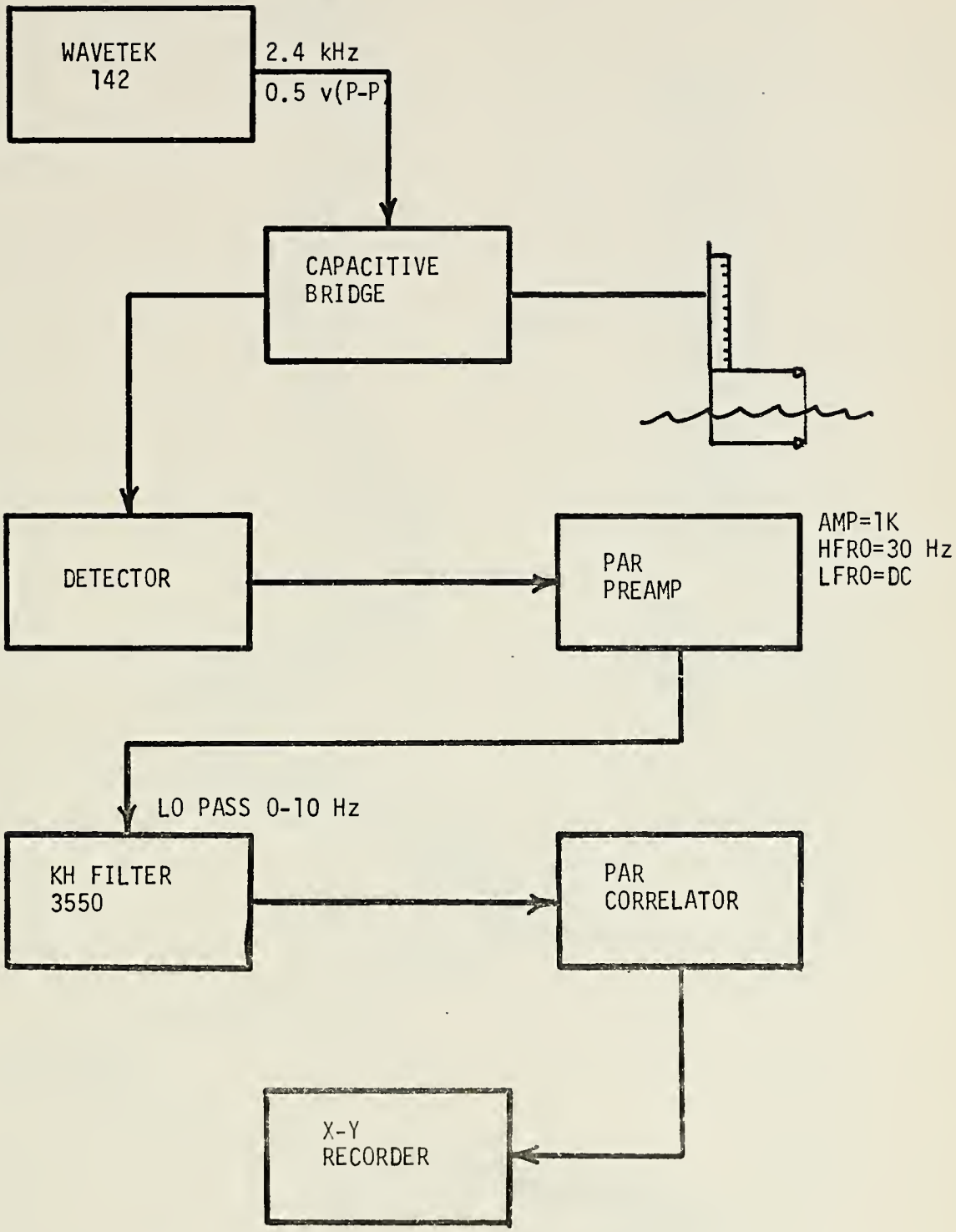

Figure 18. Experimental Setup for Determining the OAWF Surface Wave Autocorrelation Function

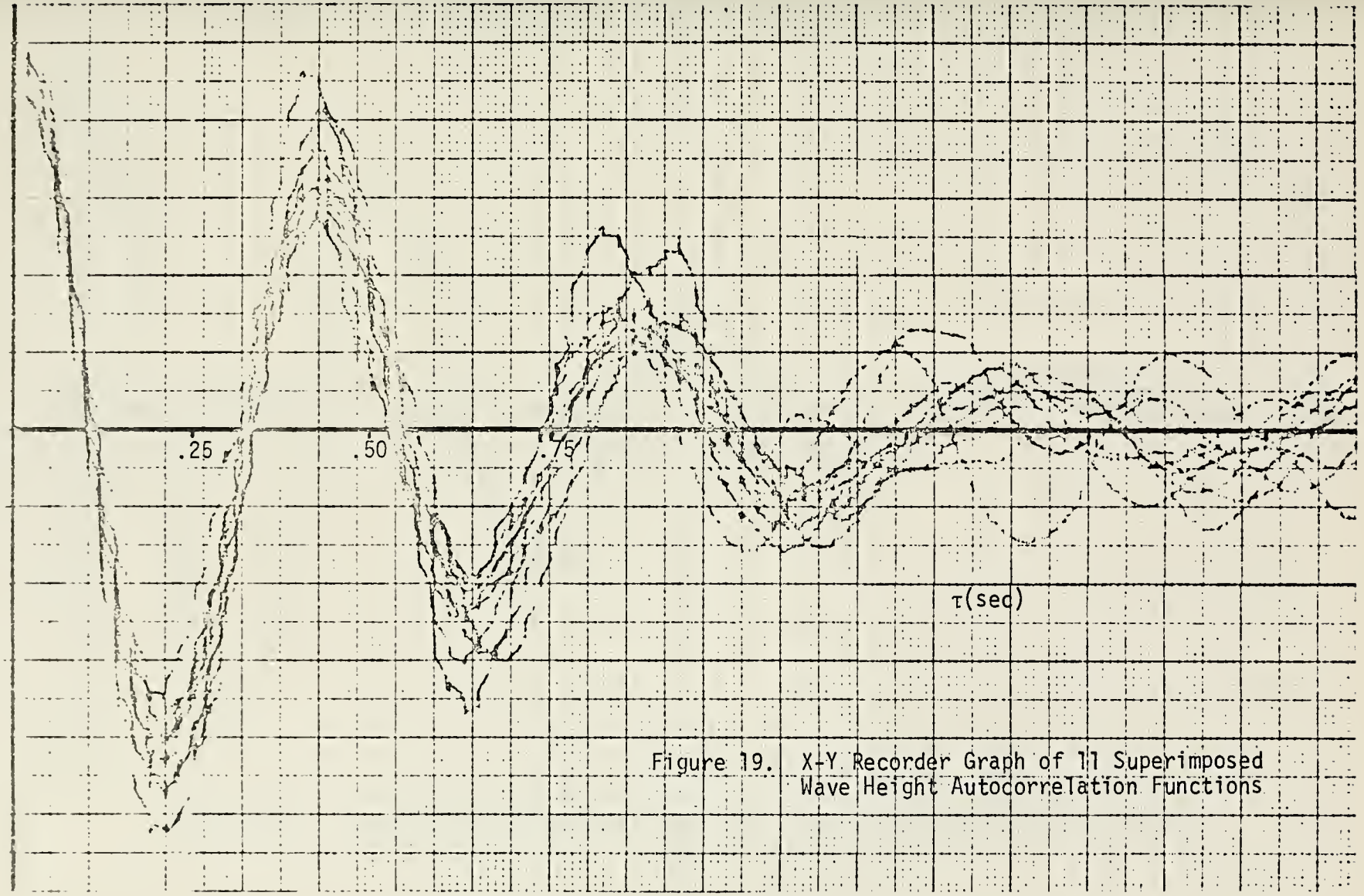

Figure 19. X-Y Recorder Graph of 11 Superimposed Wave Height Autocorrelation Functions

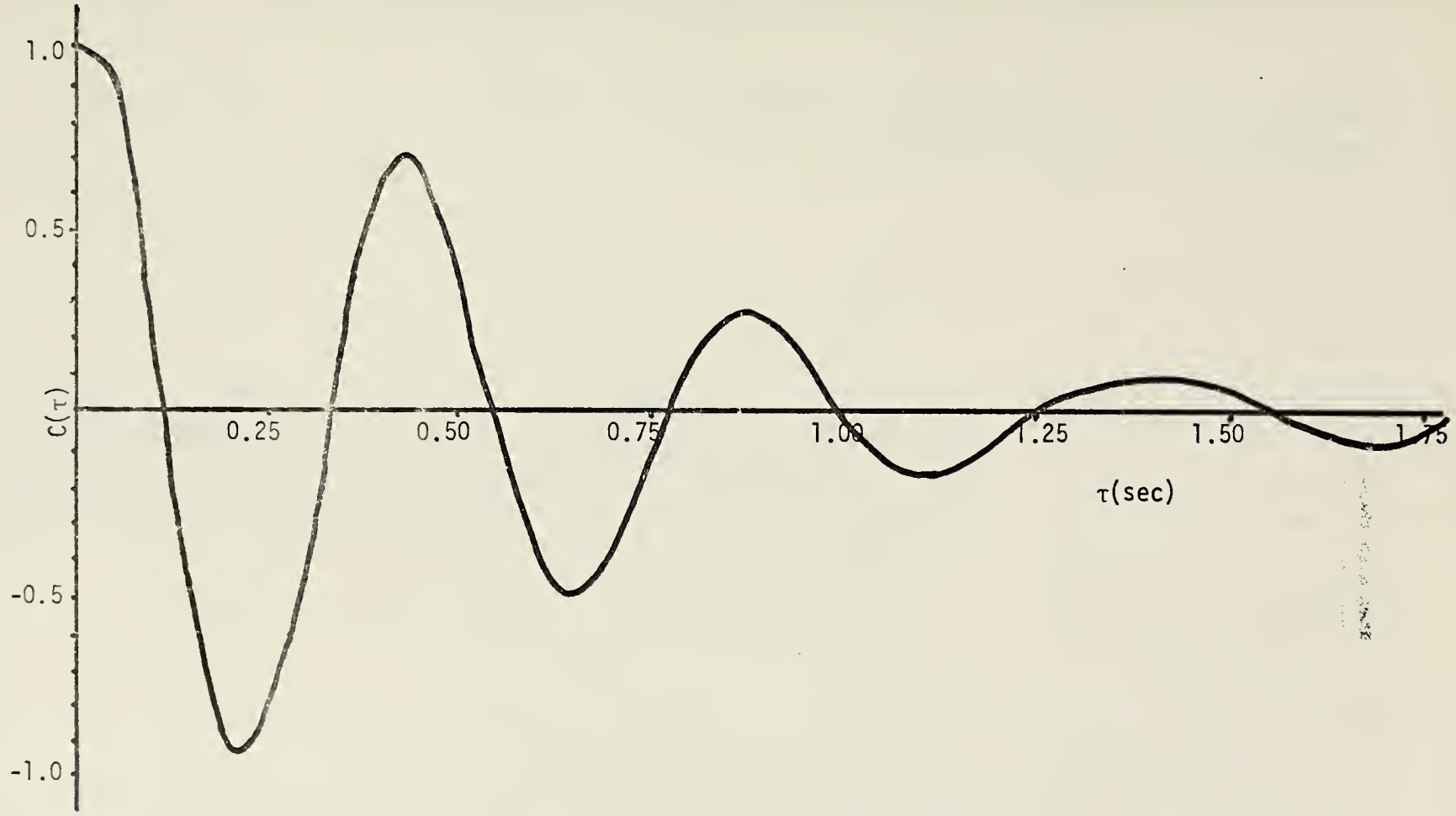

Figure 20. Average OAWF Surface Wave Height Autocorrelation Function

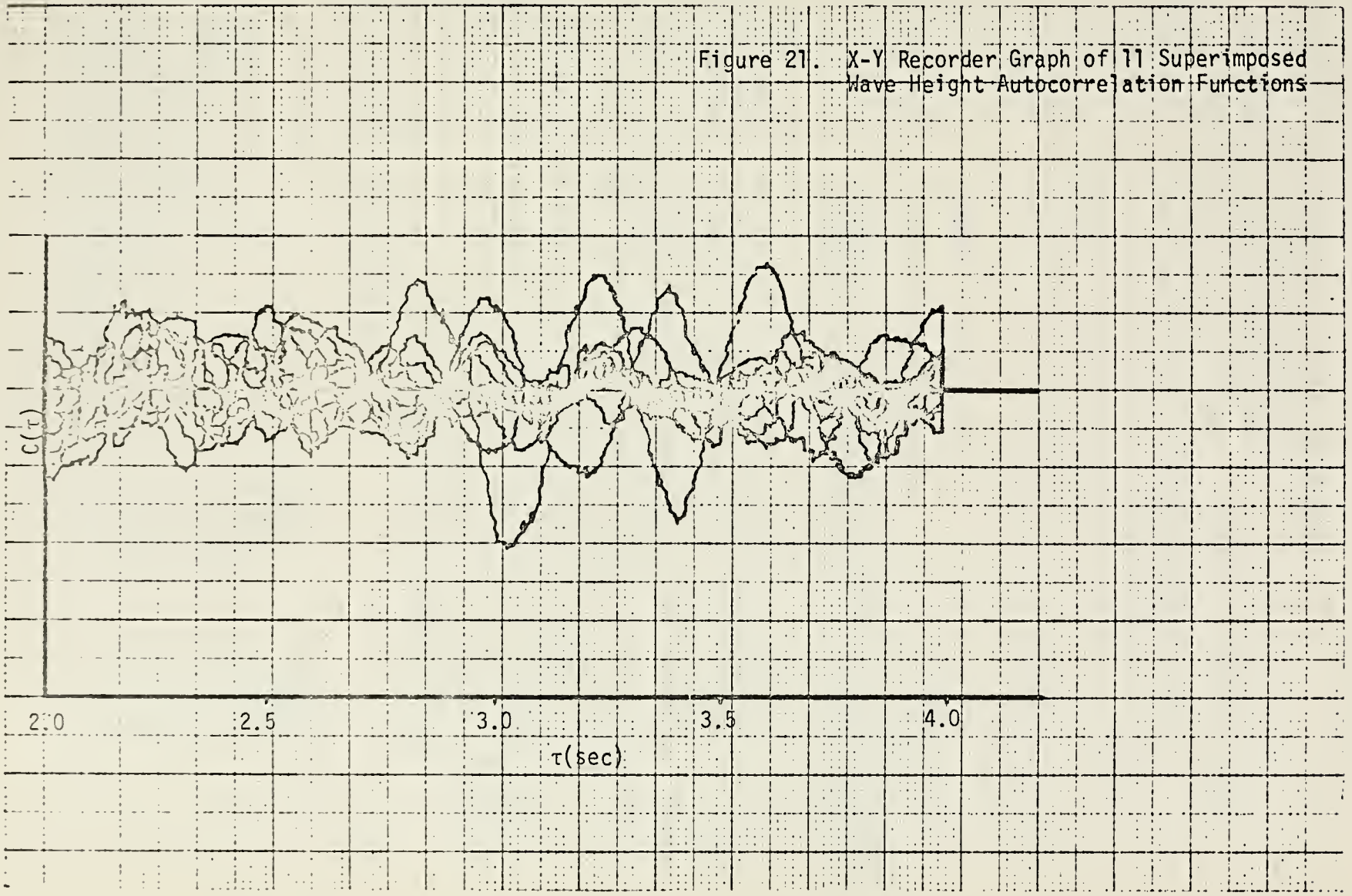

Figure 21. X-Y Recorder Graph of 11 Superimposed Wave Height Autocorrelation Functions

later in this work when comparisons are made with the modulation envelope of scattered sound.

4. The Roughness Parameter

The previously mentioned roughness parameter, $\sqrt{g}$, is defined by Beckmann and Spizzichino [Ref. 2] as:

$$\sqrt{g} = \frac{2\pi\sigma}{\lambda} [\cos \theta_1 + \cos \theta_2]$$

with σ = ocean RMS wave height

λ = acoustic wave length

θ_1, θ_2 = angles of incidence and reflection, respectively (measured from the normal to the ocean surface).

It is easily seen that a "smooth" condition ($\sqrt{g} << 1$) can be achieved through use of low acoustic frequencies or large angles of incidence (shallow grazing angles) as well as with the obvious small RMS surface wave heights. The converse is of course also true for "rough" conditions ($\sqrt{g} >> 1$). $\sqrt{g}$ was the factor that was used to model the OAWF ocean to the actual ocean in later research and an example of typical sets of conditions in both domains yielding the same $\sqrt{g} = .076$ is given below:

	OAWF	OCEAN
Wind	3 Fans	20 KTS
RMS wave height	.7 cm	54 cm
Acoustic Frequency	13 kHz	300 Hz
Source/Rcvr Depth	10 cm	200 m
Source/Rcvr Separation	150 cm	7000 m

As noted above $\sqrt{g}$ is the same for both sets of parameters and thus the typical ocean conditions noted in the right column can be reproduced if the values in the left column are employed in the OAWF.

B. COMPARISON OF WAVE HEIGHT AND DEMODULATED SCATTERED SOUND SPECTRA AND CORRELATION FUNCTIONS

As noted in the Theory section the frequency spectrum of the amplitude modulation of the scattered sound is directly related to the frequency spectrum of the wind driven waves. Hence it is important to compare these frequency spectra. Further it is of interest to compare autocorrelation functions in order to gain an insight into signal processing possibilities. In addition to these two comparisons the cross correlation function was computed.

1. Frequency Spectra Comparison

Though some trials described later in this work were conducted with a directional source, the principal study used an omnidirectional source and receiver, which were felt to best model the submarine/sonobuoy scenario. The source was a locally-constructed transducer made from a 2" (o.d.) Glennite Ceramic sphere which was covered with several coats of neopreme. This source transducer will be referred to hereafter as "OMNI". The receiver was a standard Atlantic Research LC-10 hydrophone and its response was immediately amplified by 30 dB, NUS Corporation FET preamp powered by a 12 volt DC POWER SUPPLY. Both the LC-10/NUS combination

and the OMNI, as well as a directional piston type transducer (F-27) used later, are shown in Figure 22.

As the spectra of the OAWF sea waves had already been computed from an average of forty runs, only the average sound amplitude modulation spectrum remained to be determined. To accomplish this the scattered AM sound was demodulated by the detector shown in Figure 14 and the resulting time-varying DC signal sent to the OPHELEA system. A photograph of the wave forms of the AM scattered sound, the demodulated scattered sound and the instantaneous wave height are shown in Figures 23 and 24. A complete schematic of the experimental setup is shown in Figure 25.

Forty runs were conducted with 256 A/D samples of the demodulated acoustic 20 kHz signal being taken for each run at a sampling frequency of 20 Hz, again using program PING 1C. As before, a 128-point spectral density versus frequency readout was calculated for each run and the resulting forty spectra averaged and normalized for comparisons with the previously determined average wave spectrum. These two averaged, normalized spectra are plotted in Figure 26 which shows the obvious similarity. The demodulated sound spectrum has a shape that is remarkably similar to its counterpart though its peaks are about 0.2 Hz less than the predominant wave frequencies. This difference is presumably due to the surface drift velocity [Ref. 9]. The 3 dB bandwidth of the demodulated sound spectrum is about 0.5 Hz as compared with 0.6 Hz for the wave spectrum.

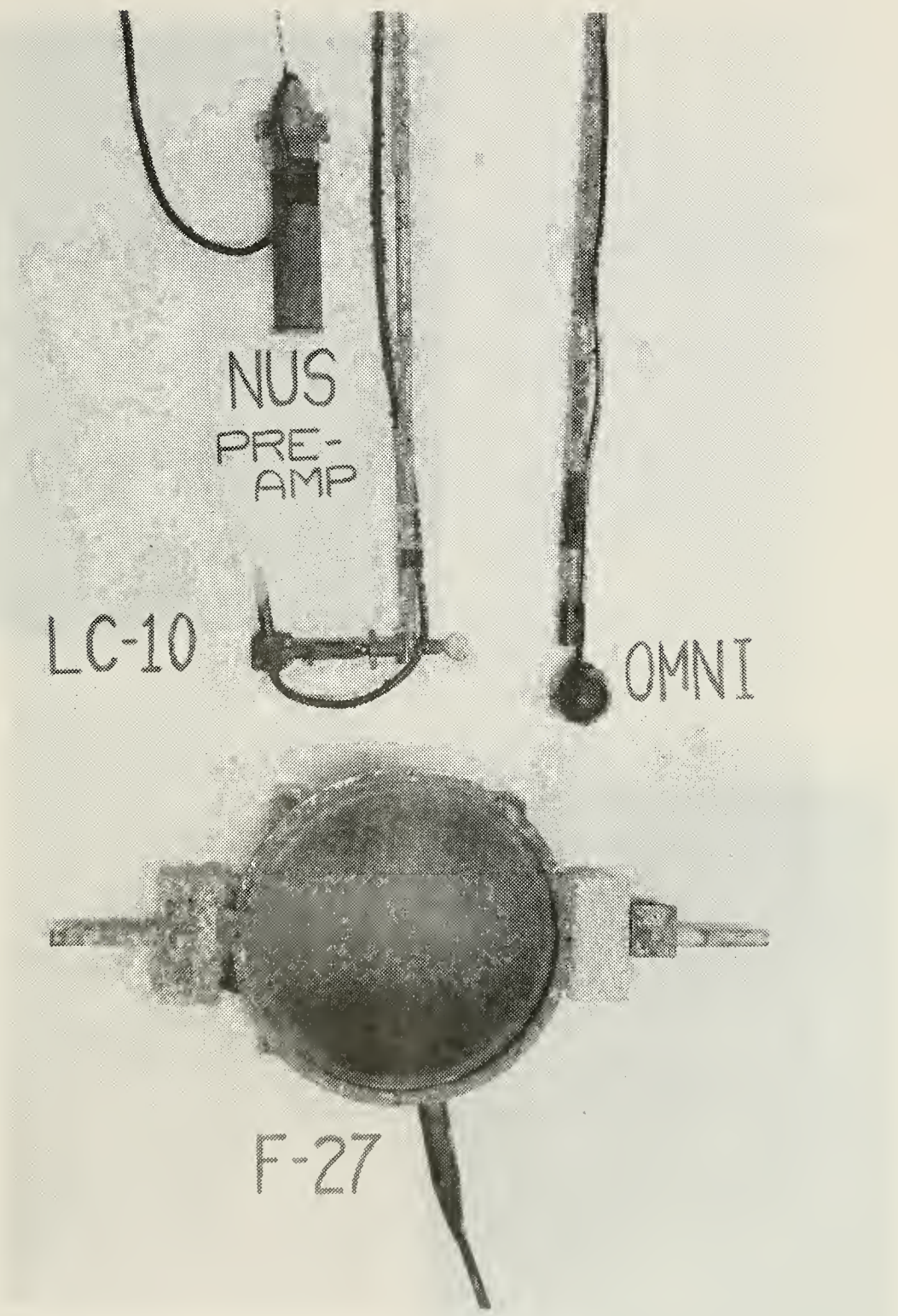

Figure 22. Hydrophone (LC-10) and Transducers Used in this Research

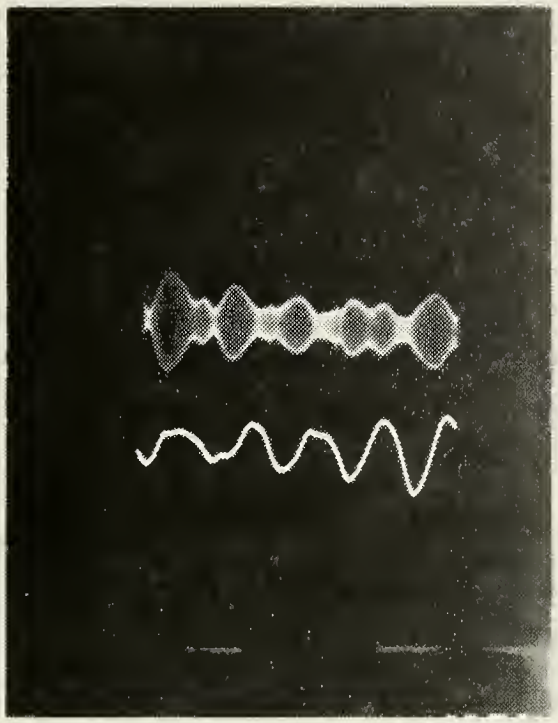

Figure 23.

Amplitude Modulated Sound (top) and Instantaneous Wave Height

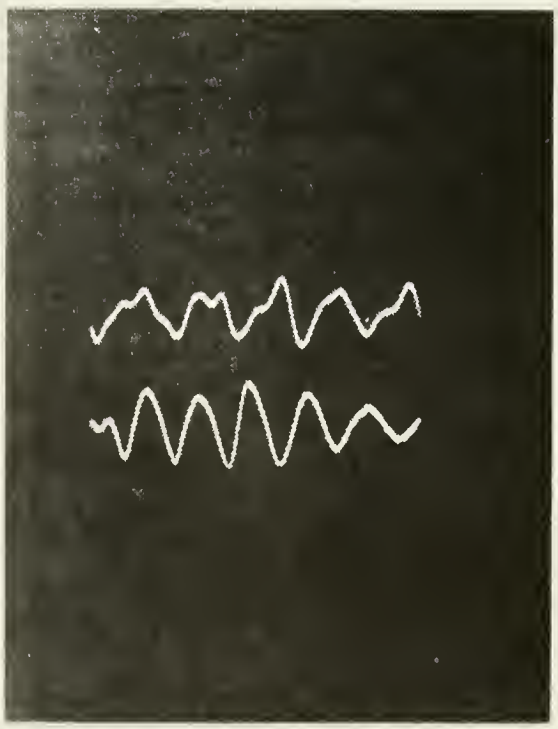

Figure 24.

Demodulated AM Sound (top) and Instantaneous Wave Height

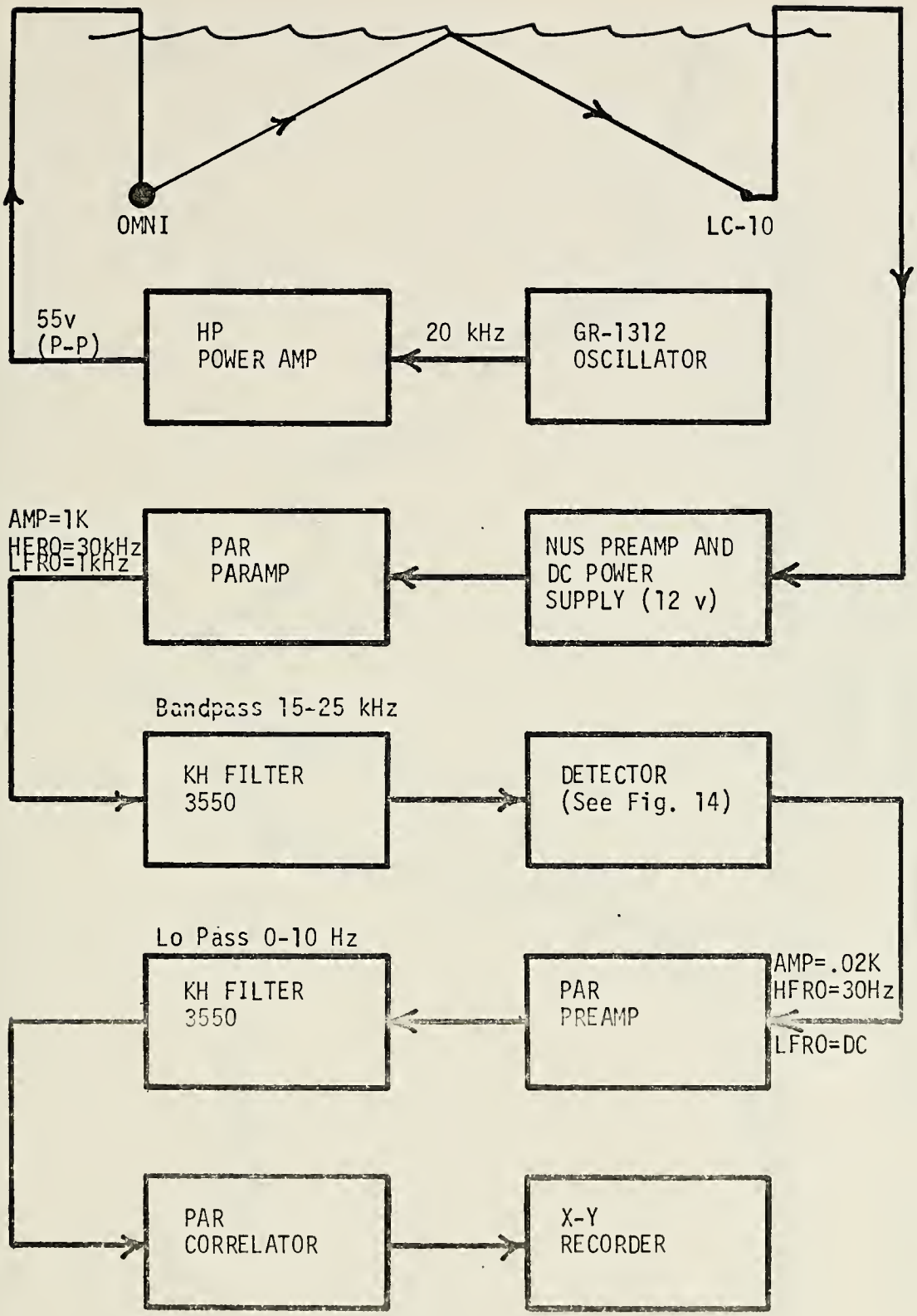

Figure 25. Experimental Setup for Determining the Spectrum of Demodulated Scattered Sound

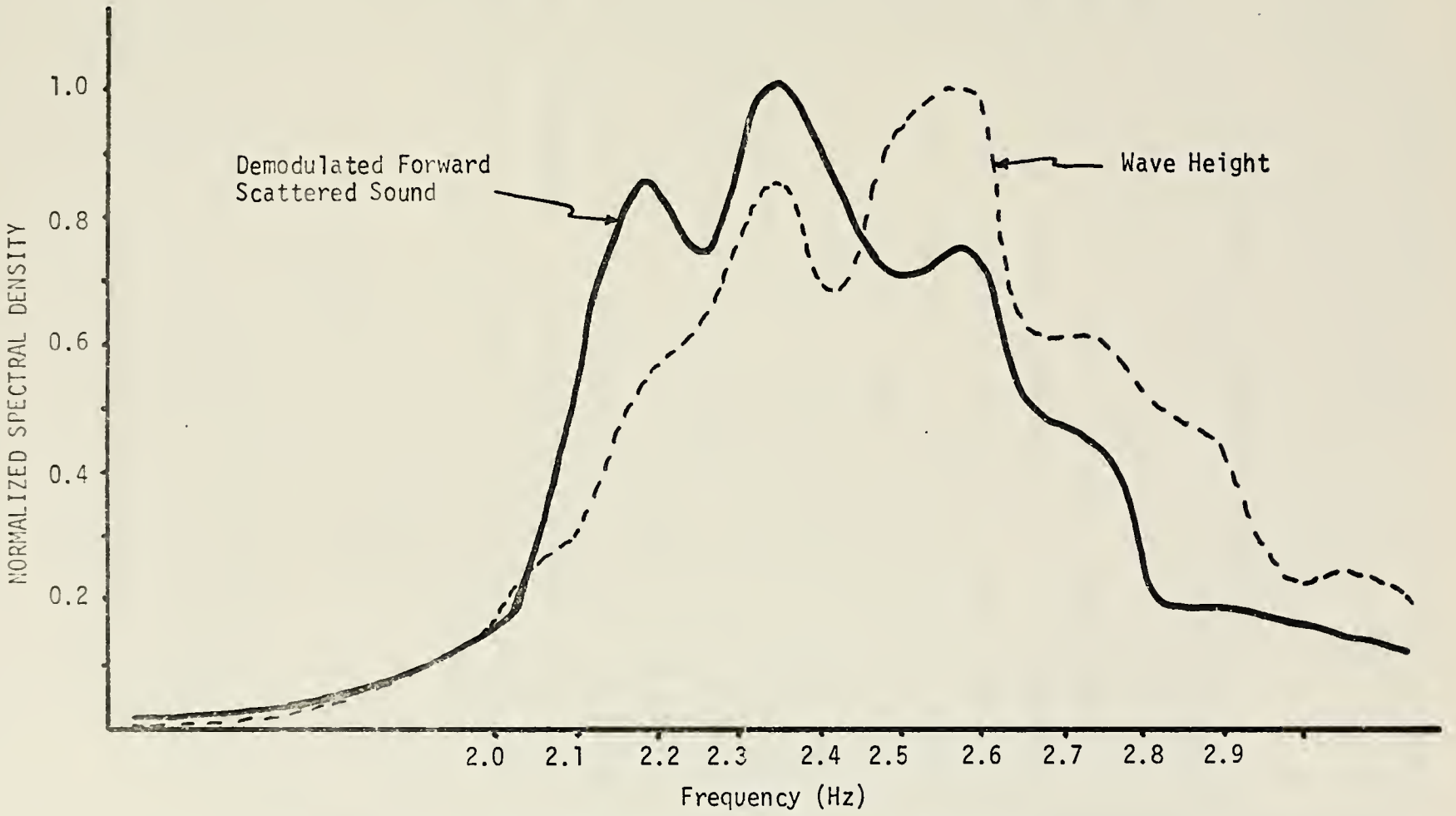

Figure 26. Normalized Frequency Spectra of Demodulated Forward Scattered Sound and OAWF Surface Wave Height

These frequency spectra, though exhibiting some minor differences, are considered to be essentially the same and confirm the theoretically expected result.

2. Autocorrelation Function Comparison

The same procedure was used in determining the demodulated scattered sound autocorrelation function as in the case of the wave height version. The output of the previous setup was terminated in the PAR CORRELATOR instead of OPHELEA and recording was done on the X-Y RECORDER as before. Again eleven runs were conducted for delays τ = 0.0 to 2.0 seconds. These recordings are shown in Figure 27. An average autocorrelation function was then fitted to this record. A plot of both records, wave height and demodulated scattered sound, is shown in Figure 28. Though the ordinate at τ = 0 is slightly different for the two functions due to idiosyncracies of the PAR CORRELATOR and X-Y RECORDER, it is apparent that the results are nearly identical for the two cases. Further, it is evident that significant correlation for both variables exists for three "peaks", that is, over two ocean periods. The demodulated sound correlation function also becomes confused for delays greater than 2.0 seconds, as is the case with the wave height, as seen in Figure 29. It should be noted that the vertical scale in Figure 29 is expanded over that of Figure 21 and no inference of greater correlation should be drawn.

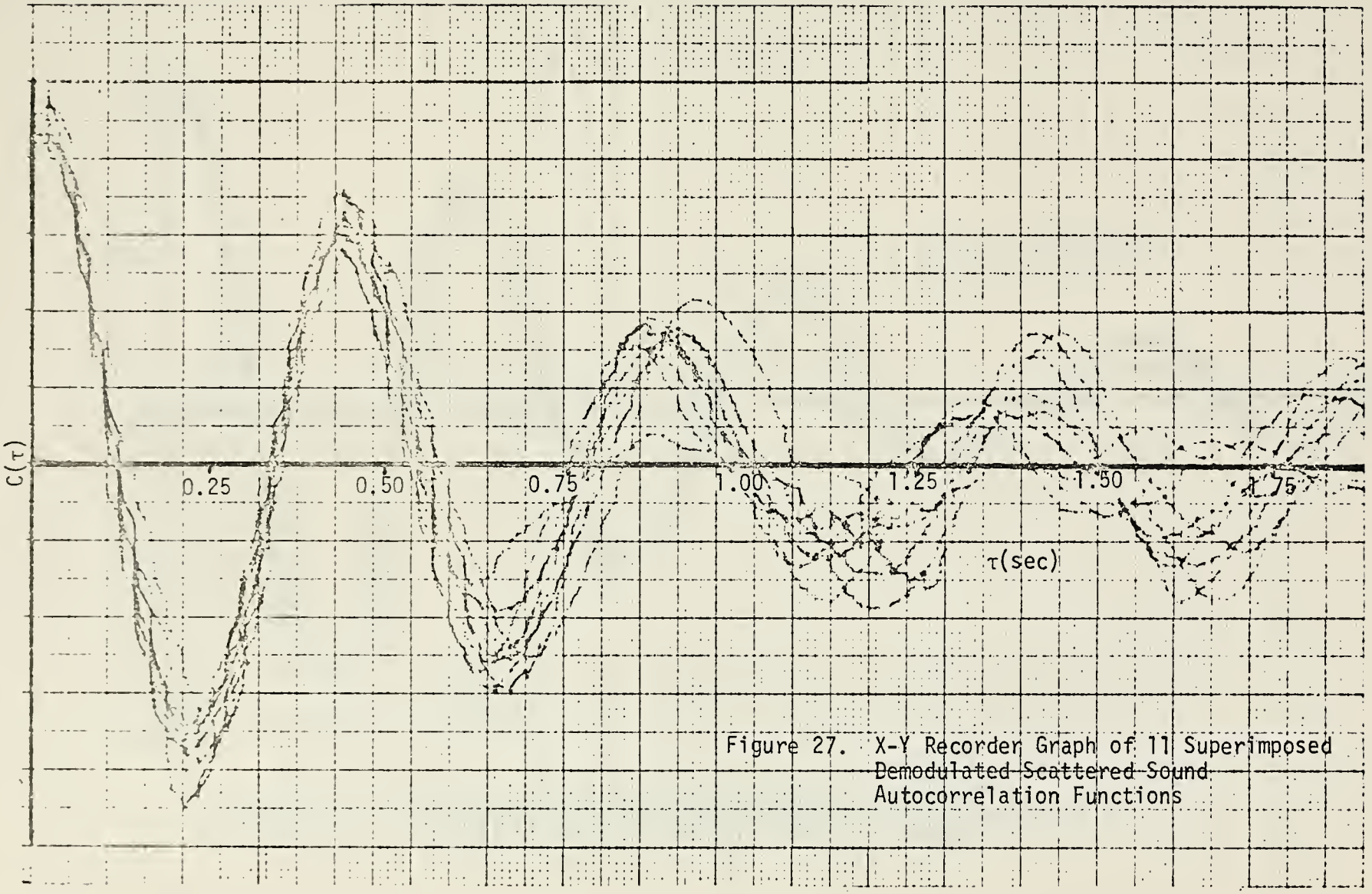

Figure 27. X-Y Recorder Graph of 11 Superimposed Demodulated Scattered Sound Autocorrelation Functions

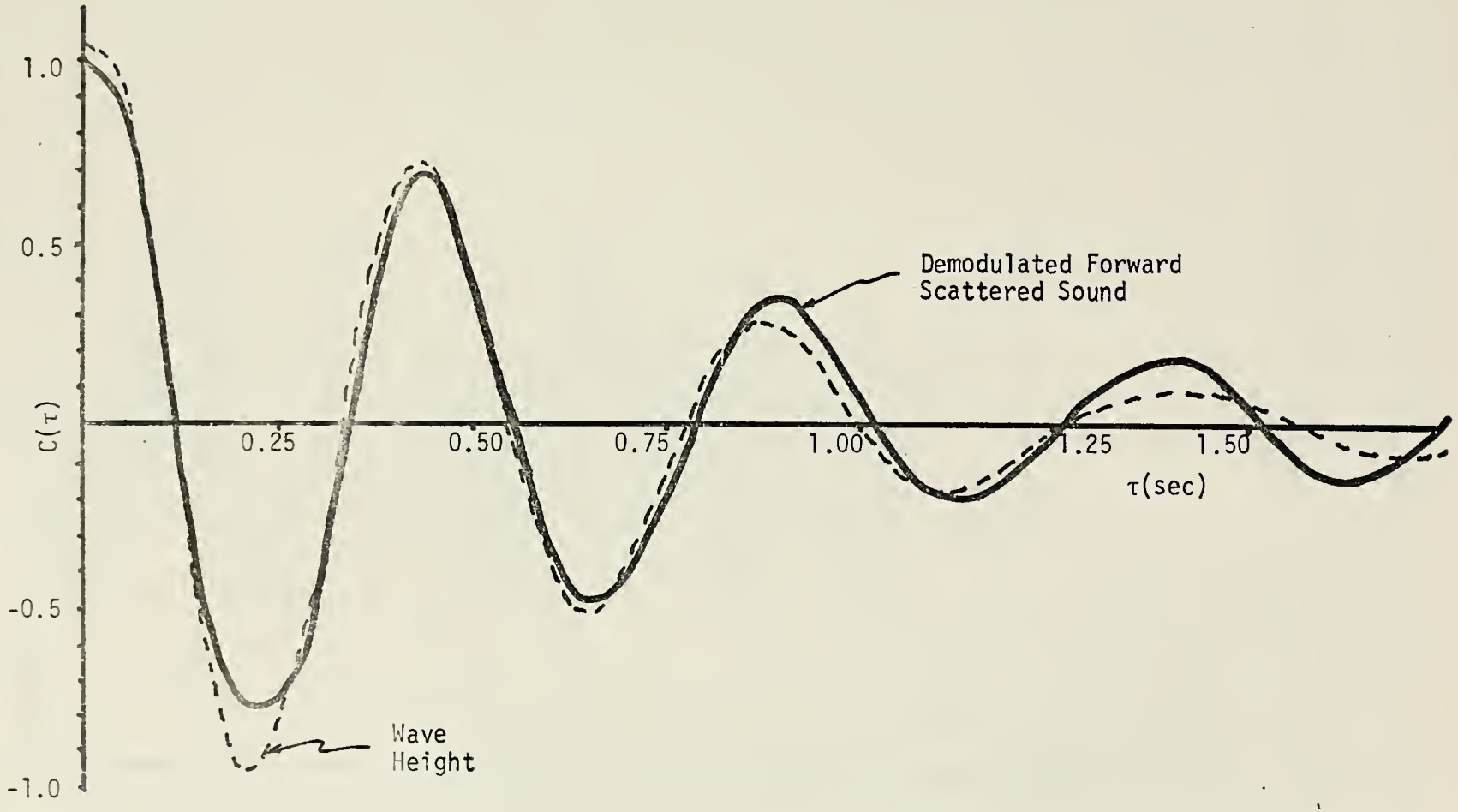

Figure 28. Average Autocorrelation Functions of Demodulated Forward Scattered Sound and Wave Height

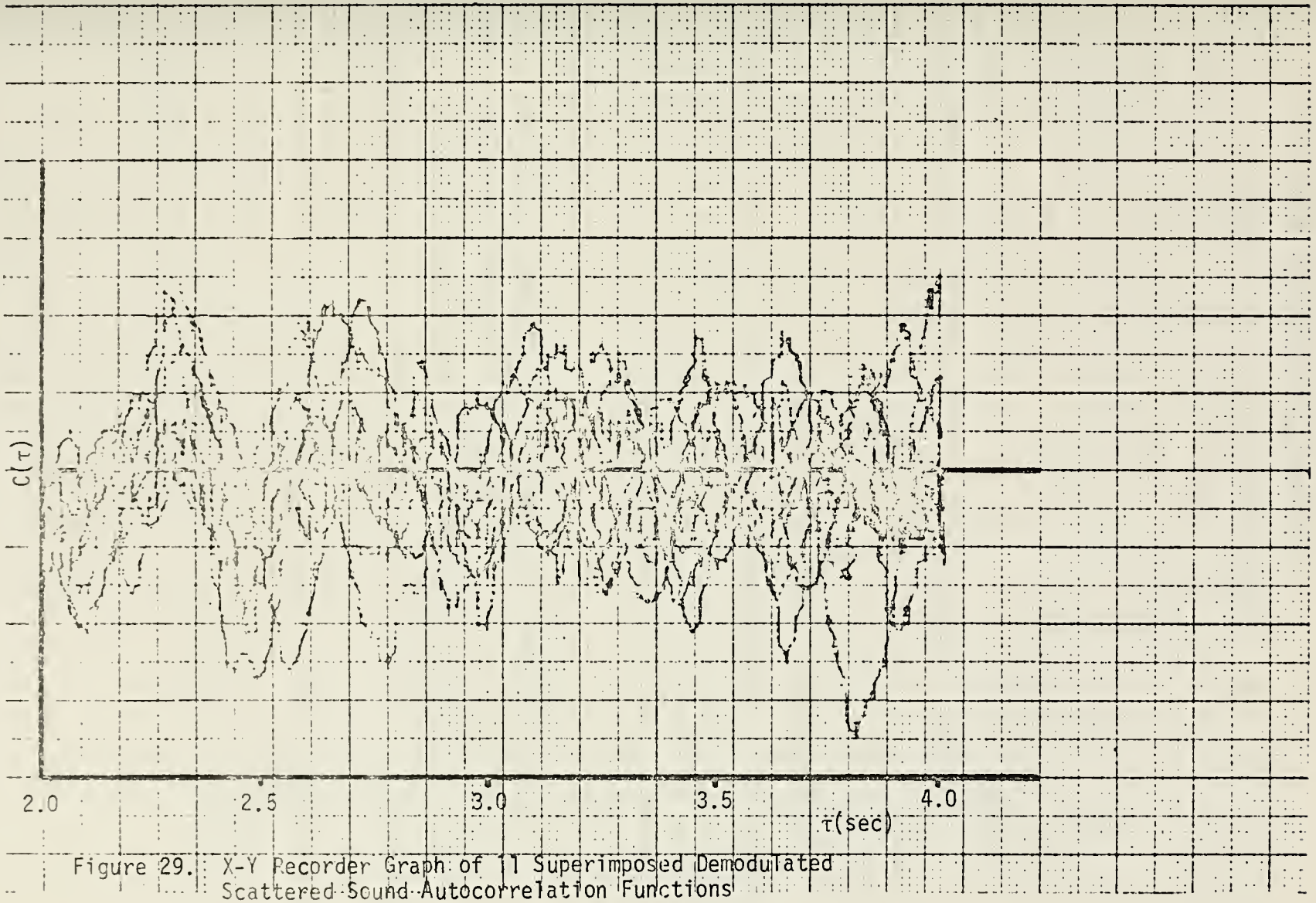

Figure 29. X-Y Recorder Graph of 11 Superimposed Demodulated Scattered Sound Autocorrelation Functions

3. Cross Correlation Function

Using the two setups described in the autocorrelation section above the two wave forms were cross correlated, again using the PAR CORRELATOR and X-Y RECORDER. The same sort of averaging process was then performed on the record shown in Figure 30 and yielded an average cross correlation function which is shown in Figure 31. The $\tau = 0$ ordinate varied considerably between positive and negative values of correlation and the choice of a near zero initial value was purely arbitrary. Again three peaks are seen to dominate, at about $\tau = 0.8$, 1.25 and 1.7 seconds. This is to be expected from the cross correlation function of two signals which both exhibit significant correlation over two ocean cycles (or have three "peaks" in their autocorrelation functions).

C. EFFECT OF FREQUENCY AND ANGLE OF INCIDENCE ON SCATTERED SOUND MODULATION

To determine whether the modulation frequency of the scattered sound remained essentially constant with changing acoustic frequency and varying angle of incidence, a series of trials was conducted with different combinations of these two parameters. It was felt at this stage of the research that there might be some advantage in using a directional hydrophone to make the detection.

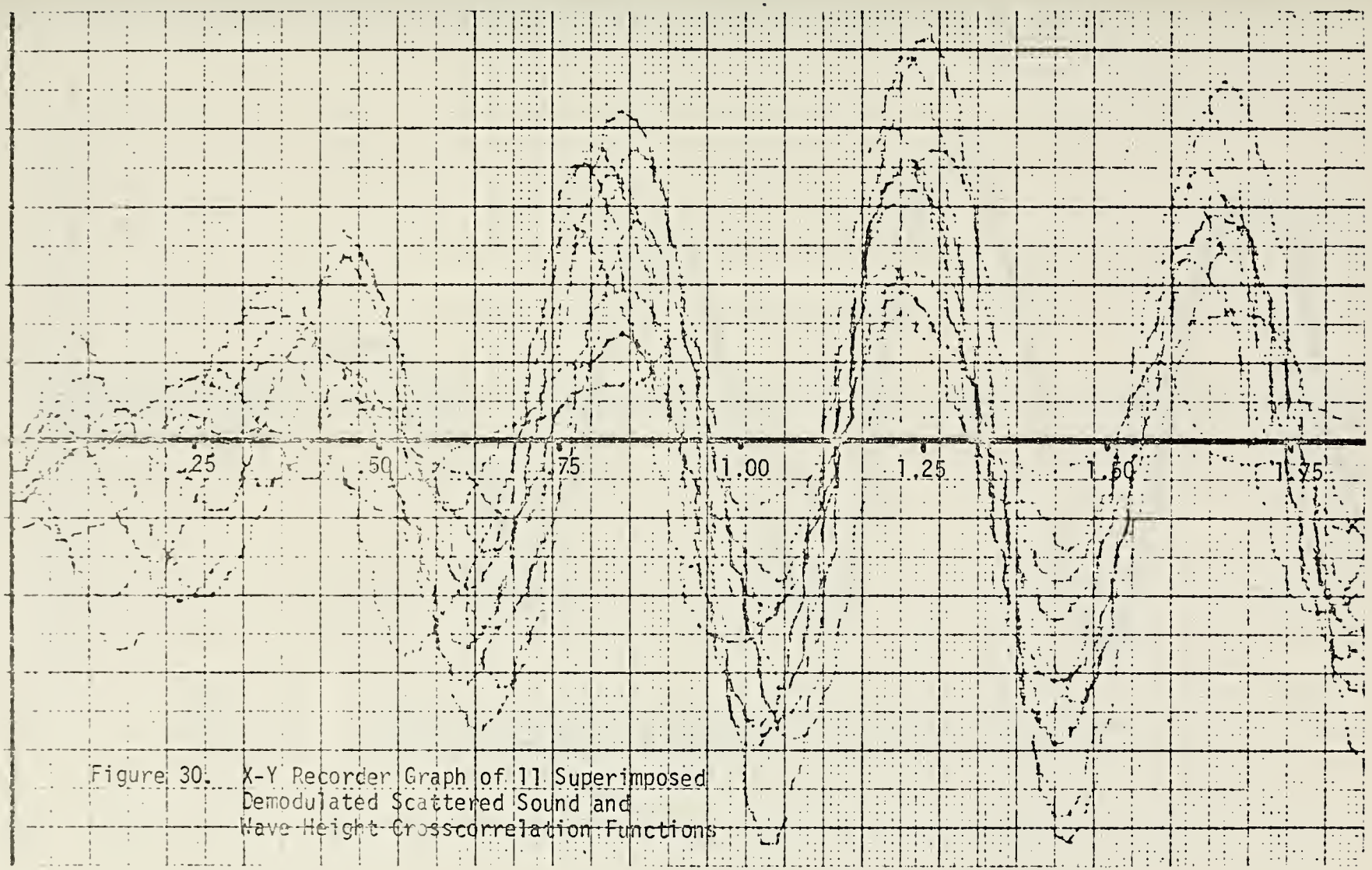

Figure 30. X-Y Recorder Graph of 11 Superimposed Demodulated Scattered Sound and Wave Height Crosscorrelation Functions

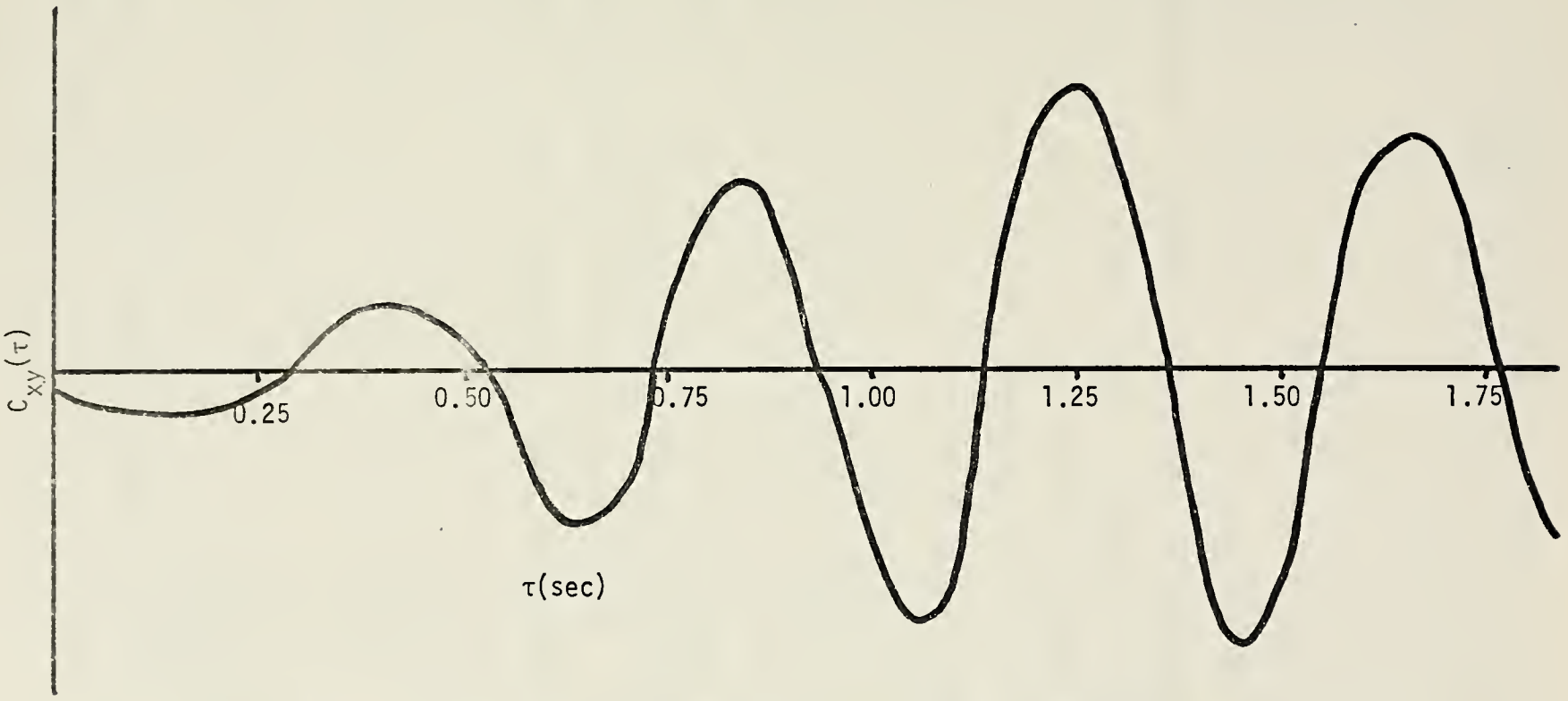

Figure 31. Average Demodulated Scattered Sound and Wave Height Cross Correlation Function

1. Changing Frequency and Angle of Incidence

In these tests a directional transducer, a USRD Type F-27, was mounted in a trainable bracket which permitted angles of incidence, measured from the surface normal, of from 0° to 90°. The F-27 is shown in Figure 22. The scattered sound was received by an omnidirectional LC-10 hydrophone which was positioned at the same depth as the F-27 and 2.75 meters away. To achieve different angles of incidence while retaining specular scatter the F-27 and LC-10 were positioned at depths of 0.99, 0.49 and 0.27 meters which equate to angles of incidence of approximately 58°, 70° and 79° respectively. Prior to each trial the F-27 was elevated and depressed, with the surface quiescent, until the maximum response ensured that the observation was of specular scatter. Ten runs, using program PING 1C (Appendix A), were conducted at each position with 256 A/D samples being taken at a sampling rate of 20 Hz. A 128-point spectral density versus frequency output was generated as in the determination of previous spectra. Again the WAVETEK oscillator provided the pulse train for proper A/D converter triggering at low frequencies. A diagram of this setup is shown in Figure 32 and a table of run parameters and particular equipment settings is found in Table II.

After the above 80 runs were completed, the ten spectra from each angle/frequency combination were averaged and normalized to permit comparison. The results were then

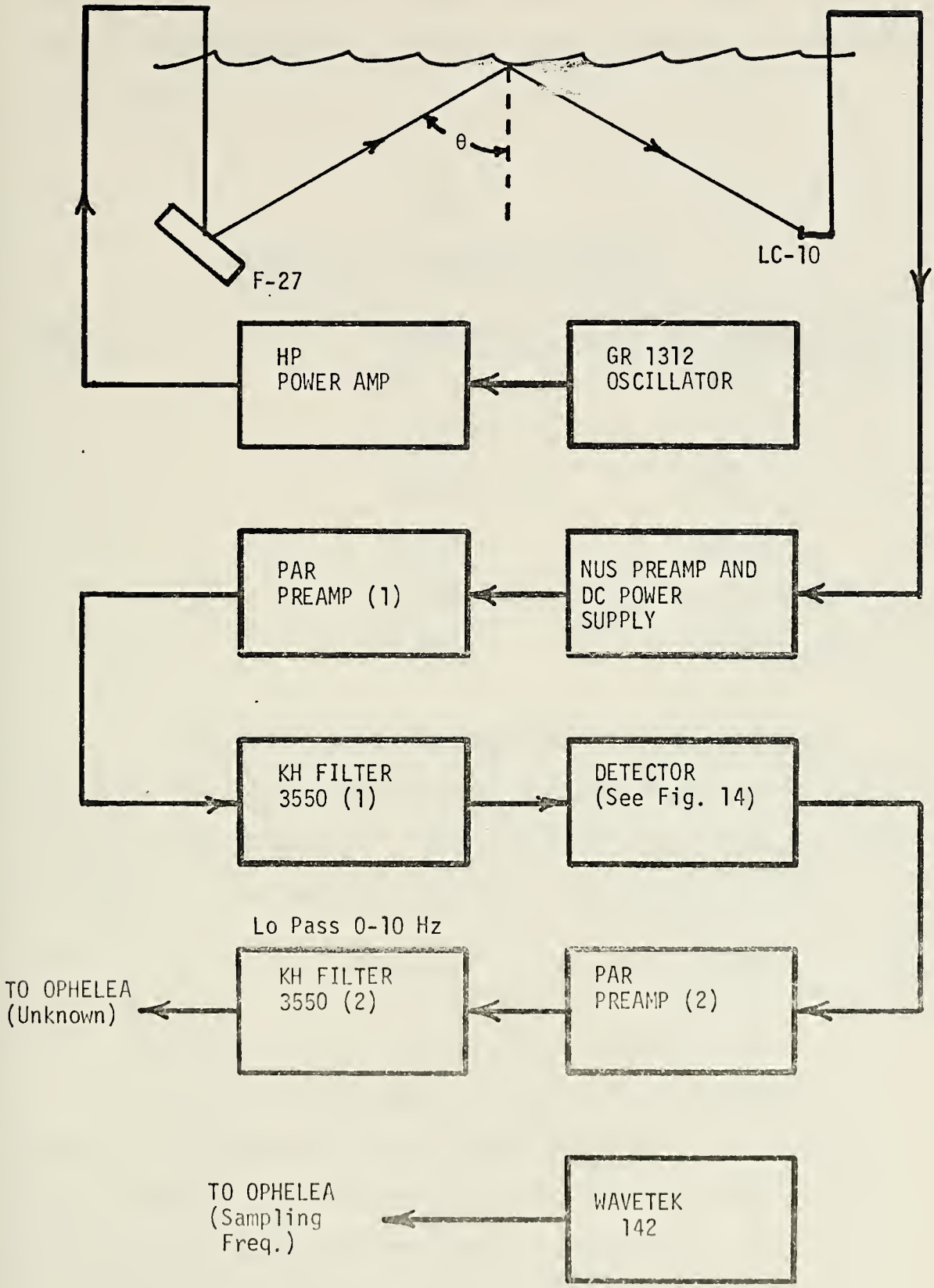

Figure 32. Experimental Setup for Determining the Effects of Varying Angle of Incidence and Frequency on Scattered Sound Modulation

plotted as indicated in Table I below with results compared for constant angle of incidence and variable frequency and vice versa.

TABLE I

SUMMARY OF VARIABLE ANGLE OF INCIDENCE AND FREQUENCY TRIALS

Figure	Acoustic Frequency	Angle of Incidence
33	30,40 kHz	79°
34	20,30,40 kHz	70°
35	20,30,40 kHz	58°
36	20 kHz	70°,58°
37	30 kHz	79°,70°,58°
38	40 kHz	79°,70°,58°

As may be seen from Figures 33 through 38 the frequency spectral peaks differ by less than 0.3 Hz in all cases except Figure 35. The somewhat wider spread, about 0.5 Hz, between peaks is thought to be due to greater contributions from the side lobes at that angle of incidence. Even this difference, though larger, is comparable to the 3 dB bandwidth of the wave frequency spectrum.

Based on this work, it was concluded that the modulation spectra of the scattered sound received by a point hydrophone are similar for variations in acoustic frequency or angle of incidence. It is felt that the differences are due to inadequate averaging and/or the dependence on side lobes.

TABLE II

Summary of Parameters Affecting Trials with Variation of Frequency and Angle of Incidence

Run No.'s	Acoustic Freq.	Angle of Incidence	AMP of PAR PREAMP (1)	AMP OF PAR PREAMP (2)	BandPass of KH-3550 (1)
1-10	20 kHz	70°	0.2K	0.02K	15 to 25 kHz
11-20	30 kHz	70°	1.0K	0.01K	25 to 35 kHz
21-30	40 kHz	70°	0.05K	0.01K	35 to 45 kHz
31-40	40 kHz	79°	0.05K	0.02K	35 to 45 kHz
41-50	30 kHz	79°	0.1K	0.05K	25 to 35 kHz
51-60	40 kHz	58°	0.02K	0.02K	35 to 45 kHz
3a-12a	20 kHz	58°	0.2K	0.02K	15 to 25 kHz
13a-22a	30 kHz	58°	0.2K	0.02K	25 to 35 kHz

Note: (1) Runs designated with an "a" were conducted on the preceding day but under precisely the same conditions.

(2) No runs were conducted for 20 kHz at 79° due to the beam width, 24° to the 3 dB points, of the F-27 at that frequency.

(3) Numbers with PREAMPS and KH-3550 refer to Figure 32.

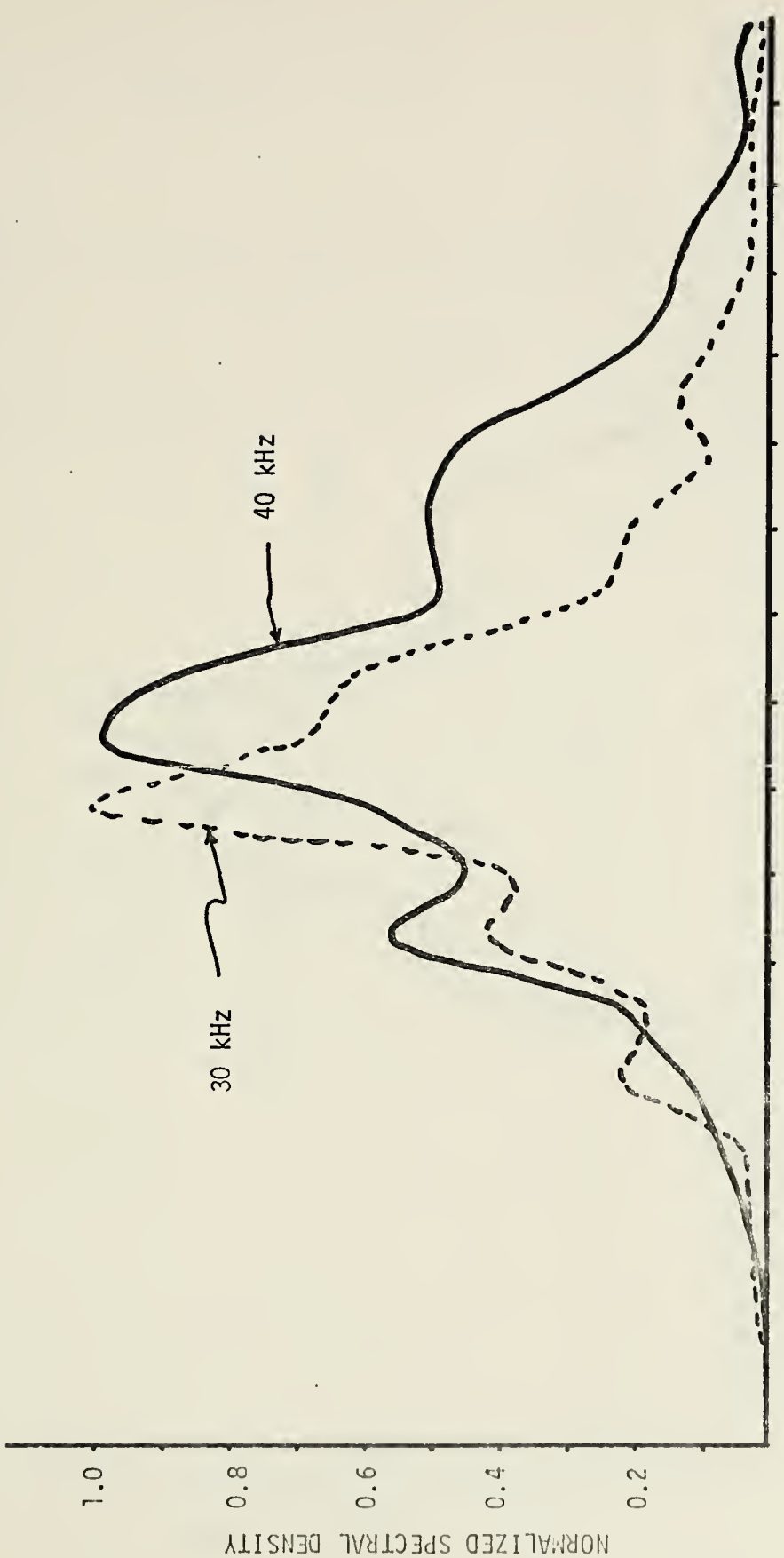

Figure 33. Normalized Frequency Spectra of 30 kHz and 40 kHz Demodulated Sound at an Angle of Incidence of 79°

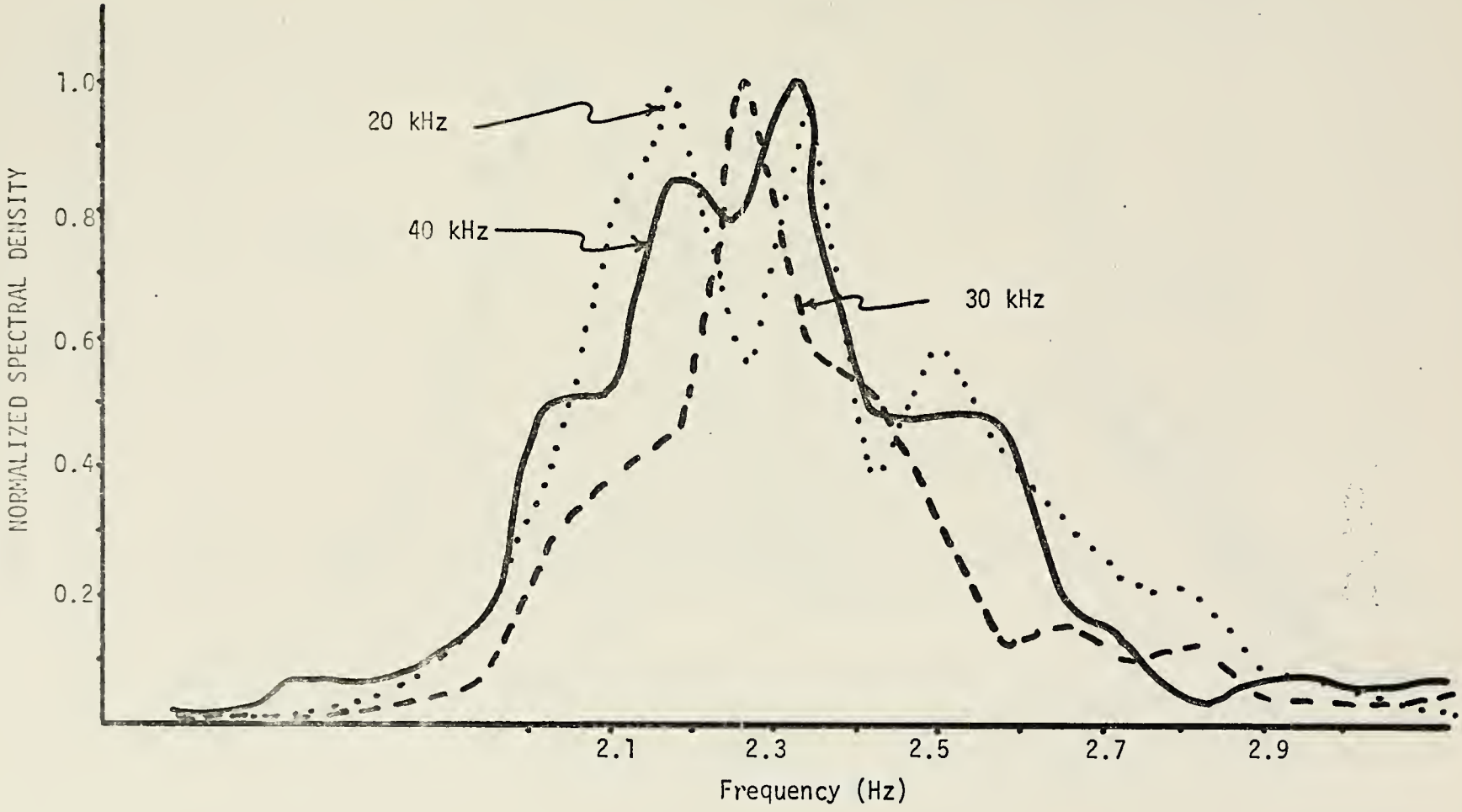

Figure 34. Normalized Frequency Spectra of 20 kHz, 30 kHz and 40 kHz Demodulated Scattered Sound at an Angle of Incidence of 70°

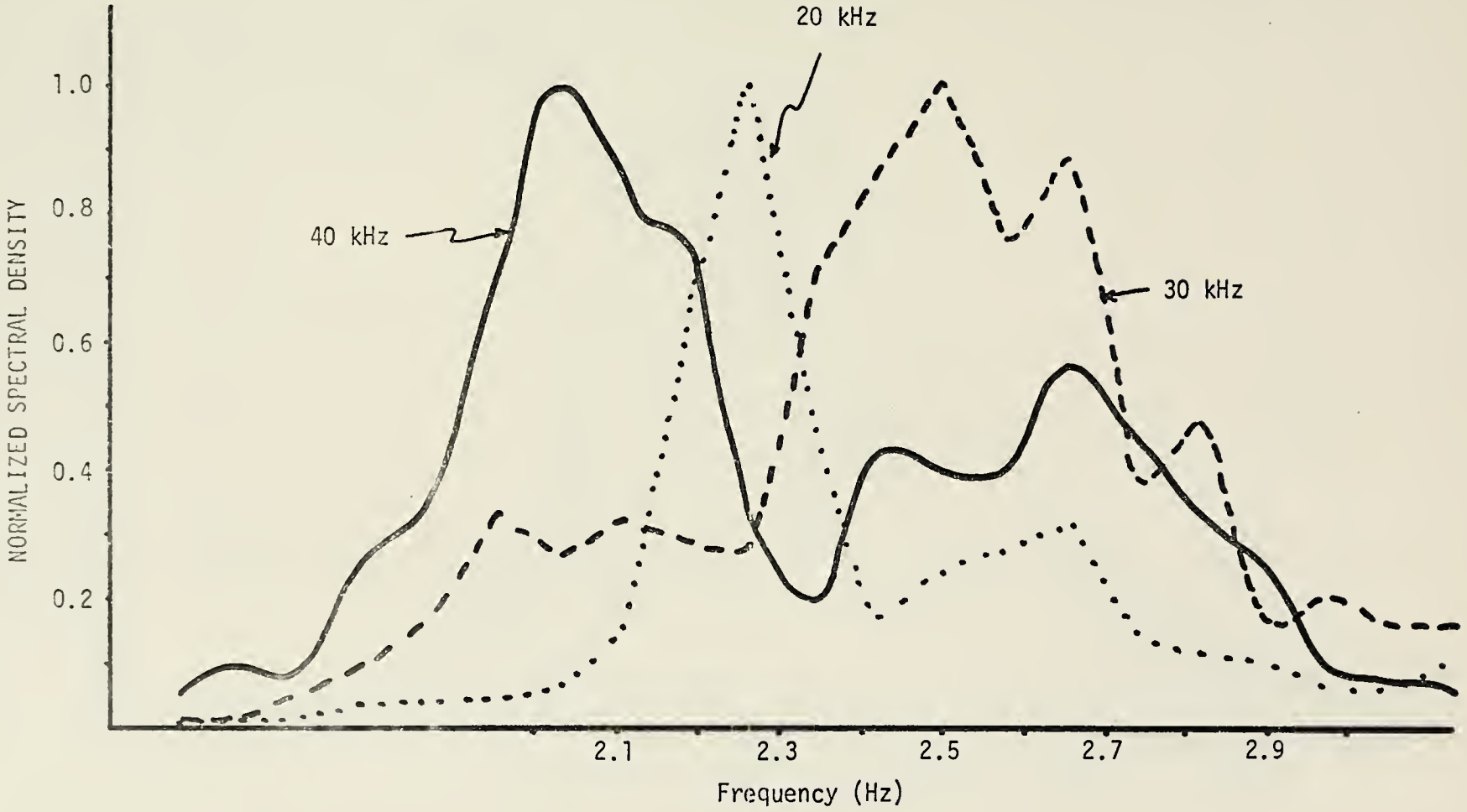

Figure 35. Normalized Frequency Spectra of 20 kHz, 30 kHz and 40 kHz Demodulated Scattered Sound at an Angle of Incidence of 58°

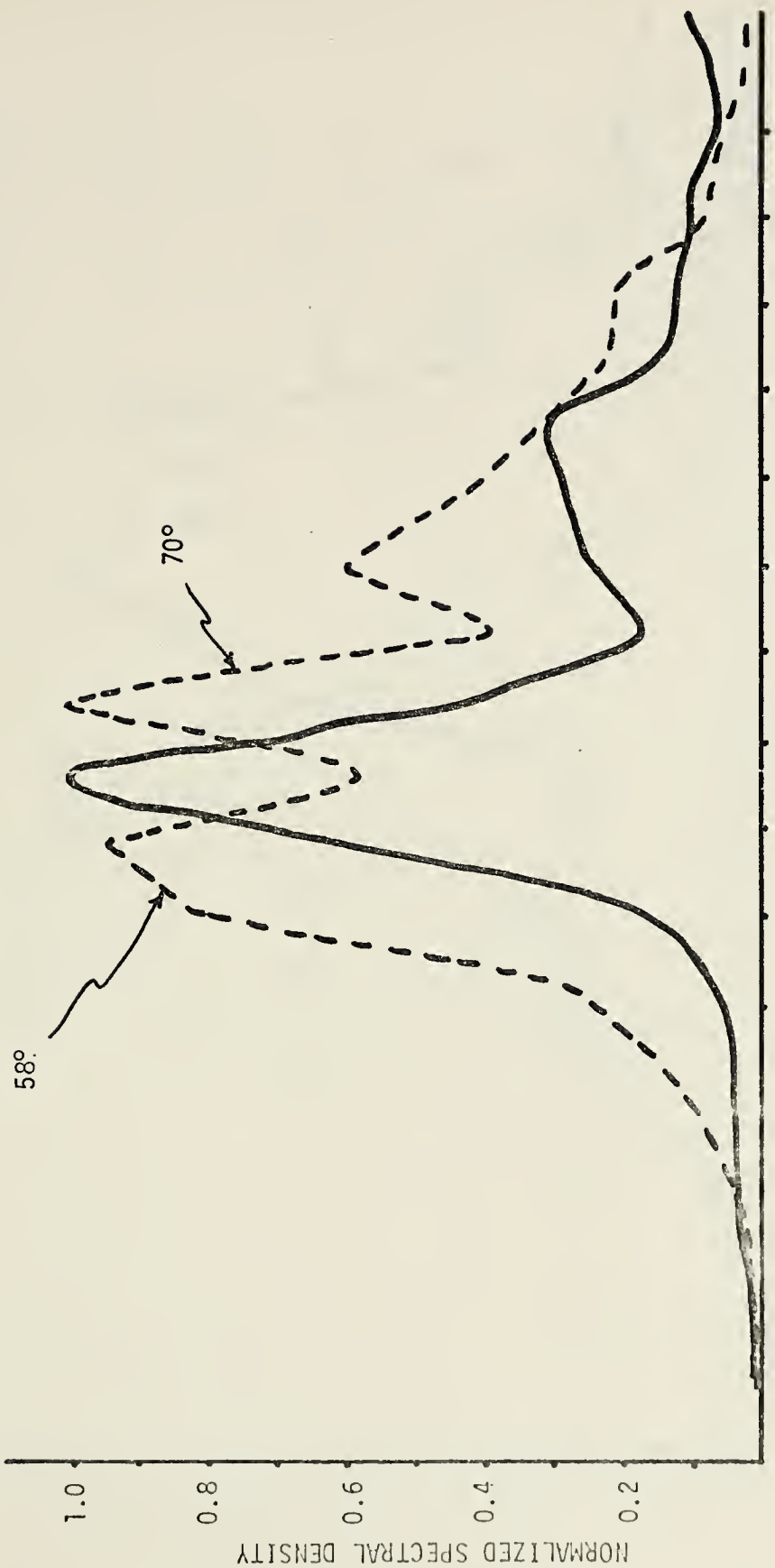

Figure 36. Normalized Frequency Spectra of 20 kHz Demodulated Scattered Sound at Angles of Incidence of 58° and 70°

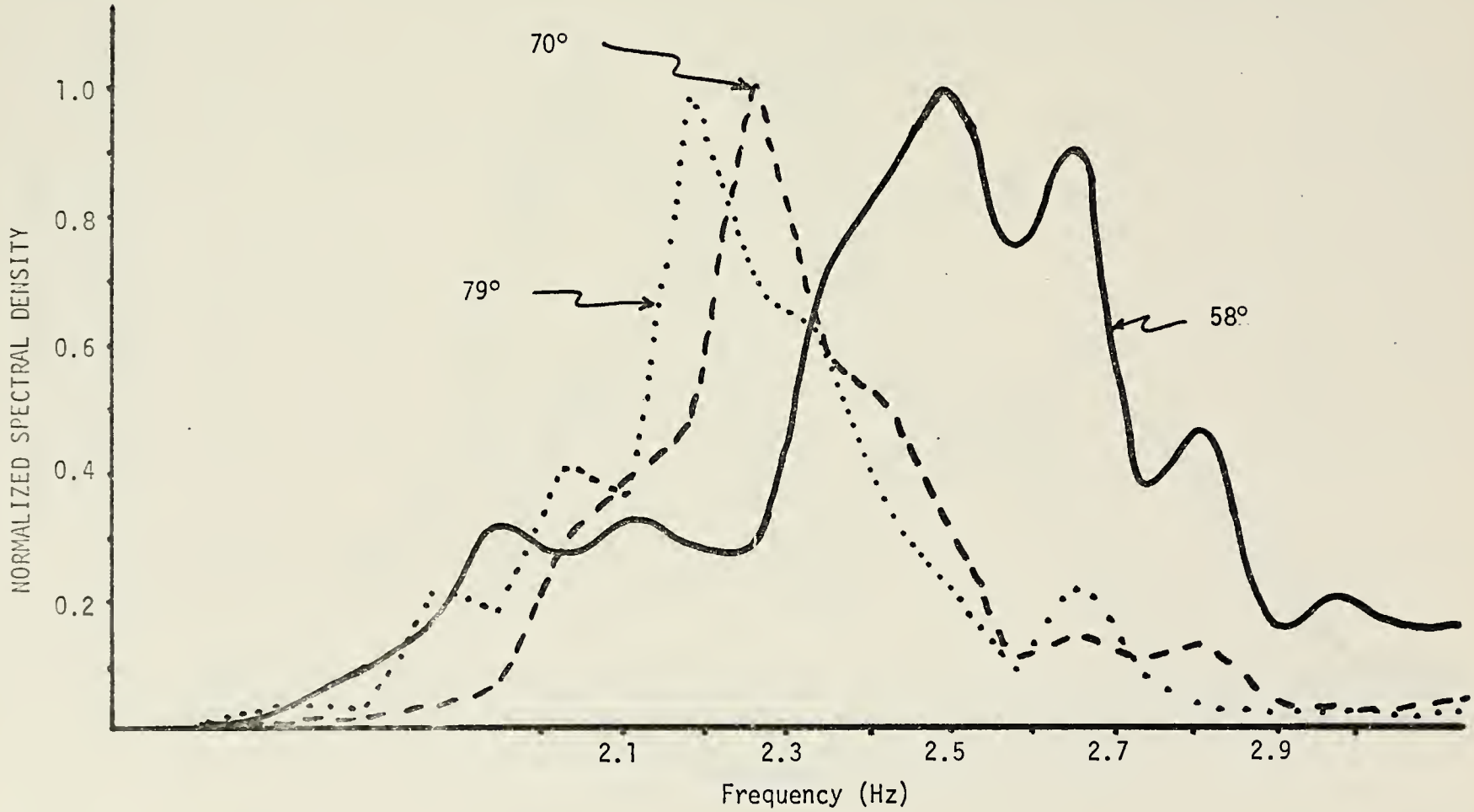

Figure 37. Normalized Frequency Spectra of 30 kHz Demodulated Scattered Sound at Angles of Incidence of 58°, 70° and 79°

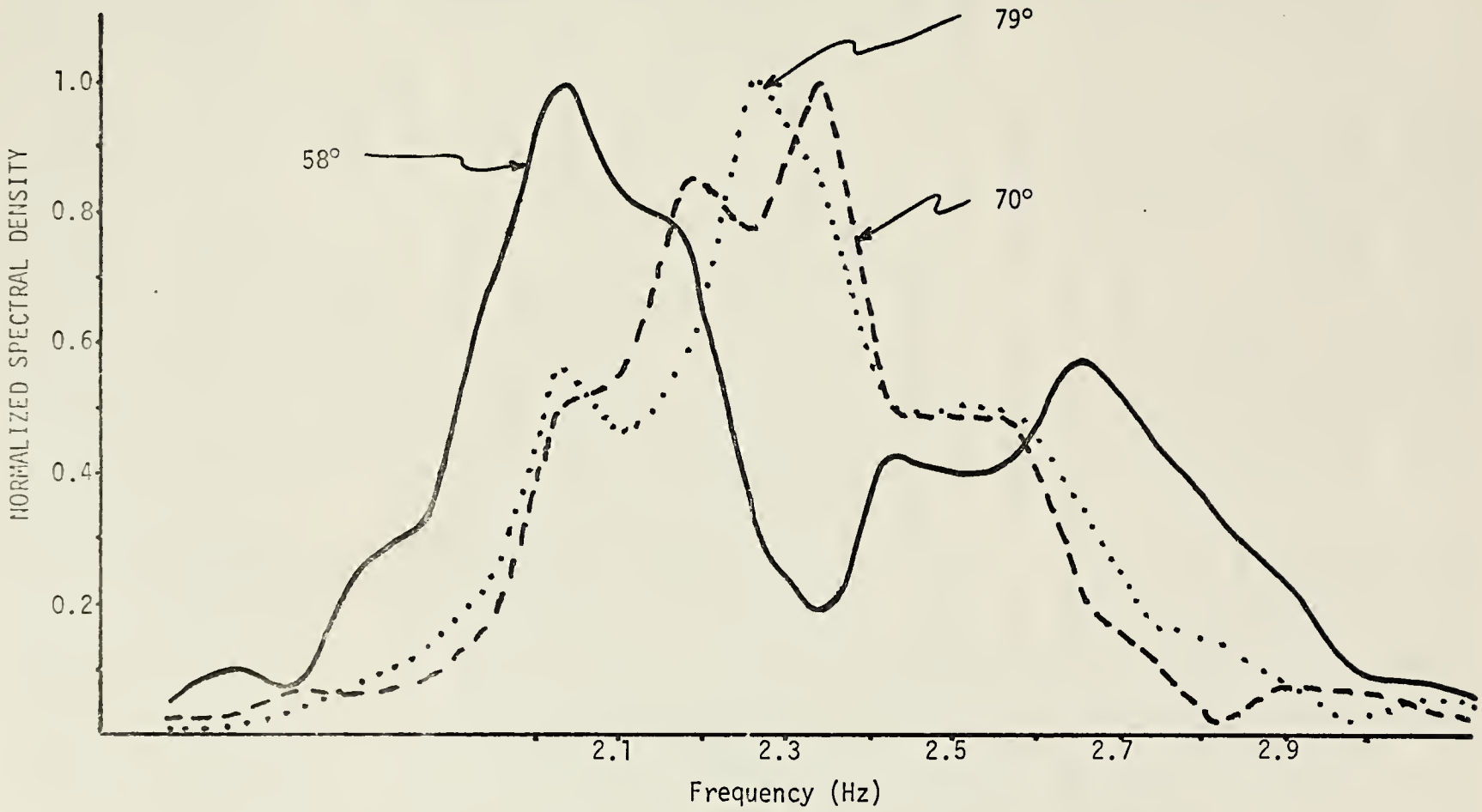

Figure 38. Normalized Frequency Spectra of 40 kHz Demodulated Scattered Sound at Angles of Incidence of 58°, 70° and 79°

2. Modulation Strength with Changing Receiver Angle

The object of this set of trials was to determine if the modulation effect could be increased by training a directional receiver to a preferred angle of reflection with a point source. Although acoustic reciprocity would be expected to hold, in this case control would be at the option of the listener. Specifically it was felt that possibly if the receiver hydrophone were directed normal to the modulating ocean surface, the relative modulation of the received scattered acoustic signal would be increased. The experimental setup was essentially as before; however, now the F-27 was the receiver and the previously referred to OMNI was the source, with both at a depth of 1.0 meters. The three fan OAWF sea was again the environment with the water level standardized as before. A setup diagram is shown in Figure 39. Ten runs were conducted at each of seven angles of incidence ranging from direct path, through specular to normal incidence. The acoustic frequency was 30 kHz and amplifier and filter settings were kept constant for all runs so that valid comparisons could be made. Table III shows a summary of these trials.

Each of the seventy runs in Table III consisted of taking 256 A/D samples at a 20 Hz sampling frequency (using program PINC 1C) as before; then averaging the spectral density information for each angular setting. The plot of these average spectra is presented in Figure 40 which shows log spectral density plotted versus scattered sound modulation frequency.

TABLE III

SUMMARY OF VARIABLE ANGLE RECEIVER TRIALS

Run Numbers	Angle of Incidence
61-70	90° (Direct)
71-80	58° (Specular)
81-90	45°
91-100	30°
101-110	0° (Normal
111-120	25°
121-130	75°

Note: Again the angle of incidence is measured normal to the surface.

All levels have been plotted without adjustment so that the amplitude of the modulation at different angles of incidence can be seen simultaneously. Summarizing:

a. The greatest modulation strength was observed at $\theta = 58°$, that is the specular direction.

b. Modulation amplitude declined regularly as the angle of receiver is changed in either direction from the specular.

c. Although the incoherent component (modulated amplitude) may possibly be increased relative to the coherent component, the modulation amplitude is down 30 dB (re specular) with the receiver trained normal to the sea surface ($\theta = 0°$).

Knowing that the amplitude modulation is greatest at or near the specular direction might provide a means of

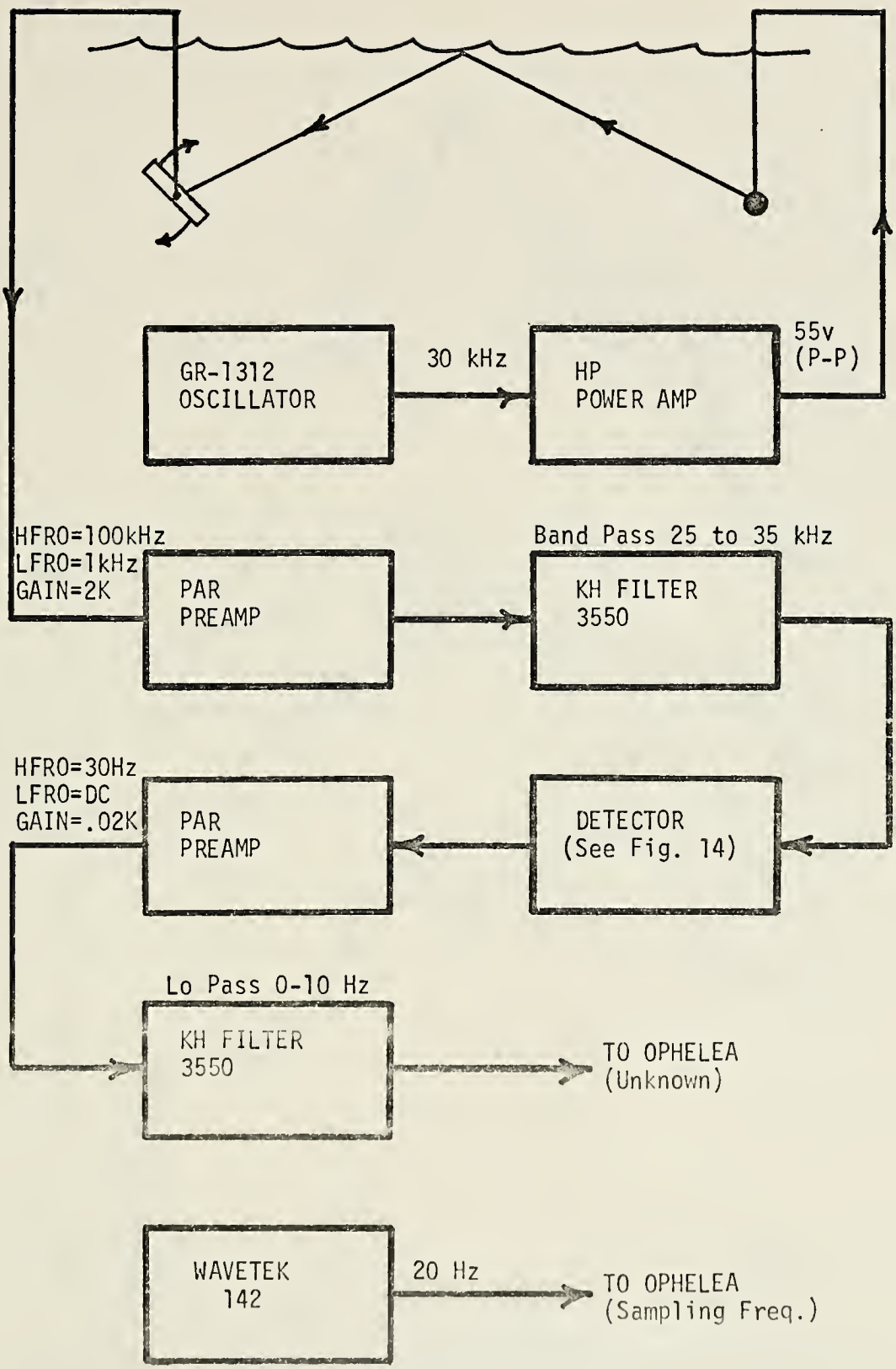

Figure 39. Experimental Setup for Determining the Effects of Changing Receiver Angle on Modulation Strength

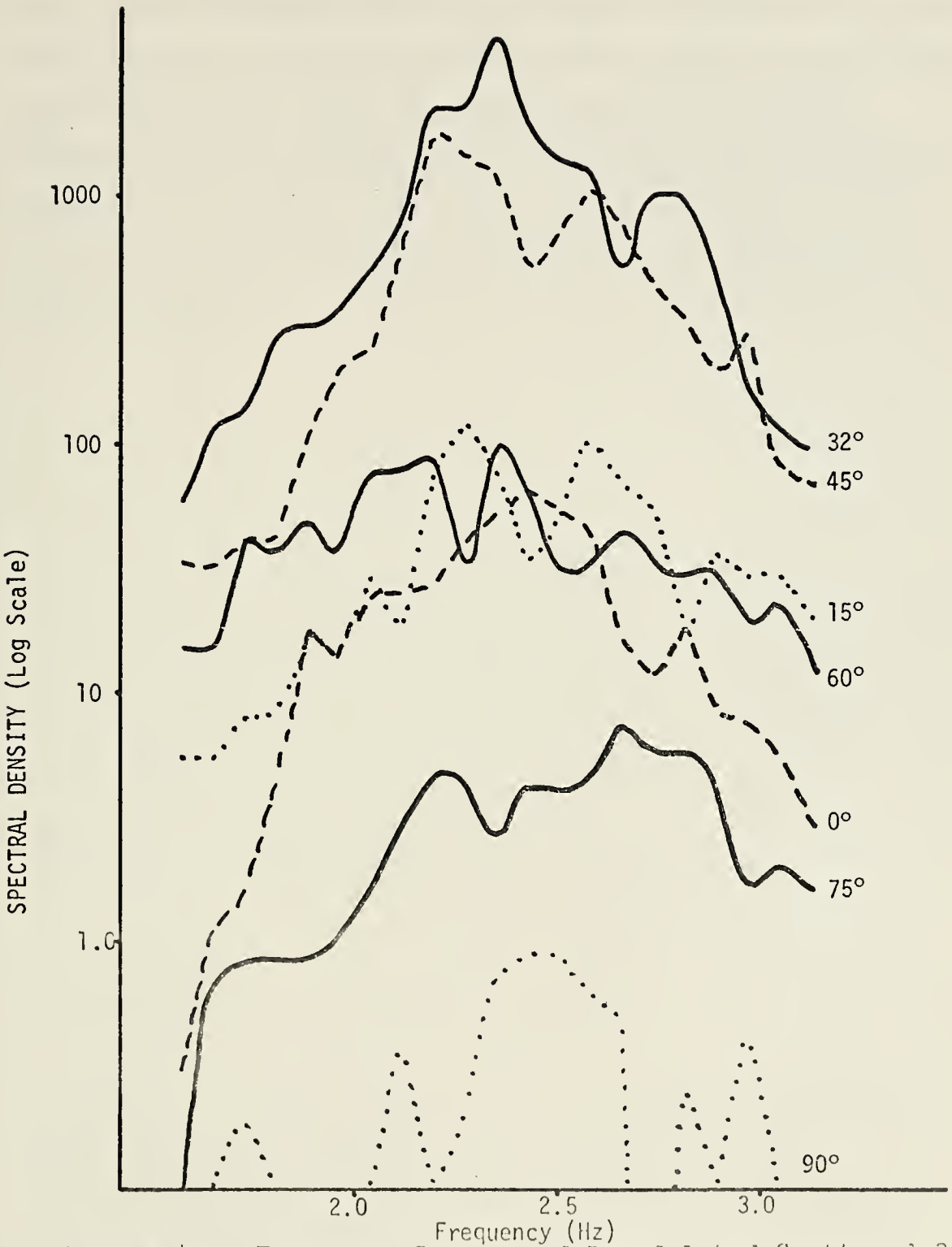

Figure 40. Frequency Spectra of Demodulated Scattered 30 kHz Sound from an Omnidirectional Source at Various Receiver Angles

arriving at a rough fix or target probability area. Assuming that target bearing could be provided by a directional hydrophone and that the local sound velocity profile is known, the approximate range could be found by applying ray path techniques once the angle of greatest modulation (specular direction) is found. This scheme would of course require a hydrophone system which is directional in both azimuth and elevation.

V. ENHANCING THE TIME-VARYING SIGNAL

At this stage, with reasonable assurance that the OAWF sea accurately modeled the actual ocean and that the modulation spectrum of the scattered sound was essentially that of the surface waves, efforts were begun toward improving signal processing using the model and the information gained to date. If the ocean wave spectrum were of a single fixed frequency the sound would fluctuate at that same single fixed frequency and sound signal enhancement would then be easy. It would be necessary merely to identify a loud point in the received signal and then to listen at later intervals equal to the ocean wave period. The ocean is regrettably not this simple as is obvious from the respective frequency spectra and therefore alternative or modified processing means had to be identified and implemented.

A. PROGRAMS PERK 1A AND PERK 1B

To begin to explore the problem, a pair of computer programs modestly named for this rookie acoustician were developed which would accomplish the following:

1. PERK 1A orders the computer to direct the A/D converter to take a group of samples (say 64), hereafter called a "BLOCK", and then to "pause".

2. The "pause" is triggered by the computer taking its last ordered sample and PERK 1A then shifts the computer into a Fortran "Do Loop" which has an index proportional to the desired time delay.

3. When the "Do Loop" has completed its preset number of operations (and the delay or pause has been completed) the program signals the A/D to take another BLOCK of samples. This is followed by another "pause", another BLOCK, etc.

The net result is a series of BLOCKS of A/D samples taken at specified intervals along the modulated signal which, when a total of 8192 data points have been taken (the present storage limit of OPHELEA), are read out to a tape cassette. This data tape is then put aside as the second program, further modestly entitled PERK 1B, is loaded.

PERK 1B reads the time series data of the previously recorded sample BLOCKS back into memory destructively and performs an FFT spectral analysis on each BLOCK. The program may then be directed to output all of the complete spectral analyses, or just the major spectral peak in each analysis. Thus a sequence of successive sound spectral density peaks is available, each separated by a fixed time delay, the "pause". The duration of the "pause" is selected to provide the desired number of spectral densities of predetermined frequency resolution during an "ocean period". An "ocean period" is here defined as the reciprocal of the peak frequency in the ocean spectrum. The effect of the modulation caused by the ocean is vividly illustrated by Figure 41, which depicts the peak sound spectral density versus time, and which shows a swing of about 18 dB between maxima and minima of signal strength. Copies of PERK 1A and PERK 1B may be found in Appendix A.

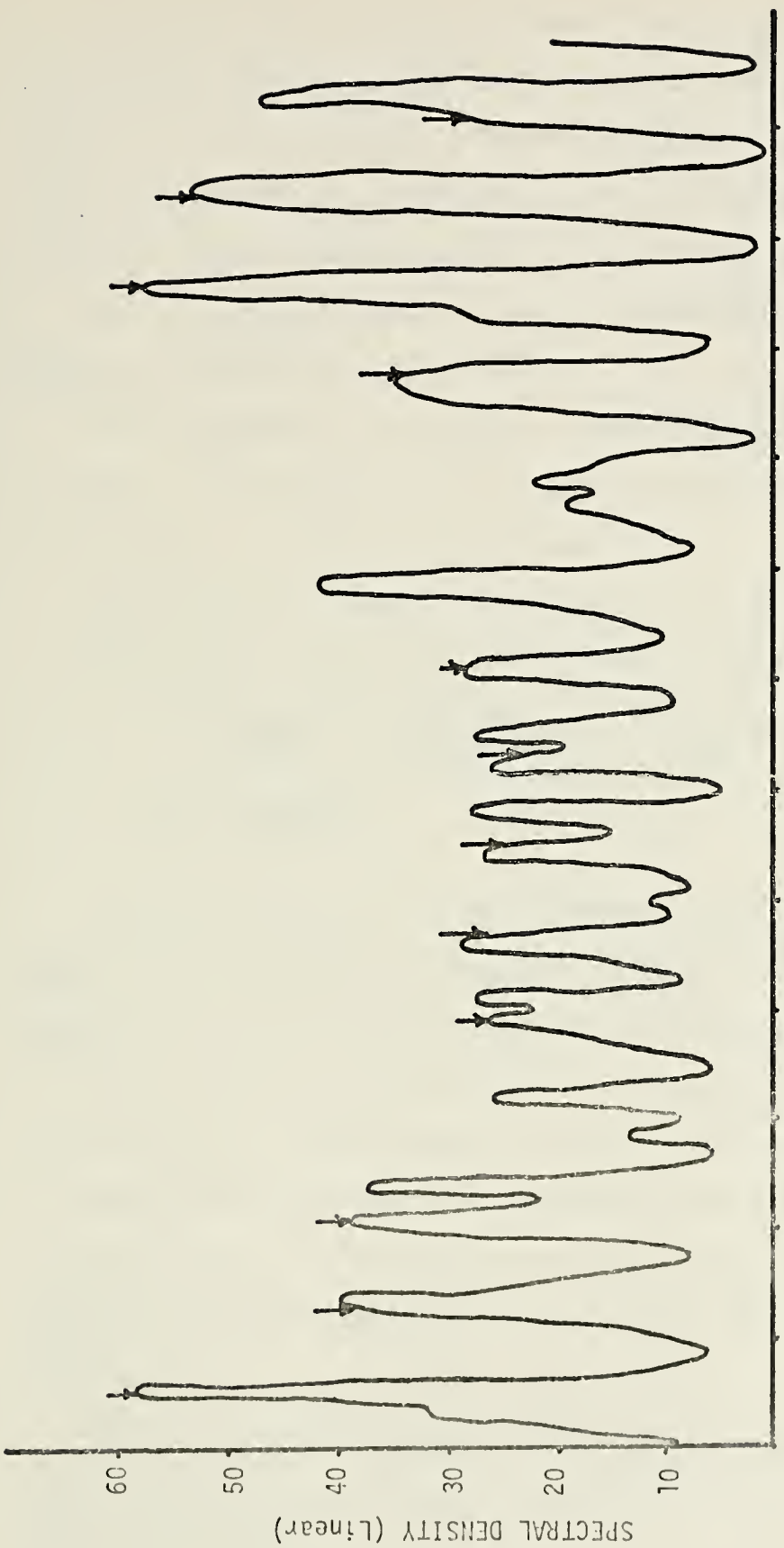

Figure 41. Changing Spectral Density Amplitude of a Forward Scattered Acoustic Signal. (Weak Signal - Large Fluctuations)

In this work, the BLOCKS almost invariably contained 64 A/D samples and the "pause" was selected to provide eight BLOCKS per ocean period. The following is a sample delay time calculation for a 20 kHz acoustic signal, modulated by a 2.5 Hz ocean (ocean period 0.4 sec.) and sampled at 80 kHz.

For 64 Samples/BLOCK at 80×10^3 samples/sec.:
sampling time/BLOCK = 0.8 msec.

For 8 BLOCKS/ocean period: sampling time/ocean period = 6.4 msec. Therefore, for one ocean period, total delay time = 400 msec - 6.4 msec = 393.6 msec.

Delay between BLOCKS = 393.6/8 = 49.2 msec.

Total data collected in 16 ocean periods

$$= \left(\frac{64 \text{ samples}}{\text{BLOCK}}\right)\left(\frac{8 \text{ BLOCKS}}{\text{ocean period}}\right)\left(\frac{16 \text{ ocean periods}}{\text{run}}\right)$$

$$= 8192 \frac{\text{samples}}{\text{run}}$$

For the purposes of this research eight BLOCKS per ocean period were considered adequate coverage. Each of the eight BLOCKS was said to be at a different PHASE lettered A through H. Every eighth BLOCK would be at the same phase. Again if the ocean were monochromatic and the spectral density peaks in each PHASE averaged, one average, corresponding to the strongest part of the signal, would predominate and the other PHASES of lesser amplitude would be distributed sinusoidally around it.

PERK 1A and PERK 1B are highly versatile programs with a number of options available as summarized in the following table (Table IV).

TABLE IV

SUMMARY OF PERK 1A AND PERK 1B PARAMETER OPTIONS

Total number of A/D data points	up to 8192
Number of data points/BLOCK	from 16 to 512 in powers of 2 (2^N)
Delay between BLOCKS	0.01 to 999.9 msec with accuracy to 0.01 msec.
Number of BLOCKS/ocean period = number of PHASES	2 to 16 in powers of 2

The program also provides a unique number for each run, based on day, month and run sequence of that day (i.e., #15101 is the first run conducted on 15 October), and also prints out input parameters such as sampling frequency, prior to displaying the output.

It should be noted at this point that PERK 1A/1B were tested on a known sinusoid of 2.5 Hz and found satisfactory. In that test, groups of 8 A/D samples separated by 0.4 seconds were taken at 80 kHz and plotted versus time. No visible discrepancy existed over 24 sinusoidal periods.

To recapitulate, the programs PERK 1A and PERK 1B were used to take BLOCKS of 64 A/D samples, properly spaced temporally to provide eight PHASES (A-H) per ocean period, over sixteen ocean periods. This equates to 128 BLOCKS or 16 BLOCKS per PHASE. Samples were taken at four times the acoustic frequency, or twice the Nyquist rate, to diminish

the effects of aliasing. A pictorial representation of this signal processing scheme is shown in Figure 42.

B. EFFECT OF SIGNAL STRENGTH ON MODULATION — LLOYD MIRROR MODELING

One of the most obvious times when signal processing enhancement is important is when the received acoustic signal is weak and may be fluctuating in and out of the background noise. In order to provide a common basis for comparing varying signal strengths, it was decided to employ different aspects of the Lloyd mirror phenomenon to observe varying strengths of the output signal.

1. Brief Review of Lloyd Mirror Effect

As every school-boy acoustician knows, the Lloyd Mirror Effect is caused by constructive and destructive interference between the direct and smooth surface reflected paths taken by an acoustic signal. For a mirror surface within a Critical Range $R_c = \frac{4hd}{\lambda}$, the effect is one of pressure peaks and valleys, with the peaks falling off as $1/r$ and the valleys going to zero (h = receiver depth, d = source depth, λ = acoustic wavelength). Beyond the critical range the pressure declines as $1/r^2$. The OAWF tank is capable of measurements both within and beyond the critical range for frequencies in the vicinity of 13 kHz. Another means of visualizing this effect is by replacing the reflected rays by an image source at I as also shown in Figure 43.

In the case of a rough surface the peaks caused by reinforcement are not as great and the coherent scattering

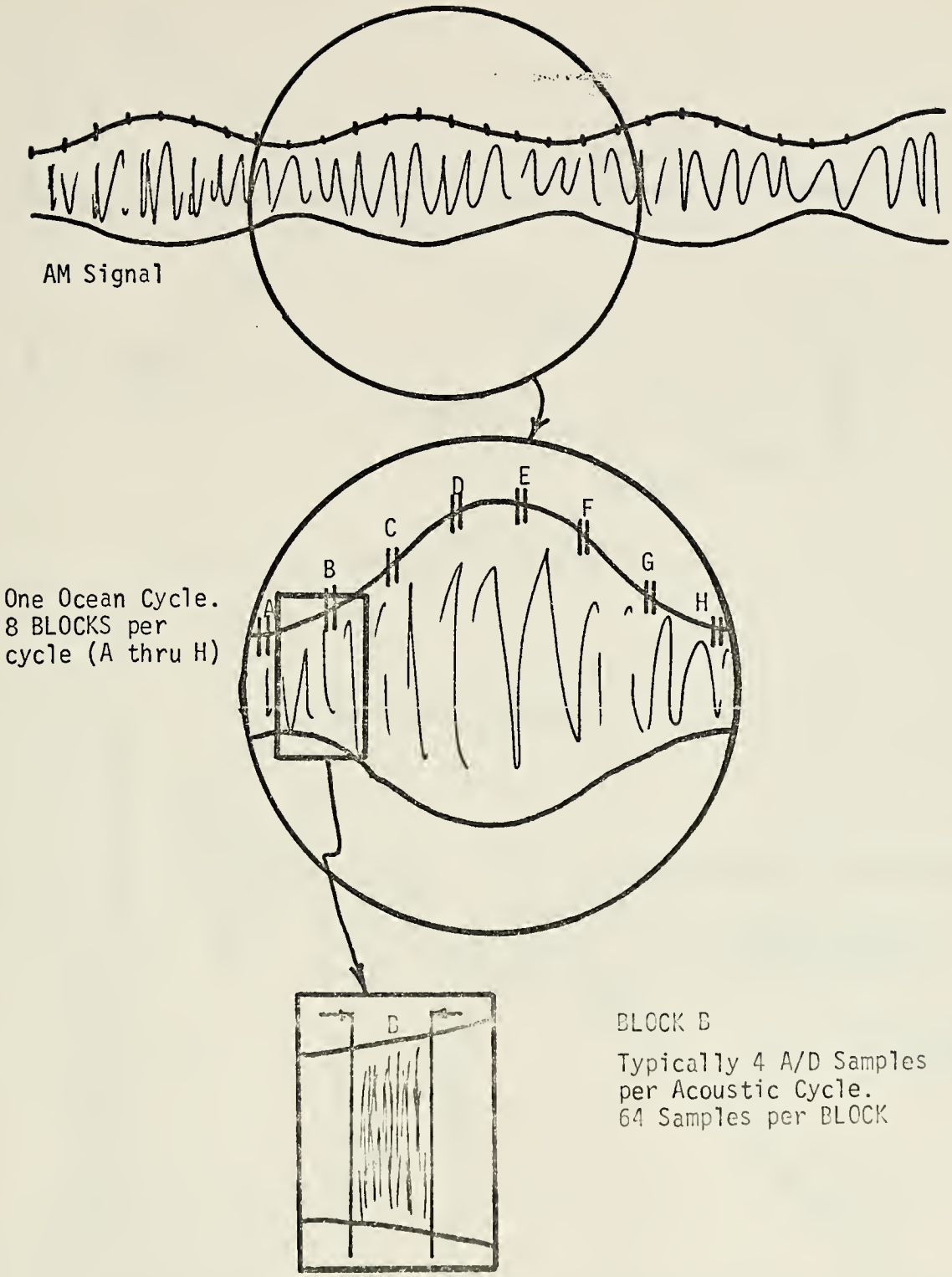

Figure 42. PERK 1A/PERK 1B Signal Processing Scheme

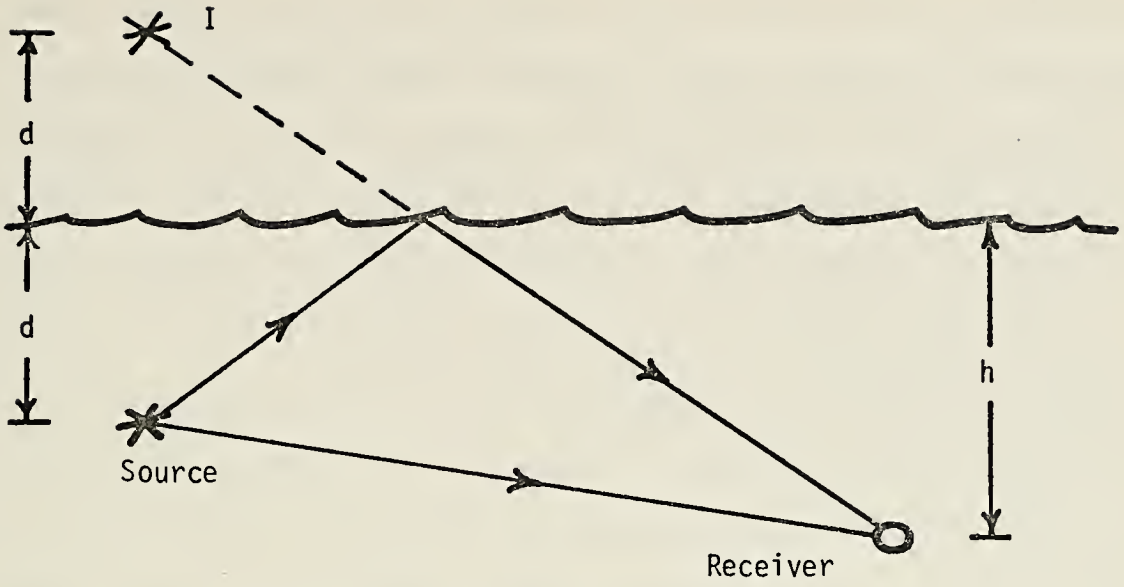

Figure 43. Lloyd Mirror Effect

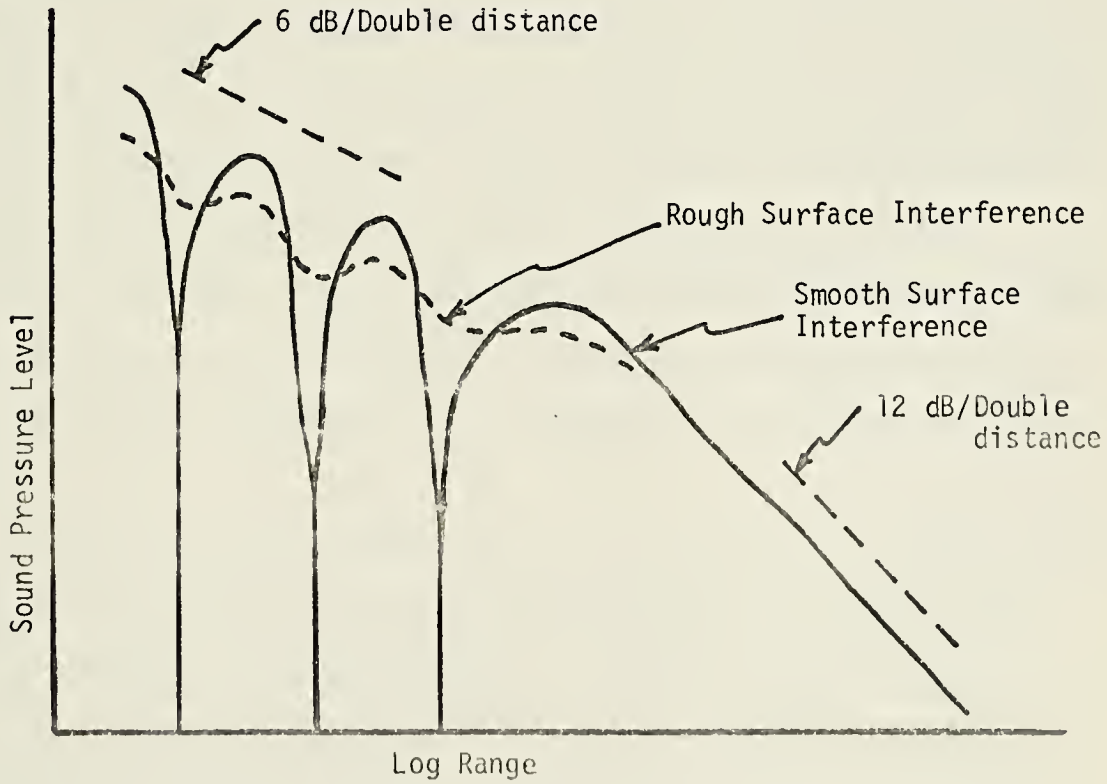

Figure 44. Differences in Lloyd Mirror Effect for Rough and Smooth Surfaces

term, given by the first Dirac delta term in the expression for the scattered sound spectrum (Theory section), predominates. Further the valleys caused by cancellation are now minima instead of zero as the incoherent or modulated term in the $S(\Omega)$ expression becomes important. This effect is shown in Figure 44 which contrasts the rough and smooth situation.

The setup used in the following three trials was essentially the same as in all signal processing runs. The OMNI was the source and the LC-10 served as receiver (both at a depth of 10 cm.), with a 3 Fan OAWF sea, set to the standard water level, modulating the transmitted 20 kHz acoustic signal. A/D samples were taken with program PERK 1A at a sampling rate of 80.0 kHz and analysis was performed by PERK 1B. A setup diagram is shown in Figure 45. The rack on which the LC-10 was mounted was moved back and forth with the water surface quiescent (fans off) until a Lloyd mirror maximum and adjacent minimum were identified. A third position was then chosen arbitrarily between the two extremes and designated "Intermediate". Runs were conducted at each of these three locations and a summary is presented in Table V below.

From the output of PERK 1B it was possible to compare the signal fluctuations at the three positions. At the Lloyd mirror maximum, corresponding to a strong signal (larger constant amplitude coherent and smaller variable incoherent contribution from the surface scattered sound), the maximum

TABLE V

TRIALS CONDUCTED AT VARIOUS LLOYD MIRROR POSITIONS

Run No.	Lloyd Mirror	Samples/ BLOCK	Delay	No. of PHASES	Total Ocean Periods Covered
10101	Min	64	47.69 msec	8	16
10102	Max	64	(assumed ocean freq.	8	16
10.03	Inter-mediate	64	2.578 Hz)	8	16

spectral density peak exceeded the overall average by about 2.1 dB and the minimum peak fell about 2.0 below the average. The total range of amplitudes was about four decibels. Applying the same comparison technique to the other two runs yields a swing of about 8.5 dB at the "Intermediate" position and almost 19 dB at the position of the weak signal where there is a maximum fluctuation of the amplitude.

It is apparent that in this model fluctuations do exist regardless of signal strength and that they are of greatest importance when the signal is weak. This further points up the importance of adapting knowledge of the sound modulation to enhancing a signal processing method as a means of acquiring and/or retaining low strength signals in a noisy or highly variable environment.

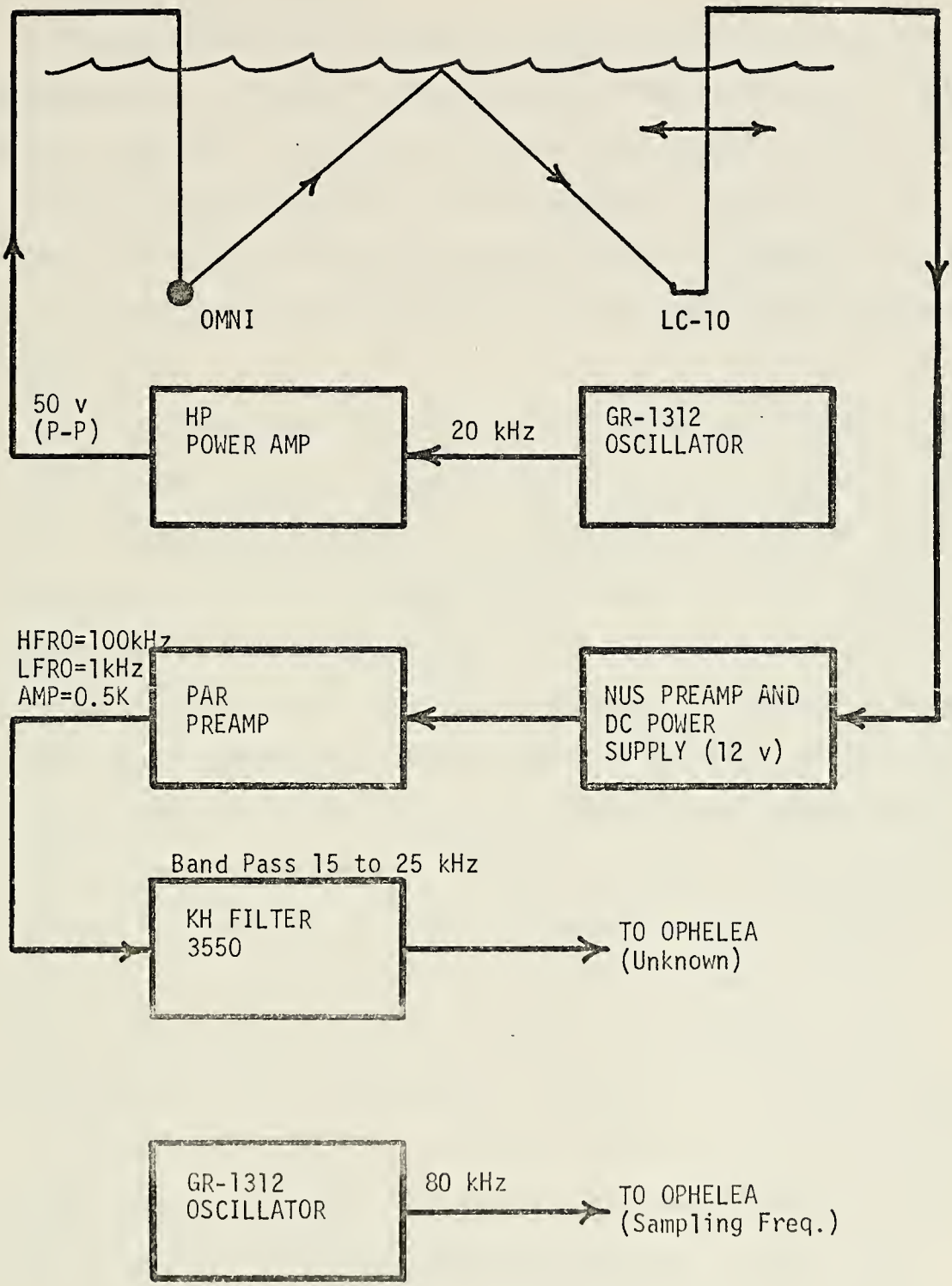

Figure 45. Experimental Setup for Determining the Effect on Spectral Density Variation with Time at Three Lloyd Mirror Positions

C. "BEST PHASE" METHOD

As previously mentioned, if the scattered sound were modulated at a single fixed frequency there would be a PHASE which, when once correctly chosen, would always yield the strongest average signal. The modulation frequency is of course not monochromatic as shown earlier in Figure 41 and in fact its spectrum has about a 0.5 Hz half-power bandwidth (Figure 26).

This not withstanding it was felt both instructive and possibly rewarding to compare the relative strengths of the eight PHASES. Thus an annex was appended to PERK 1B which averaged all of the spectral density peaks in each PHASE (every eighth peak in this case) and printed out a PHASE average as well as the overall average of all peaks. These values for 8 runs are shown in Figures 46(a-h), which depict PHASE average spectral density plotted versus PHASE with the dashed line indicating the overall average. All of the runs are seen to, in fact, follow a rough sinusoidal pattern particularly Figures 46(c) and 46(g) but others such as Figure 46(a) appear to be at double the ocean frequency. The Figures 46(a-h) show spectral density on a linear scale.

If the "BEST PHASE", or highest PHASE average is compared to the overall average, the gain is in the range of 0.3 dB (for the Lloyd mirror max-strong signal case) to 0.5 dB (for the weak signal), which is hardly anything to write home about.

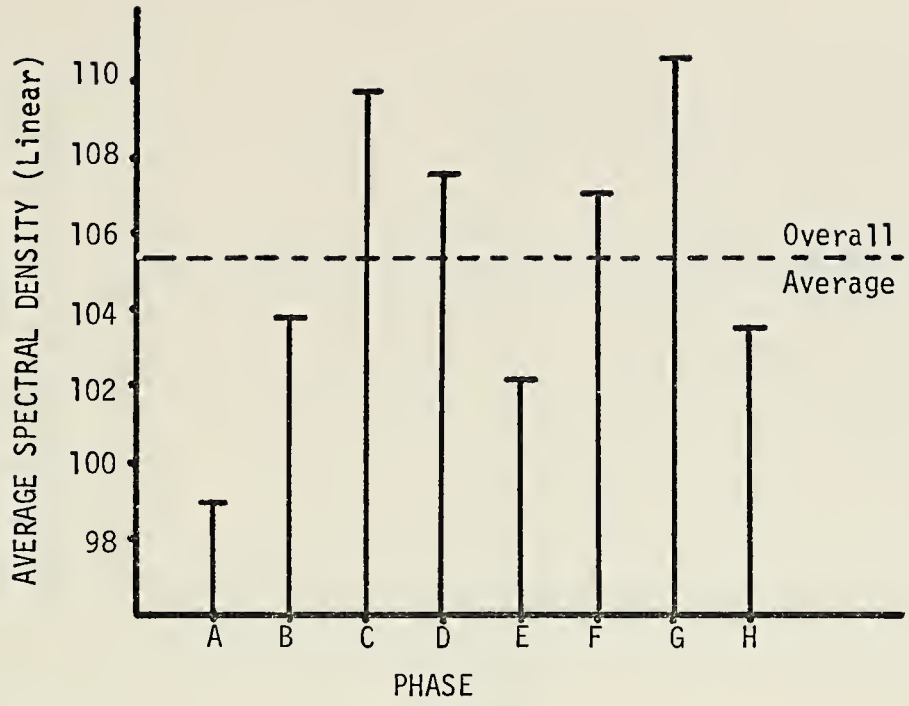

(a) Run 18901

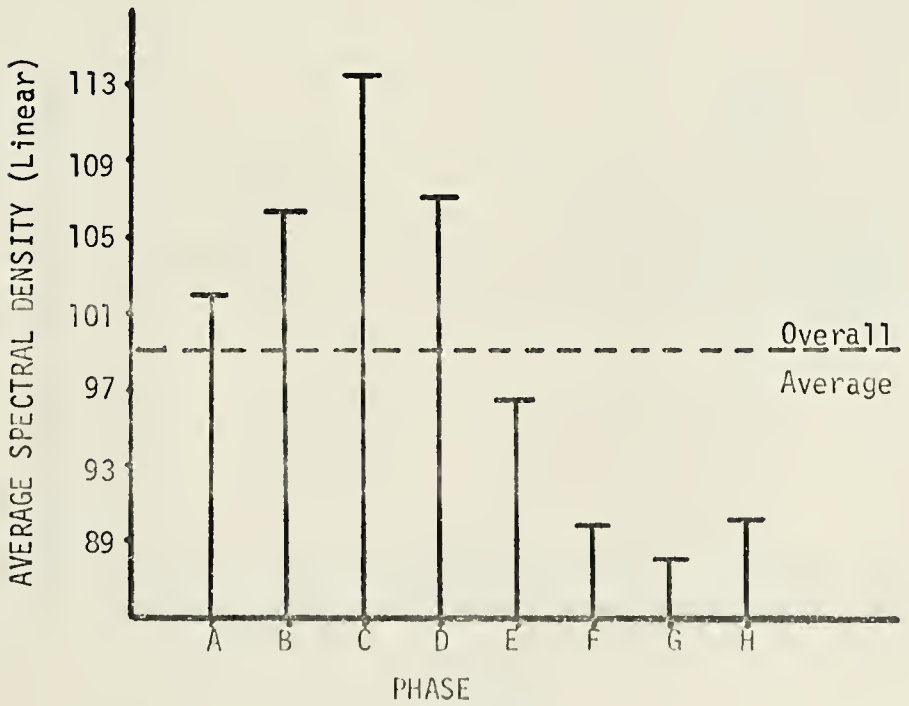

(b) Run 20901

Figure 46. Average PHASE Spectral Densities

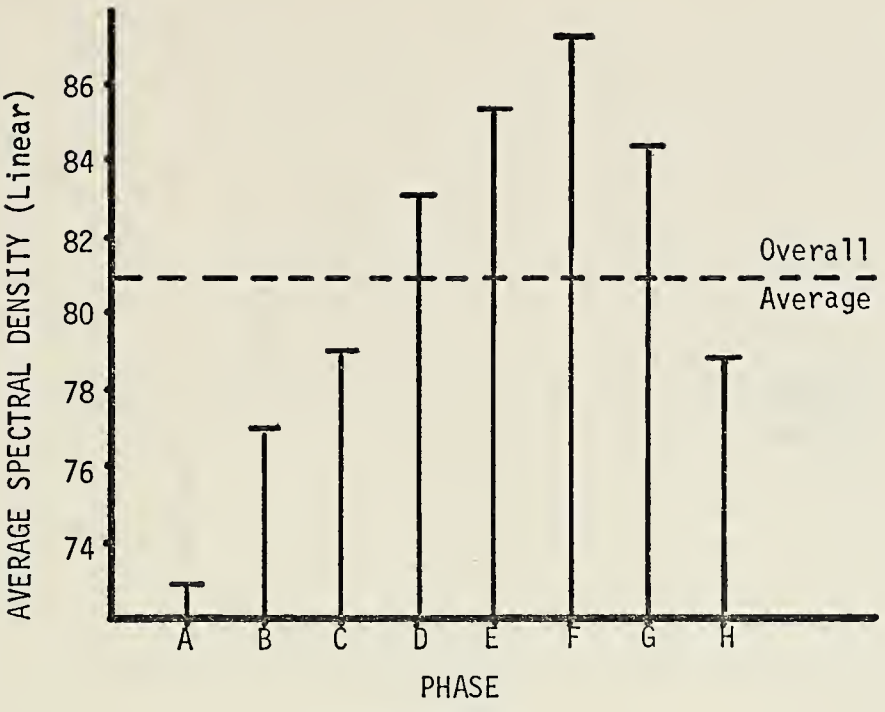

(c) Run 20902

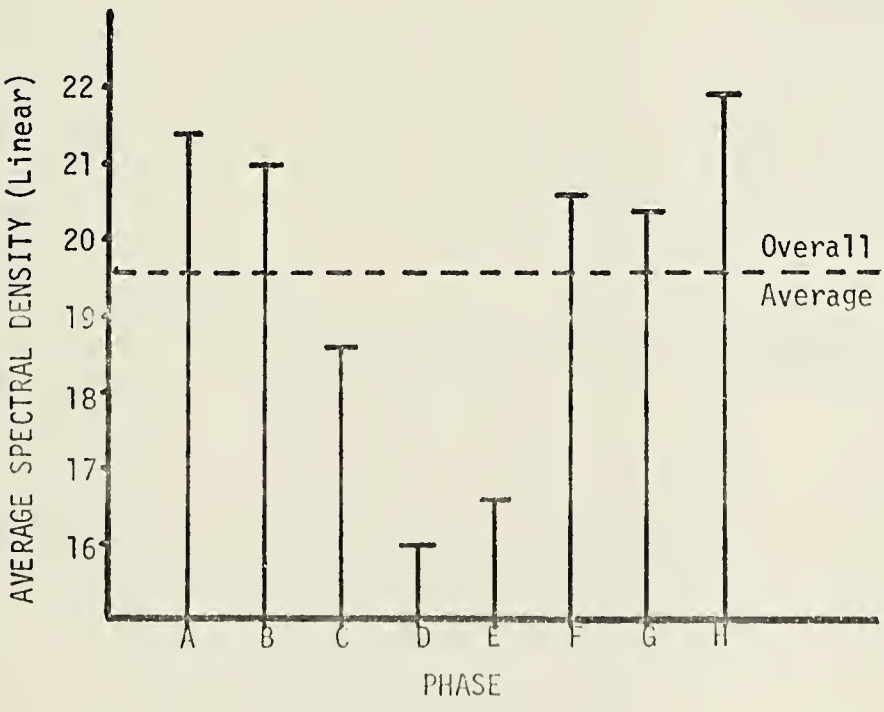

(d) Run 10101

Figure 46. Average PHASE Spectral Densities

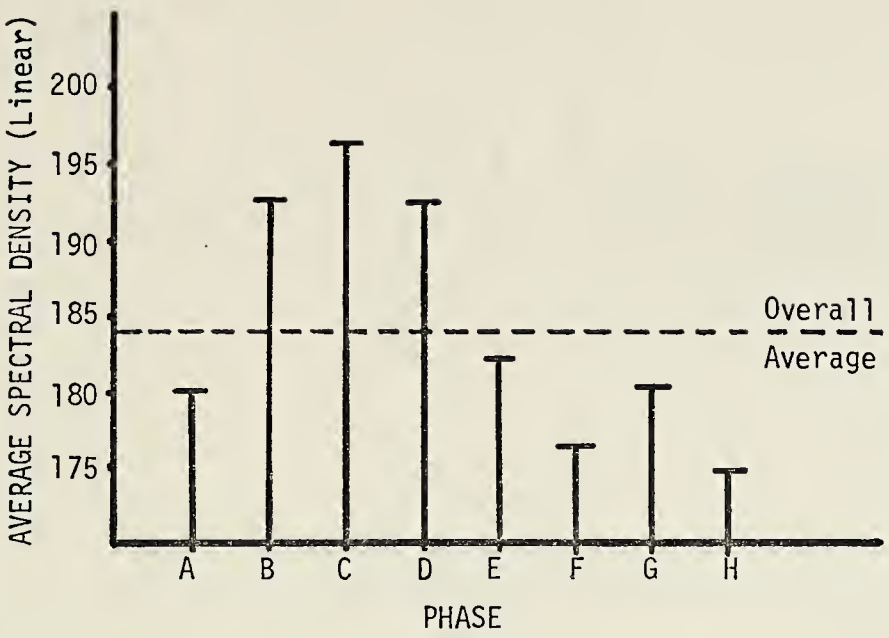

(e) Run 10102

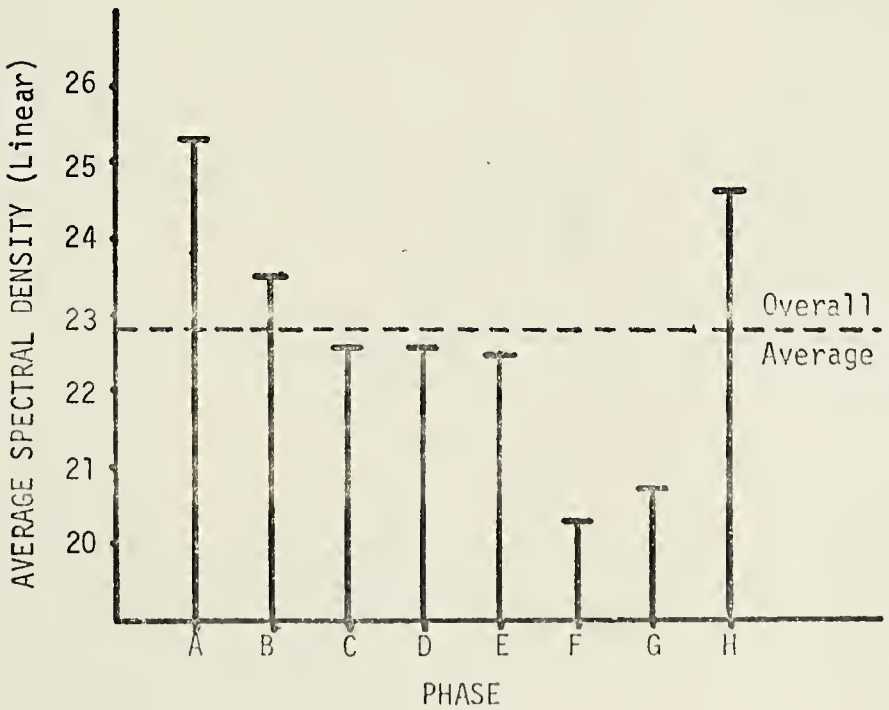

(f) Run 10103

Figure 46. Average PHASE Spectral Densities

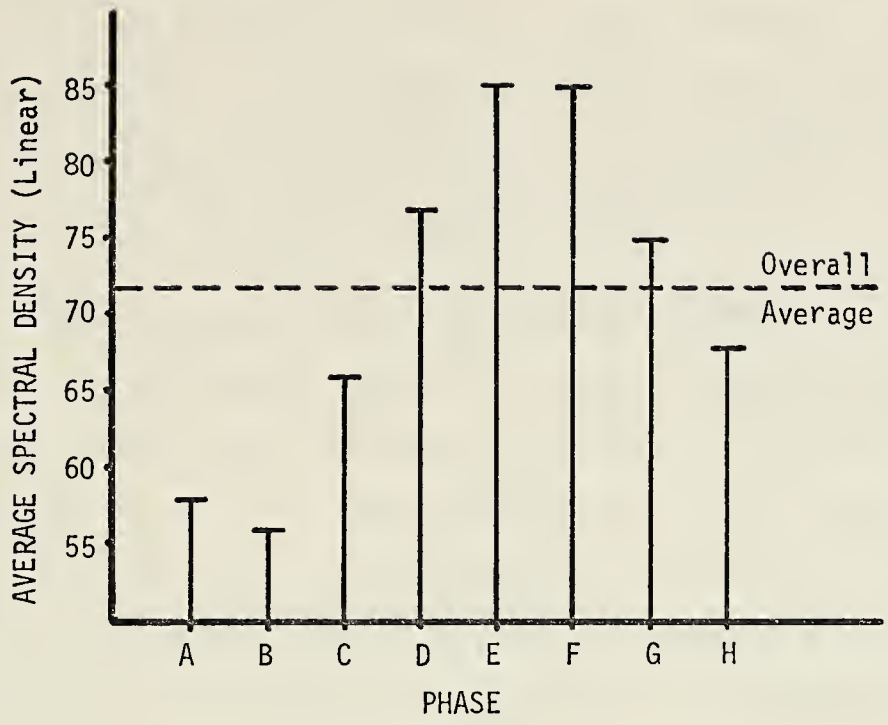

(g) Run 15101

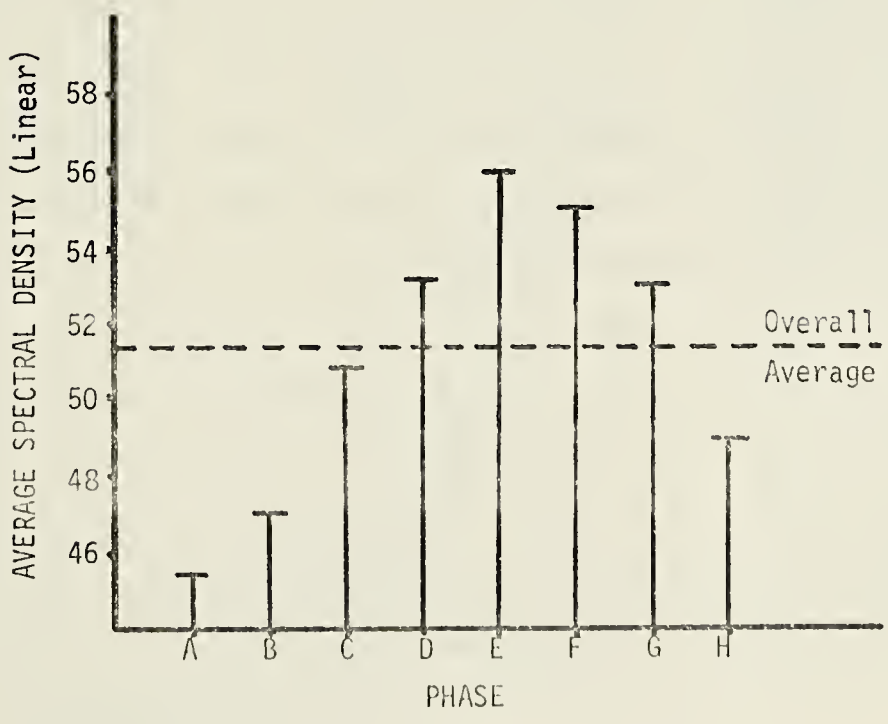

(h) Run 15102

Figure 46. Average PHASE Spectral Densities

In summary the "BEST PHASE" method applied innocently over 16 ocean periods is seen to offer some small advantage. However, because of the broad band modulation of the scattered sound modulation and the drift of the best phase over many ocean periods the gain realized is minimal.

D. "MONDAY MORNING SIGNAL PROCESSING" METHOD

The next approach began with hand plotting the spectral density versus time information presented by PERK 1B and examining it to see if any combinations would become apparent. Samples of the plots are included in Figures 41, 47 and 48 and show the fluctuations of spectral density with time for the Lloyd mirror minimum, "intermediate" and maximum, respectively.

To analyze this displayed information a clear plastic mask was constructed with a sinusoid of the same frequency as the assumed peak OAWF ocean frequency printed on it. The mask was then moved along the time axis of the spectral density versus time plot to determine how many peaks or near peaks corresponded to the ideal sinusoid peaks. Typically groups of at least three but up to five would line up prior to an irregularity or "glitch" which would require shifting phase to a subsequent group. This was not unexpected as the auto- and cross-correlation functions discussed earlier in this work indicated good correlation for at least two or three ocean periods.

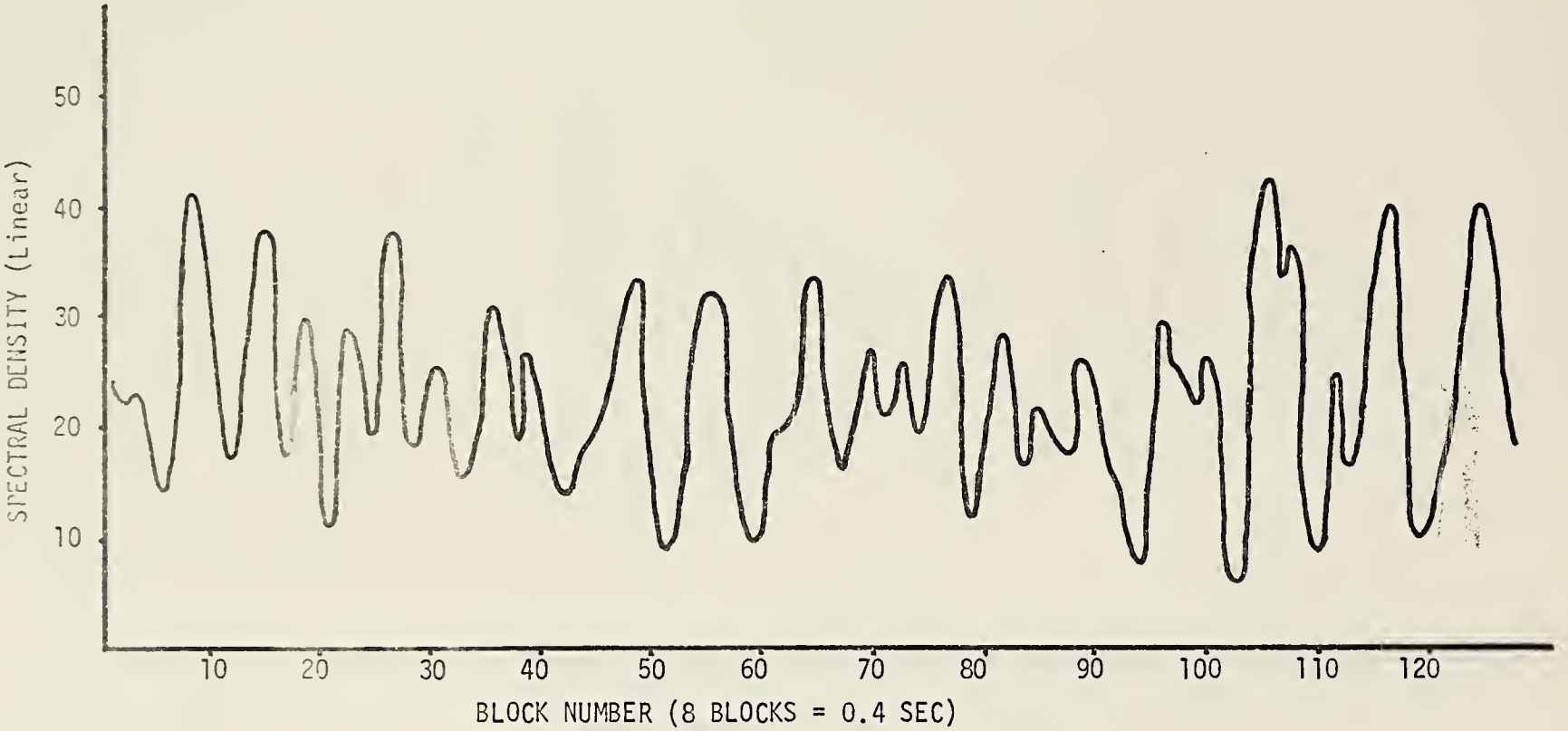

Figure 47. Changing Spectral Density Amplitude of a Forward Scattered Acoustic Signal ("Intermediate" Strength Signal)

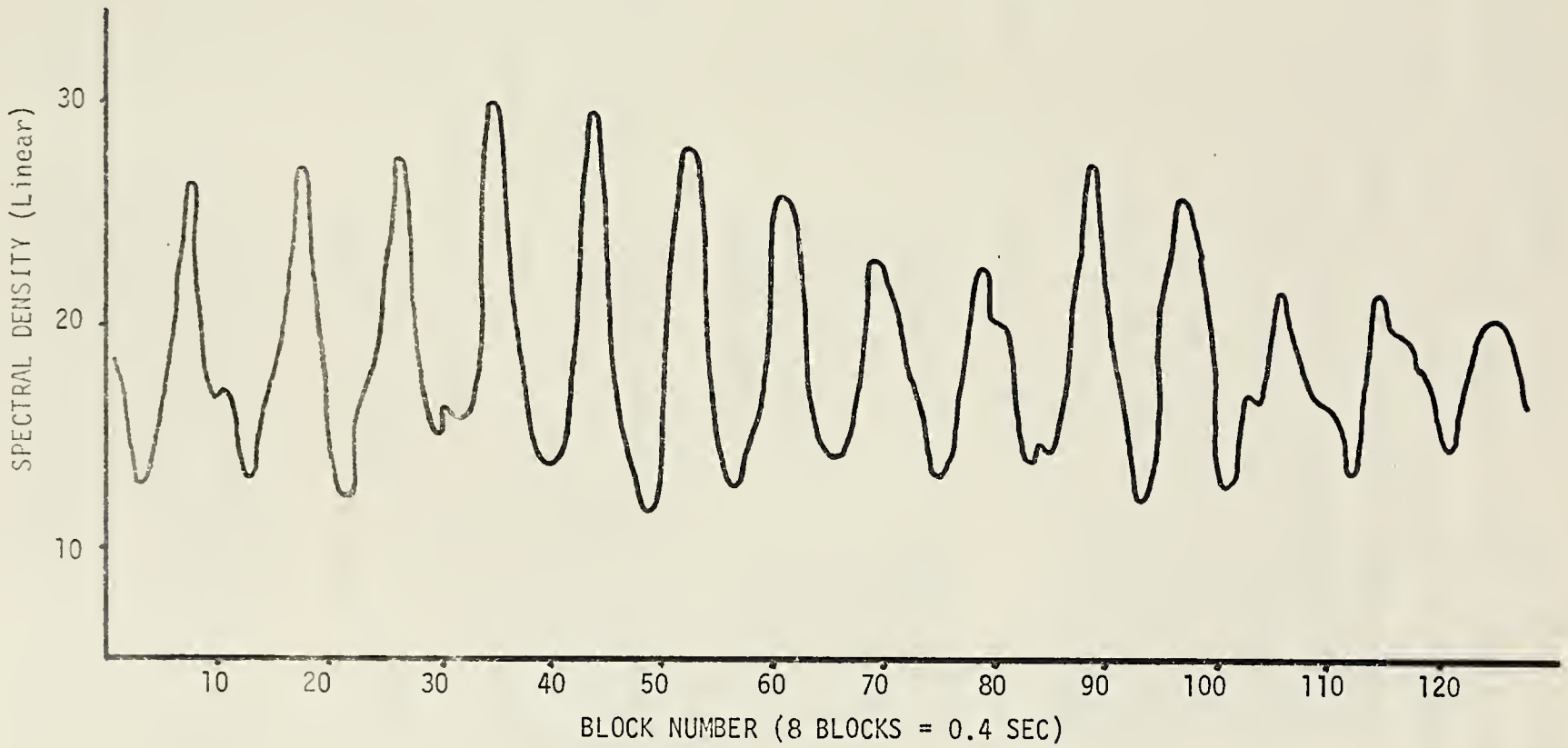

Figure 48. Changing Spectral Density Amplitude of a Forward Scattered Acoustic Signal (Strong Signal - Small Fluctuations)

The above procedure was felt to simulate a signal processor which would identify a strong signal and then sample later, only at intervals which are multiples of the ocean period, three to five times to gain signal enhancement over continuous integration. The results of this signal processing in hindsight – hence the Monday Morning label – are interesting and are illustrated below:

Referring to Figure 41, the Lloyd mirror weak signal (large fluctuations) case; if the BLOCKS indicated by arrows are chosen and averaged as follows:

Group	BLOCKS	M^2SP Ave.
1	5,13,21	44.70
2	39,47,55,63,71	25.20
3	98,106,114,122	42.55

These groups of BLOCKS correspond to identifying initial strong signal (i.e. BLOCKS 5,39 or 98), then sampling at the ocean frequency for only three to five peaks further. The payoff becomes apparent when these Monday Morning averages are compared to the overall average of 19.6 which yields gains of +3.6, +1.1 and +3.4 dB for groups 1, 2, and 3, respectively.

Gains in the case of the modeling strong signal (weak fluctuations) ranged from +1.0 to +1.4 dB and those for the Lloyd Mirror "Intermediate" response were in the +0.4 to +1.1 dB range. The interested reader is invited to verify

these values, or try to improve on them with other combinations, by marking a ruler or like object in intervals of 0.4 seconds and sliding it along Figures 41, 47 and 48.

The advantage of Monday Morning Signal Processing, is obvious in the weak signal environment (where it is most needed, of course) and is at least worthwhile, though not vital, when observing a stronger signal. The author will consider modifications to this technique and suggestions for real time analysis in the final section.

E. SUCCESSIVE AVERAGING

In an attempt to validate statistically the "seat of the pants" notion that three to five ocean periods is the maximum extent to which sampling at multiples of the ocean period can be profitably employed, a system of averaging was developed and appended to PERK 1B (which became PERK 1C).

The spectral density peaks were first divided into eight PHASES (A through H) of sixteen peaks each. These PHASE groups were then blindly averaged in ensemble group as follows:

Taking PHASE B for example,

Average by two's $\frac{B1+B2}{2}$, $\frac{B2+B3}{3}$, ... , $\frac{B16+B1}{2}$

Average by three's $\frac{B1+B2+B3}{3}$, $\frac{B2+B3+B4}{3}$, ... , $\frac{B16+B1+B2}{3}$

etc.

Up to Average by eights

These averages were then compared with the overall average and the number that exceeded it noted. Rather than confirming the initial hypothesis, however, the results were contradictory; indicating that groups of three to five were most profitable in some PHASES while averages of five to eight were most beneficial in others. In fact one PHASE indicated that it made little difference how many were averaged — that all combinations were equally profitable.

The author remains convinced however, that, though it has not been statistically proven, when compared with blind averaging, the Monday Morning technique demonstrates that averaging more than three to five peaks in a group is counterproductive.

In summary the blind Best Phase method provides only a minimal gain of about half a decibel when applied to a weak signal while the Mondary Morning technique provides nearly a +3 dB enhancement of the signal processing for very weak signals if sampling is limited to three to five ocean cycles.

VI. FUTURE RESEARCH, CRYSTAL BALL GAZING AND OTHER MUSINGS

The author feels that the research described in the foregoing pages has only scratched the surface of a viable means of acoustic signal enhancement. Some basic parameters and features of the modulation of surface scattered sound have been identified or confirmed and in some cases loosely quantized. These ideas may be of immediate use to signal processors, however additional research is felt to be indicated in the following two areas:

A. Further investigation of the phenomenon for additional clues which might increase its value/utility and prove more rigorously some notions presented herein.

The initial concept of identifying a signal peak (or loud point), then sampling later at multiples of the ocean period, which at this point might be charitably described as simplistic, could be more effective in a modified form. If a peak were identified and the next sampling interval were sought within the interval $T \pm \Delta T$, where T is the ocean period and ΔT is related in some unknown way to the bandwidth of the ocean spectrum and/or the rate of "attenuation" of its autocorrelation function, greater improvement might be realized. Of course the interval of sampling would increase by additional multiples of ΔT if the starting point were not reset at a peak after each group of samples was taken and the peak identified. (See Figure 49.) It is felt that the previously mentioned limit of three to five sampling intervals

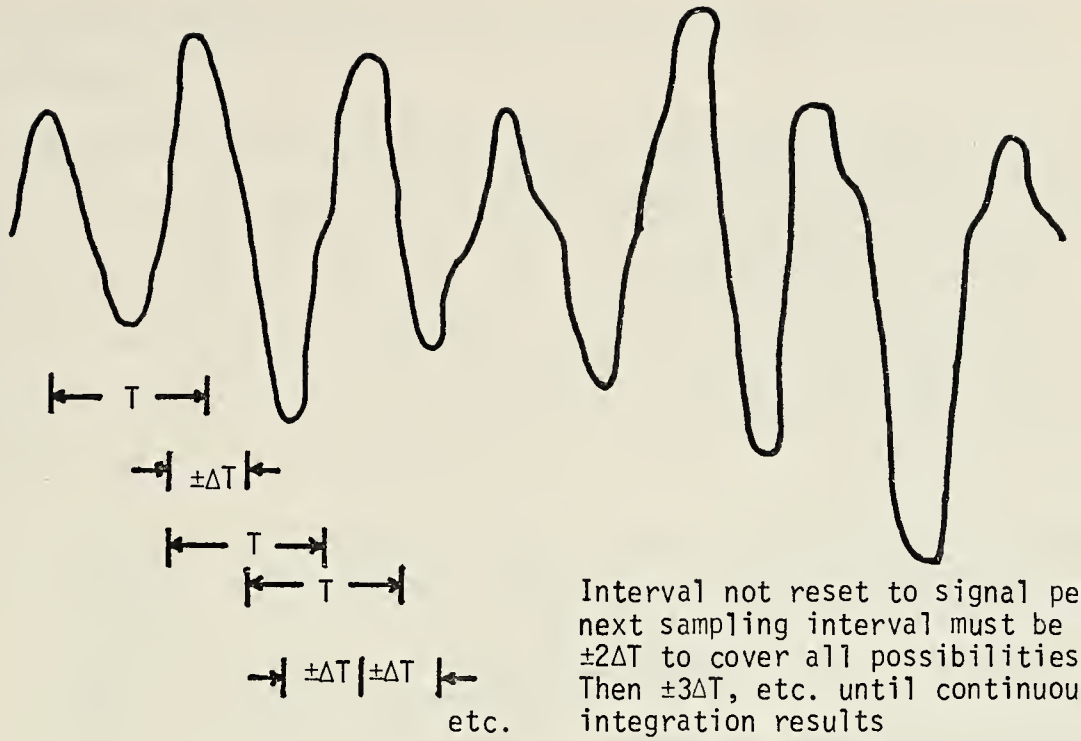

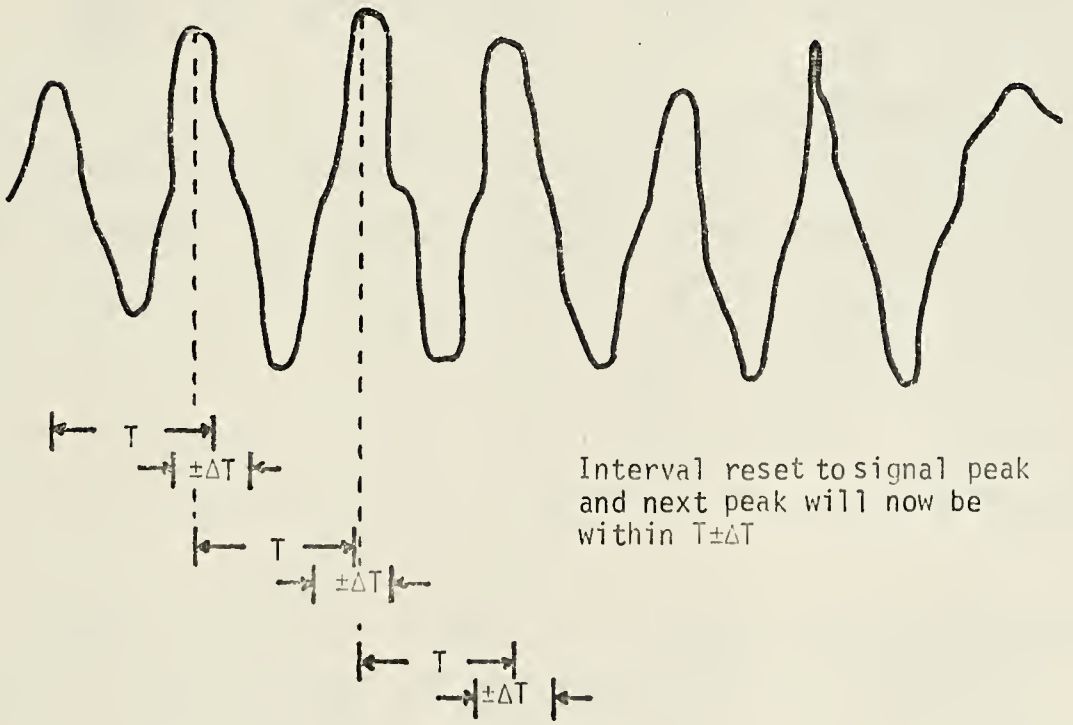

Figure 49. Improving on the "Best Phase" Processing Method

before the diminishing returns point is reached may also apply here.

It might be even more profitable to take samples at a rate of several BLOCKS per ocean period over some observation interval (greater than the ocean period) as done in this research and then to compute, sort and rank the spectral density peaks by magnitude. Once so arranged the following options would be available:

1. use only the highest peak in each observation interval
2. use only the highest peak in each ocean period and average over the observation interval
3. use the five (or any other arbitrary number) highest peaks observed and average as in 2.).
4. use only those peaks which exceed the overall average, which would also have to be computed, by 3 dB (or employ some lesser standard, such as 2 or 3, if none did).

As an aside it should be noted that when speaking of the "highest spectral peak" it is implicit that the highest for each frequency observed is computed, compared and utilized. This research was conducted with a single acoustic frequency but future trials might include several tranducers operating at various frequencies and signal output levels. A BLOCK of more than 64 samples may be required in this case to provide the desired frequency resolution.

Another possibility might be to continuously process for most of the "loud" half of the ocean period (5 seconds or so in the actual ocean), then process and use the received frequency spectral information to image correlate during the quieter half cycle. Again the three to five period

profitable limit is felt to pertain. This method might provide even better results than those obtained by active sonar image correlating as the changing doppler effects and attendant correlation mismatches would not be a factor over such short time spans.

B. The second major area of suggested study would be to spectrally analyze, plot, and employ the Monday Morning Signal Processing Technique on actual passively-recorded submarine tapes to see if gains comparable to this research are realized. Additionally the modulation frequency spectrum and autocorrelation functions could be determined and compared with both the locally observed wind/sea data and the results of this work.

In summary, there is no doubt as to the fact that sound scattered from the ocean surface is amplitude modulated at the basic surface wave frequencies. The ability to estimate the ocean wave frequency and spectrum is of course vital to taking advantage of this phenomenon and has not been addressed to this point. The author feels that ballpark estimates could be arrived at on station through a knowledge of fetch and surface wind speed and duration and assuming a Pierson-Moskowitz wave height spectrum. Further it is felt that meteorological organizations such as Fleet Numerical Weather Central could supply this information if tasked to do so, so that signal processors would be provided with up-to-date, tactically-useful data.

Though other mechanisms such as internal waves and temperature microstructure also contribute to fluctuations, the surface scattering is of particular importance for near-surface sources and/or receivers. What remains in the author's opinion is to find the means to most effectively use the various ocean modulation effects to enhance signal processing. It is felt that clever signal processors, if properly informed, could devise numerous techniques far more subtle and comprehensive than the rather simplistic methods suggested in this and the foregoing sections and that even greater gains might be realized. It should be emphasized that use of these techniques is not contended to be the miracle cure for the Anti-Submarine Warfare problem. The author does feel however that ocean modulation phenomena, if used to best advantage, will provide part of the answer required to cope with quieter next generation targets.

```
C
C       PING1C     4 SEPTEMBER 1974     CCH
C
C       THIS PROGRAM TAKES DATA FROM TWO ADC CHANNELS,PERFORMS
C       AN FFT ON IT,CALCULATES PSD AND ANGLES,PRINTS ONLY
C       SPECIFIED PEAKS,THEN CALCULATES 10LOG10(PSD1/PSD2)
C       AND THE DIFFERENCE BETWEEN THE ANGLES FOR EACH CHANNEL
C
C       THIS PROGRAM HAS THE ABILITY TO USE UP TO 1024
C       DATA POINTS PER CHANNEL
C
C       IARY IS THE ANALOG ARRAY (INTEGER)
C       ARY IS THE REAL DATA ARRAY
C       N IS THE POWER OF 2 EQUAL TO THE ARRAY SIZE
C       1 = YES, 0 = NO
C
C
      INTEGER*2 IARY
      DIMENSION IARY(2,1030),ARY(2,1024)
      DIMENSION OUT(2,515)
      EQUIVALENCE (OUT(1,1),IARY(1,1))
C
C       CLEAR IARY
C
  800 DO 10 I=1,1024
      IARY(1,I) = 9
      IARY(2,I) = 9
   10 CONTINUE
C
C       REQUEST INPUT PARAMETERS
C
   16  WRITE(3,300)
  300 FORMAT (/28HINPUT VALUE OF N ? (00=END) )
      READ (5,301) N
  301 FORMAT (I2)
      IF (N.EQ.0) GO TO 860
      IF(N.GT.10)GO TO 16
       NV=2**N
       INV=(NV/2)+2
       WRITE (3,310) NV
  310  FORMAT(17HNO COMPLEX PTS = ,I4)
       WRITE(3,315)
  315  FORMAT(/19HINPUT SAMPLE FREQ ?)
        READ(5,316) SF
  316   FORMAT (F9.4)
      WRITE(3,850)
  850 FORMAT(/13HWHICH PIDS ? )
      READ(5,301)IPID
      WRITE(3,302)
  302  FORMAT(/18HINPUT LIST DESIRED)
      READ(5,350)IL
  350 FORMAT (I1)
      WRITE (3,462)
  462 FORMAT (/15HPID PRINTOUT ? )
      READ (5,350) IP
       WRITE(3,303)
      READ(5,350)IT
  303 FORMAT(/14HTRIHAN DESIRED)
C
C       COMPUTE RESOLUTION AND TOTAL BANDWIDTH
```

```
C
      FPSD = FLOAT(IPSD)
      PES = FPSD/(FLOAT(NV)*(1.0/SF))
      TB=1.0/(2.0*(1.0/SF))
      WRITE (3,870)
  870 FORMAT (11HCONTINUE ? )
      READ (5,350) ICO
      IF (ICO.EQ.0) GO TO 800
C
C      INPUT DATA ON CHANNEL B/C ADC
C      192  = HEX C0
C
      NVV = NV+2
      IOC = 192
      CALL ADCDAC(IOC,IARY,NVV)
C
C       ADC DATA NOW IN
C
      WRITE (3,870)
      READ (5,350) ICO
      IF (ICO.EQ.0) GO TO 800
      INX = 2*NV
      IF (IT-1)8,9,8
C
C
    9 C = FLOAT(NV)
      C = 1.0/(C/2.0)
      B = C
      A = C
      DO 700 I=1,NV
      K = I+2
      D = FLOAT(IARY(1,K))
      E = D*B
      IARY(1,K) = IFIX(E)
      D = FLOAT(IARY(2,K))
      E = D*B
      IARY(2,K) = IFIX(E)
      IF(A.GE.1.0) GO TO 703
      B = B+C
      GO TO 701
  703 B = B-C
  701 A = A+C
  700 CONTINUE
C
C       TRANSFER TO COMPLEX ARRAY
C
    8 DO 15 ICHAN=1,2
      WRITE (3,320) ICHAN
  320  FORMAT(/,13HCHANNEL NO. ,I1,/)
      IF (ICHAN.EQ.2) GO TO 400
      DO 1 I=1,NV
      II = I+2
      ARY(1,I) = FLOAT(IARY(ICHAN,II))
    1 ARY(2,I)=0.0
      GO TO 490
  400 DO 410 I=1,NV
      IARY(2,I) = IARY(2,I+2)
  410 CONTINUE
      KK = (NV+4) 2
      OUT(1,KK) = ARY(1,KK)
```

```
      OUT(2,KK) = ARY(2,KK)
      OUT(1,KK-1) = ARY(1,KK-1)
      OUT(2,KK-1) = ARY(2,KK-1)
      K = NW
      DO 420 I=1,NW,2
      KK = K/2
      TEMP1 = FLOAT(IARY(2,K))
      TEMP2 = FLOAT(IARY(2,K-1))
      OUT(1,KK) = ARY(1,KK)
      OUT(2,KK) = ARY(2,KK)
      ARY(1,K) = TEMP1
      ARY(2,K) = 0.0
      ARY(1,K-1) = TEMP2
      ARY(2,K-1) = 0.0
      K = K-2
  420 CONTINUE
C
  490 IF (IL-1) 7,6,7
C
C
    6 DO 3 I=1,NW,8
      II = I+7
      WRITE (3,602) (ARY(1,M),M=I,II)
  602 FORMAT (8F7.0)
    3   CONTINUE
    7 WRITE (3,870)
      READ (5,350) ICO
      IF (ICO.EQ.0) GO TO 800
C
C
      IX = -1
       CALL FOUR1(ARY,NW,IX)
      WRITE (3,870)
      READ (5,350)   ICO
      IF (ICO.EQ.0) GO TO 800
      IF (IP.EQ.0) GO TO 611
      WRITE (3,610)
  610 FORMAT (16X,3HPSI,13X,4HPRED,6X,5HANGLE/)
  611 P2 = 0.0
C
C       OUTPUT ( IIT = 1/2 NO. COMPLEX POINTS + 2
C
      DO 2 I=1,NW,IPSD
      IF(ARY(1,I),NE.0.0)GO TO 500
      IF(ARY(2,I))501,502,503
  501 ANGLE = 270.0
      GO TO 530
  502 ANGLE=0.0
      GO TO 530
  503 ANGLE=90.0
      GO TO 530
  500 ANGLE=ATAN(ARY(2,I)/ARY(1,I))
      ANGLE = ANGLE*57.29577951
      IF (ARY(1,I),GE,0.0) GO TO 505
      ANGLE = ANGLE+180.0
      GO TO 530
  505 IF (ARY(2,I),GE,0.0) GO TO 530
      ANGLE = ANGLE+360.0
  530 P2 = ARY(1,I)**2+ARY(1,I)+ARY(2,I)*ARY(2,I)
      IF (IP.EQ.0) GO TO 612
```

```
      WRITE (3,600) PSD,RS,ANGLE
  612 ARY(1,I) = PSD
      ARY(2,I) = ANGLE
  600 FORMAT (3X,F16.1,3X,F14.3,3X,F8.3)
       IF(PS.LT.TB) GOTO 20
      PS=6.0
      GOTO 2
   20  PS=PS+PES
    2 CONTINUE
C
C
      WRITE (3,870)
      READ (5,350) ICO
      IF (ICO.EQ.0) GO TO 800
   15 CONTINUE
C
C
      PS = 0.0
      WRITE (3,460)
  460 FORMAT (/13X,4HFREQ,3X,16H10LOG(PSD1/PSD2),3X,13HANGLE1-ANGLE2/)
C
      DO 430 I=1,INW,IPSD
      IF (ARY(1,I).NE.0.0) GO TO 450
      PSD = 9999.0
      GO TO 451
  450 PSD = 10.0*ALOG10(OUT(1,I)/ARY(1,I))
  451 ANGLE = OUT(2,I)-ARY(2,I)
      WRITE (3,461) PS,PSD,ANGLE
      IF (PS.LT.TB) GO TO 440
      PS = 0.0
      GO TO 430
  440 PS = PS+PES
  430 CONTINUE
  461 FORMAT (3X,F14.3,3X,F16.5,3X,F13.3)
C
C
       GO TO 800
  860 STOP
      END
```

```
C
C       PERK1A  2F AUGUST 1974      CCH
C       PROGRAM TO SAMPLE,PAUSE,AND WRITE DATA ON CASSETTE
C
C       A SPECIFIED NUMBER OF POINTS ARE TAKEN FROM ADC/C IN A
C       SPECIFIED BLOCK SIZE WITH A SPECIFIED DELAY BETWEEN
C       EACH BLOCK
C       INPUT DATA:
C            RUN = IDENTIFYING NUMBER (INTEGER)
C            N = POWER OF 2 EQUAL TO ARRAY SIZE
C            NS = POWER OF 2 EQUAL TO BLOCK SIZE
C            SF = SAMPLE FREQUENCY
C            NP = NUMBER OF PHASES
C            DELAY = DELAY BETWEEN BLOCKS IN MILLISECONDS * 100
C            1 = YES, 0 = NO
C
      INTEGER*2 N,TNP,NS,PPS,DELAY,CON
      INTEGER*2 I,IND%,IARY,KEND,II,M
      INTEGER*2 NP,J,JJ
      INTEGER*2 NTOTB
      INTEGER*2 RUN
      DIMENSION IARY(8200)
      KEND = 32767
C
C       REQUEST INPUT PARAMETERS
C
  100 WRITE (3,900)
  900 FORMAT (2HN = ? (I2) (00=END) )
      READ (5,901) N
  901 FORMAT (I2)
      IF (N) 100,200,110
  110 IF (N.GT.13) GO TO 100
      TNP = 2**N
C
  120 WRITE (3,902)
  902 FORMAT (13HNS = ? (I2) )
      READ (5,901) NS
      IF (NS) 120,130,130
  130 IF (NS.GT.9) GO TO 120
      IF (NS.LT.4) GO TO 120
      PPS = 2**NS
      NTOTB = TNP/PPS
      IF (NTOTB.GT.512) GO TO 100
      TNP = NTOTB*PPS
C
      WRITE (3,903)
  903 FORMAT (15HDELAY = ? (I5) )
      READ (5,904) DELAY
  904 FORMAT (I5)
C
      WRITE (3,905)
  905 FORMAT (25HRUN NO. = ? (I5) (DUMRP) )
      READ (5,904) RUN
C
      WRITE (3,909)
  909 FORMAT (14HSF = ? (F8.1) )
      READ (5,910) SF
  910 FORMAT (F8.1)
C
  140 WRITE (3,911)
```

```
 911   FORMAT (12HNP = ? (I2) )
       READ (5,901) NP
       IF ((NTOTB/NP)*NP.NE.NTOTB) GO TO 140
C
       WRITE (2,906)
 906   FORMAT (11HCONTINUE ? )
       READ (5,907) CON
 907   FORMAT (I1)
       IF (CON.EQ.0) GO TO 100
C
C
       I = TNP/PPS
       TNP = I*PPS
C
C       CLEAR THE ARRAY
C
       DO 150 I=1,8200
       IARY(I) = KEND
 150   CONTINUE
C
C       GET DATA FROM ADC CHANNEL 0
C
       CALL SAMP(IARY,TNP,PPS,IDELAY)
C
C       OUTPUT DATA
C
       WRITE (2,920) RUN,TNP,PPS,DELAY,SF,NP,NTOTB
 920   FORMAT (4I6,F8.1,2I6)
 908   FORMAT (8I6)
       DO 160 I=1,TNP,8
       II = I+7
       WRITE (2,908) (IARY(M),M=I,II)
 160   CONTINUE
       WRITE (2,908) KEND
       GO TO 100
C
C
 900   WRITE (2,908) KEND
       STOP
       END
```

```
C
C     PERK1C  15 OCTOBER 1974     OCH
C      PROGRAM TO ANALYZE BLOCK DATA
C
C      ALL INPUT PARAMETERS AND DATA ARE ON A
C      CASSETTE GENERATED BY PERK1A
C
       DIMENSION APY(2,512),PHASE(2,512),APSD(2,16)
C
C        GET INPUT PARAMETERS FROM TAPE
C
  100  READ (2,900) NRUN,NTNP,NPPS,NDELAY,SF,NP,NTOTB
  900  FORMAT (4I6,F8.1,2I6)
       IF (NRUN.EQ.32767) GO TO 400
       WRITE (3,902)
  902  FORMAT (9HTPIHAN ? )
       READ (5,903) IT
  903  FORMAT (I1)
       WRITE (3,930)
  930  FORMAT (6HEND ? )
       READ (5,903) IE
       IF (IE.EQ.1) GO TO 400
       WRITE (3,940)
  940  FORMAT (14HTEST PRINTOUT ? )
       READ (5,903)ITPO
       WRITE (3,941)
  941  FORMAT (24HINTERMEDIATE PRINTOUT ? )
       READ (5,903) IPO
C
C
       WRITE (3,931)
  931  FORMAT (/48H************************************************)
       WRITE (3,913) NRUN
  913  FORMAT (/8HRUN,1X,I5)
       WRITE (3,914) SF
  914  FORMAT (11HSAMPLE FREQ,1X,F8.1)
       WRITE (3,915) NDELAY
  915  FORMAT (7HDELAY,1X,I5)
       WRITE (3,931)
       WRITE (3,932)
  932  FORMAT (/)
C
C
       DO 270 NB=1,NTOTB
C
C
       DO 110 I=1,NPPS,8
       II = I+7
       READ (2,901) (APY(1,J),J=I,II)
  110  CONTINUE
  901  FORMAT (8F8.0)
       DO 120 I=1,NPPS
       APY(2,I) = 0.0
  120  CONTINUE
C
C
       IF (IT.EQ.0) GO TO 150
C
C
       C = 2.0/FLOAT(NPPS)
```

```
      B = C
      A = C
      DO 140 I=1,NPPS
      ARY(1,I) = ARY(1,I)+B
      IF (A.GE.1.0) GO TO 130
      B = B+C
      GO TO 135
  130 B = B-C
  135 A = A+C
  140 CONTINUE
C
C
  150 IF (IPO.EQ.0) GO TO 410
      WRITE (3,904)
  904 FORMAT (/10X,29H******************************)
      WRITE (3,905) NRUN,NB
  905 FORMAT (/10X,3HRUN=,1X,I5,10X,5HBLOCK,1X,I4)
      WRITE (3,904)
C
C
  410 PES = SF/FLOAT(NPPS)
      TB = SF/2.0
C
C
      PHASE(1,NB) = 0.0
C
C
      IX = -1
      CALL FOUR1(ARY,NPPS,IX)
C
C
      IF (IPO.EQ.0) GO TO 420
      WRITE (3,906)
  906 FORMAT (16X,3HPSD,13X,4HPREQ,6X,5HANGLE/)
  420 PS = 0.0
      INDX = (NPPS/2)+2
C
C
      DO 260 I=1,INDX
      IF (ARY(1,I).NE.0.0) GO TO 210
      IF (ARY(2,I)) 180,190,200
  180 ANGLE = 270.0
      GO TO 230
  190 ANGLE = 0.0
      GO TO 230
  200 ANGLE = 90.0
      GO TO 230
  210 ANGLE = ATAN(ARY(2,I)/ARY(1,I))
      ANGLE = ANGLE*57.29577951
      IF (ARY(1,I).GE.0.0) GO TO 220
      ANGLE = ANGLE+180.0
      GO TO 230
  220 IF (ARY(2,I).GE.0.0) GO TO 230
      ANGLE = ANGLE+360.0
  230 PSD = ARY(1,I)*ARY(1,I)+ARY(2,I)*ARY(2,I)
      IF (PSD.LT.PHASE(1,NB)) GO TO 240
      PHASE(1,NB) = PSD
      PHASE(2,NB) = PS
  240 IF (IPO.EQ.0) GO TO 430
      WRITE (3,907) PSD,PS,ANGLE
```

```
 907  FORMAT (3X,F16.1,3X,F14.3,3X,F8.3)
 430  IF (RS.LT.TR) GO TO 250
      PS = 0.0
      GO TO 260
 250  RS = RS+RES
 260  CONTINUE
      WRITE (3,932)
      WRITE (3,932)
C
C
 270  CONTINUE
      WRITE (3,942)
 942  FORMAT (2X,5HBLOCK,12X,7HMAX PSD,13X,4HFREQ)
      DO 440 I=1,NTOTB
      WRITE (3,943) I,PHASE(1,I),PHASE(2,I)
 440  CONTINUE
 943  FORMAT (4X,I3,3X,F16.1,3X,F14.3)
C
C
      DIV = FLOAT(NTOTB/NP)
      DO 310 I=1,NP
      PSD = 0.0
      II = I
      FREQ = PHASE(2,I)
      DO 280 J=1,NTOTB,NP
      PSD = PHASE(1,II)+PSD
      IF (ITPO.EQ.0) GO TO 450
      WRITE (3,944) PSD,PHASE(1,II)
 944  FORMAT (2F16.1)
 450  IF (FREQ.NE.PHASE(2,II)) GO TO 300
      II = II+NP
 280  CONTINUE
      APSD(1,I) = PSD/DIV
      IF (ITPO.EQ.0) GO TO 460
      WRITE (3,944) APSD(1,I),DIV
 460  II = I
      SUM = 0.0
      DO 290 J=1,NTOTB,NP
      PSD = PHASE(1,II)-APSD(1,I)
      SUM = SUM+(PSD*PSD)
      II = II+NP
 290  CONTINUE
      APSD(2,I) = SQRT(SUM/DIV)
      GO TO 310
 300  WRITE (3,908) I
 908  FORMAT (22HFREQ DIFFERENCE PHASE ,I2)
 310  CONTINUE
C
C
      PSD = 0.0
      WRITE (3,931)
      WRITE (3,910)
 910  FORMAT (  2X,5HPHASE,12X,7HAVERAGE,7X,13HSTANDARD DEV)
      DO 320 I=1,NP
      WRITE (3,909) I,APSD(1,I),APSD(2,I)
 909  FORMAT (5X,I2,3X,F16.2,3X,F16.2)
      PSD = APSD(1,I)+PSD
 320  CONTINUE
      AVG = PSD/FLOAT(NP)
      SUM = 0.0
```

```
      DO 330 I=1,NP
      PSD = APSD(1,I)-AVG
      SUM = SUM+(PSD*PSD)
330   CONTINUE
      SD = SQRT(SUM/FLOAT(NP))
      WRITE (3,931)
      WRITE (3,911) AVG
911   FORMAT (/3X,18HOVERALL AVERAGE = ,F16.2)
      WRITE (3,912) SD
912   FORMAT (3X,29HOVERALL STANDARD DEVIATION = ,F16.2)
      WRITE (3,931)
C
C
      NBP = NTOTB/NP
      WRITE (3,932)
      WRITE (3,931)
      DO 520 JJ=1,NP
      WRITE (3,950) JJ
950   FORMAT (/1X,5HPHASE,1X,I2)
      WRITE (3,955)
955   FORMAT (/5X,5HCYCLE,17X,3HPSD)
      NN = JJ
      DO 505 N=1,NBP
      WRITE (3,956) N,PHASE(1,NN)
      NN = NN+NP
956   FORMAT (8X,I2,4X,F16.2)
505   CONTINUE
      WRITE (3,957)
957   FORMAT (/1X,5HSTART)
      WRITE (3,951)
951   FORMAT (/1X,5HCYCLE,10X,4HAVG2,10X,4HAVG3,10X,4HAVG4,10X,4HAVG5)
      WRITE (3,952)
952   FORMAT (30X,4HAVG6,10X,4HAVG7,10X,4HAVG8)
      I = JJ
      K = 1
      DO 510 J=1,NBP
      II = I+NP
      IF (II.GT.NTOTB) II=JJ
      SUM2 = PHASE(1,I)+PHASE(1,II)
      II = II+NP
      IF (II.GT.NTOTB) II=JJ
      SUM3 = SUM2+PHASE(1,II)
      II = II+NP
      IF (II.GT.NTOTB) II=JJ
      SUM4 = SUM3+PHASE(1,II)
      II= II+NP
      IF (II.GT.NTOTB) II=JJ
      SUM5 = SUM4+PHASE(1,II)
      II = II+NP
      IF (II.GT.NTOTB) II=JJ
      SUM6 = SUM5+PHASE(1,II)
      II = II+NP
      IF (II.GT.NTOTB) II=JJ
      SUM7 = SUM6+PHASE(1,II)
      II= II+NP
      IF (II.GT.NTOTB) II=JJ
      SUM8 = SUM7+PHASE(1,II)
      AVG2 = SUM2/2.0
      AVG3 = SUM3/3.0
      AVG4 = SUM4/4.0
```

```
      AVG5 = SUM5/5.0
      AVG6 = SUM6/6.0
      AVG7 = SUM7/7.0
      AVG8 = SUM8/8.0
      WRITE (3,953) K,AVG2,AVG3,AVG4,AVG5
  953 FORMAT (4X,I2,4F14.1)
      WRITE (3,954) AVG6,AVG7,AVG8
  954 FORMAT (20X,3F14.1)
      K = K+1
      I = I+NP
  510 CONTINUE
  520 CONTINUE
C
C
      READ (2,900) KEND
      IF (KEND.EQ.32767) GO TO 100
C
C
  400 STOP
      END
```

BIBLIOGRAPHY

1. Parkins, B.E., "Scattering From The Time Varying Surface of the Ocean", The Journal of the Acoustical Society of America, v. 42, no. 6, p. 1262-1267, 1967.

2. Beckmann, P. and Spizzichino, A., The Scattering of Electromagnetic Waves From Rough Surfaces, The Macmillan Company, 1963.

3. Stratton, J.A., Electromagnetic Theory, p. 427, McGraw-Hill Book Co., 1941.

4. Lastinger, J.L., "Acoustic Characteristics of Woods at High Hydrostatic Pressure", The Journal of The Acoustic Society of America, v. 47, no. 1 (part 2), p. 285-289, 1970.

5. Kinsman, B., Windwaves, p. 451, Prentice Hall, 1965.

6. Scheibel, J.W. and Fowler, R.C., Specular Scatter of Underwater Sound From a Wind Driven Model Sea Surface, M.S. Thesis, U.S. Naval Postgraduate School, 1968.

7. Kinsman, B., Wind Waves, p. 342-345, Prentice Hall, 1965.

8. Cheasapeake Bay Institute Tech. Report 19, Johns Hopkins, Surface Waves At Short Fetches and Low Wind Speeds, A Field Study, by B. Kinsman, 1960.

9. Medwin, H., Clay, C.S., Berkson, J.M., and Jaggard, D.L., "Traveling Correlation Function of the Height of Wind Blown Water Waves", The Journal of the Acoustical Society of America, v. 75, no. 24, p. 4522, 1970.

INITIAL DISTRIBUTION LIST

		No. Copies
1.	Defense Documentation Center Cameron Station Alexandria, Va. 22314	2
2.	Library, Code 0210 Naval Postgraduate School Monterey, Ca. 93940	2
3.	Professor H. Medwin (Code 61 Md.) Physics Department Naval Postgraduate School Monterey, Ca. 93940	10
4.	LCDR J.B. Perkins III Armed Forces Staff College Norfolk, Va. 23511	2
5.	Mr. William Smith Department of Physics Naval Postgraduate School Monterey, Ca. 93940	1
6.	Manager Anti-Submarine Warfare Systems Project Office Attn: ASW -01 Department of the Navy Washington, D.C. 20360	1
7.	Manager Anti-Submarine Warfare Systems Project Office Attn: ASW -12 Department of the Navy Washington, D.C. 20360	2
8.	Commander Naval Electronics Systems Command Attn: PME -124 Naval Electronics Systems Command Headquarters Washington, D.C. 20360	1
9.	CDR Ned Mayo Commanding Officer USS Glover (AGDE-1) c/o F.P.O. New York, N.Y. 09501	1

10. Commander 1
Naval Air Development Center
Attn: J. Kacergis, Special Projects Group
Warminster, Pa. 18974

11. Dr. Jack Harris, Vice President 1
Pinkerton Computer Consultants Inc.
65 West Street Road
Warminster, Pa. 18974

12. Mr. Tom Lee, Vice President 1
Pinkerton Computer Consultants Inc.
65 West Street Road
Warminster, Pa. 18974

13. Director of Acoustic Programs (Code 468) 1
Office of Naval Research
800 N. Quincy Street
Arlington, Va. 22219